



# **NAVAL POSTGRADUATE SCHOOL**

**MONTEREY, CALIFORNIA**

## **THESIS**

**ASSESSING THE OPERATIONAL ROBUSTNESS OF THE  
HOMER MODEL FOR MARINE CORPS USE IN  
EXPEDITIONARY ENVIRONMENTS**

by

Matthew M. Morse

June 2014

Thesis Co-Advisors:

Daniel Nussbaum

Eugene Paulo

Second Reader:

Imre Balogh

**This thesis was performed at the MOVES Institute  
Approved for public release; distribution is unlimited**

THIS PAGE INTENTIONALLY LEFT BLANK

REPORT DOCUMENTATION PAGE			Form Approved OMB No. 0704-0188	
Public reporting burden for this collection of information is estimated to average 1 hour per response, including the time for reviewing instruction, searching existing data sources, gathering and maintaining the data needed, and completing and reviewing the collection of information. Send comments regarding this burden estimate or any other aspect of this collection of information, including suggestions for reducing this burden to Washington headquarters Services, Directorate for Information Operations and Reports, 1215 Jefferson Davis Highway, Suite 1204, Arlington, VA 22202-4302, and to the Office of Management and Budget, Paperwork Reduction Project (0704-0188) Washington DC 20503.				
1. AGENCY USE ONLY (Leave Blank)		2. REPORT DATE 06-20-2014	3. REPORT TYPE AND DATES COVERED Master's Thesis	
4. TITLE AND SUBTITLE ASSESSING THE OPERATIONAL ROBUSTNESS OF THE HOMER MODEL FOR MARINE CORPS USE IN EXPEDITIONARY ENVIRONMENTS			5. FUNDING NUMBERS	
6. AUTHOR(S) Matthew M. Morse				
7. PERFORMING ORGANIZATION NAME(S) AND ADDRESS(ES) Naval Postgraduate School Monterey, CA 93943			8. PERFORMING ORGANIZATION REPORT NUMBER	
9. SPONSORING / MONITORING AGENCY NAME(S) AND ADDRESS(ES) N/A			10. SPONSORING / MONITORING AGENCY REPORT NUMBER	
11. SUPPLEMENTARY NOTES  The views expressed in this document are those of the author and do not reflect the official policy or position of the Department of Defense or the U.S. Government. IRB Protocol Number: N/A.				
12a. DISTRIBUTION / AVAILABILITY STATEMENT Approved for public release; distribution is unlimited			12b. DISTRIBUTION CODE	
13. ABSTRACT (maximum 200 words)  As the Marine Corps pursues greater energy efficiency in expeditionary operations, the HOMER micropower optimization model provides potential to serve as a powerful tool for improving Marine Corps power planning. The HOMER software was developed for the modeling and simulation of micropower systems over long periods of time. Although a deterministic model, HOMER uses stochastic input data, specifically solar irradiance, temperature, and load profiles. HOMER simulation fidelity is therefore affected by the inter-annual variability of these profiles. This research quantifies HOMER robustness with regard to solar irradiance and temperature profile variability through full-factorial experimental designs. The effect of shortening HOMER simulation duration on the variability of HOMER simulation outputs is also investigated, and though statistically significant, the resulting increase in variability is not large enough to preclude the use of HOMER for expeditionary operations. This thesis also demonstrates how HOMER can assist in developing power planning doctrine, showing that the fuel consumption benefits of using multiple generators of different sizes is no longer present once a renewable energy asset is added to the micropower system. This analysis of HOMER's robustness and operational potential provides insight for improving the Marine Corps' use of HOMER for power planning in an expeditionary environment.				
14. SUBJECT TERMS micropower system, solar irradiance, inter-annual variability, simulation, design of experiments, deterministic model			15. NUMBER OF PAGES 139	
			16. PRICE CODE	
17. SECURITY CLASSIFICATION OF REPORT Unclassified	18. SECURITY CLASSIFICATION OF THIS PAGE Unclassified	19. SECURITY CLASSIFICATION OF ABSTRACT Unclassified	20. LIMITATION OF ABSTRACT UU	

NSN 7540-01-280-5500

Standard Form 298 (Rev. 2-89)  
Prescribed by ANSI Std. Z39-18

THIS PAGE INTENTIONALLY LEFT BLANK



**Approved for public release; distribution is unlimited**

**ASSESSING THE OPERATIONAL ROBUSTNESS OF THE HOMER MODEL  
FOR MARINE CORPS USE IN EXPEDITIONARY ENVIRONMENTS**

Matthew M. Morse  
Captain, United States Marine Corps  
B.S., United States Naval Academy, 2008  
M.S.B.A., Boston University, 2011

Submitted in partial fulfillment of the  
requirements for the degree of

**MASTER OF SCIENCE IN MODELING, VIRTUAL ENVIRONMENTS, AND  
SIMULATION**

from the

**NAVAL POSTGRADUATE SCHOOL  
June 2014**

Author: Matthew M. Morse

Approved by: Daniel Nussbaum  
Thesis Co-Advisor

Eugene Paulo  
Thesis Co-Advisor

Imre Balogh  
Second Reader

Christian Darken  
Chair, MOVES Academic Committee

Peter Denning  
Chair, Department of Computer Science

THIS PAGE INTENTIONALLY LEFT BLANK

## **ABSTRACT**

As the Marine Corps pursues greater energy efficiency in expeditionary operations, the HOMER micropower optimization model provides potential to serve as a powerful tool for improving Marine Corps power planning. The HOMER software was developed for the modeling and simulation of micropower systems over long periods of time. Although a deterministic model, HOMER uses stochastic input data, specifically solar irradiance, temperature, and load profiles. HOMER simulation fidelity is therefore affected by the inter-annual variability of these profiles. This research quantifies HOMER robustness with regard to solar irradiance and temperature profile variability through full-factorial experimental designs. The effect of shortening HOMER simulation duration on the variability of HOMER simulation outputs is also investigated, and though statistically significant, the resulting increase in variability is not large enough to preclude the use of HOMER for expeditionary operations. This thesis also demonstrates how HOMER can assist in developing power planning doctrine, showing that the fuel consumption benefits of using multiple generators of different sizes is no longer present once a renewable energy asset is added to the micropower system. This analysis of HOMER's robustness and operational potential provides insight for improving the Marine Corps' use of HOMER for power planning in an expeditionary environment.

THIS PAGE INTENTIONALLY LEFT BLANK

---

---

# Table of Contents

---

<b>1 Thesis Introduction and Discussion of Marine Corps Energy</b>	<b>1</b>
1.1 Introduction . . . . .	1
1.2 Marine Corps Energy Challenges . . . . .	3
1.3 The Marine Corps Expeditionary Energy Strategy . . . . .	5
1.4 Changing How the Marine Corps Decreases Fuel Consumption . . . . .	8
1.5 Marine Corps Employment of HOMER . . . . .	10
 <b>2 HOMER</b>	 <b>11</b>
2.1 HOMER and Its Potential Marine Corps Application . . . . .	11
2.2 How HOMER Models Micropower Systems . . . . .	13
2.3 Modeling Solar Energy . . . . .	17
2.4 HOMER Model Resource Inputs . . . . .	23
 <b>3 HOMER in Expeditionary Operations</b>	 <b>25</b>
3.1 HOMER Robustness for Expeditionary Operations . . . . .	25
3.2 Solar Irradiance Variability . . . . .	27
3.3 Temperature Variability . . . . .	32
3.4 Effects of Load Profile Variability on HOMER . . . . .	32
 <b>4 Methodology</b>	 <b>35</b>
4.1 Experiment Design . . . . .	35
4.2 Assessing HOMER Robustness with Regard to Solar Irradiance Variation . .	45
4.3 Assessing HOMER Robustness with Regard to Temperature Variability . . .	54
4.4 Accessing the HOMER API . . . . .	57
 <b>5 Analysis and Findings</b>	 <b>59</b>
5.1 Analysis Techniques . . . . .	59
5.2 Analysis of HOMER Robustness with Regard to Inter-annual Solar Irradiance Variability . . . . .	60

5.3	HOMER Fuel Savings Predictions Using TMY3 Profiles Compared to Fuel Savings Predictions Using Measured Solar Irradiance Profiles . . . . .	79
5.4	Analysis of HOMER Robustness With Regard to Inter-Annual Temperature Variability . . . . .	82
5.5	Comparing the Effects of Solar Irradiance and Temperature Inter-annual Variability on the Robustness of HOMER Predictions . . . . .	91
5.6	Using HOMER to Assess Grid-tie versus Standalone Converters for PV Systems . . . . .	93
<b>6</b>	<b>Conclusions, Recommendations, and Future Research</b>	<b>97</b>
6.1	Evaluation of HOMER Model Robustness with Regard to Inter-Annual Variability in Solar Irradiance and Temperature Profiles. . . . .	98
6.2	HOMER Robustness with Regard to Global Dimming. . . . .	101
6.3	Using HOMER to Weigh the Benefits of Different Generator Compositions for a Micropower System . . . . .	102
6.4	Fuel Savings Associated with Existing versus Grid-Tie Capable Converters for the GREENS System. . . . .	104
6.5	Future Work . . . . .	105
	<b>Appendix: ReadMe for the Interface Built to Access HOMER 3.0 API</b>	<b>111</b>
	<b>References</b>	<b>115</b>
	<b>Initial Distribution List</b>	<b>119</b>

---



---

## List of Figures

---

Figure 1.1	GREENS employed with all PV arrays and HELBs, from [11]. . .	7
Figure 1.2	Examples of common Marine Corps equipment the GREENS system can power with associated power requirements, after [11]. . .	8
Figure 2.1	30kW modified seasonal profile . . . . .	15
Figure 2.2	30kW standard seasonal profile . . . . .	15
Figure 2.3	30kW standard profile data map . . . . .	15
Figure 2.4	30kW modified profile data map . . . . .	15
Figure 2.5	Representation of temperature effects on current and voltage in a PV cell . . . . .	21
Figure 2.6	HOMER model equation for calculating PV cell power output . .	21
Figure 2.7	HOMER model equation for calculating PV cell temperature . .	22
Figure 2.8	PV percent power production change for a PV cell with a temperature coefficient of power of -0.336 . . . . .	22
Figure 3.1	Effects of solar irradiance and temperature discrepancies in Major Brandon Newell's 2010 solar panel and HOMER model experiment, from [32]. . . . .	27
Figure 3.2	Monthly temporal CV (percent) of DNI across the United States, 1998-2005, from [33]. . . . .	30
Figure 3.3	Monthly spatial CV (percent) of DNI across the United States, 1998-2005. Seasonal effects are visibly similar to changes in mean temporal DNI CV seen across the seasons and climates of the United States in Figure 3.2, from [33]. . . . .	31
Figure 4.1	The 6 DOE factors, number of levels for each factor, and a brief description of each factor . . . . .	36

Figure 4.2	Generator usage chart, based on 767 historical records of real world 10kW, 30kW, 60kW and 100kW tactical quiet generators. Probability refers to the likelihood of the load equaling the given percentage of peak power, from [16]. . . . .	37
Figure 4.3	Composition of diesel generator and GREENS/SPACES systems factors for DOE energy generation scenarios. "Diesel Generators" refers number of Marine Corps TQGs included in each scenario design. . . . .	38
Figure 4.4	2010 NREL solar irradiance variability report visualization of 1998-2005 solar irradiance variability, adjusted to show the ten locations selected as location factor levels for this research, from [33]. . . .	43
Figure 4.5	Koppen-Geiger climate classification system applied to the continental United States, from [36]. . . . .	44
Figure 4.6	Measurements of long-term GHI that suggest a shift in Europe's solar irradiance trend from global dimming to global brightening, from [38]. . . . .	47
Figure 4.7	Modification of the Wilcox and Gueymard equation for calculating the cumulative GHI CV for each scenario across the available years of data, after [33]. . . . .	49
Figure 4.8	Linear regression plots show the negative linear relationship between years since 1961 and cumulative surface solar radiation for the first 6 months of each year per location. Top row: Albuquerque, Bismarck, Boulder, El Paso; Middle row: Eugene, Madison, Salt Lake City, Seattle; Bottom row: Sterling, Tallahassee . . . . .	50
Figure 4.9	Example demonstrating the effect of different cumulative solar irradiance means on RMSE representation of variability and how CVRMSE removes the effects of different quantities of cumulative solar radiation . . . . .	52
Figure 4.10	The effect of varying means on RMSE representation of variability and how CVRMSE removes these effects of varying means . . . .	53
Figure 4.11	Relationship between scenarios' mean temperature values and variability in temperature in RMSE . . . . .	55



Figure 4.12	Relationship between scenarios' mean temperature values and variability in temperature in RMSE described with a linear fit (left) and described with a quadratic fit (right) . . . . .	56
Figure 5.1	Partition tree showing peak load as the most influential factor in determining RMSE of percent fuel savings with regard to solar irradiance variation effects . . . . .	61
Figure 5.2	Graphical representation of the relationship between scenario peak load and interannual variability in predicted fuel savings . . . . .	62
Figure 5.3	Table shows the maximum PV power available for each scenario relative to the scenario's peak load level . . . . .	63
Figure 5.4	Graph shows strong linear relationship between mean predicted fuel savings and variability in predicted fuel savings for 5kW, 30kW and 60kW scenarios for HOMER prediction variability resulting from inter-annual solar irradiance variability . . . . .	64
Figure 5.5	Partition tree showing differences between peak load scenarios in what qualifies as the second most influential factor in determining RMSE of percent fuel savings with regard to solar irradiance variation effects . . . . .	66
Figure 5.6	The relationship between simulation duration on mean predicted fuel savings and on inter-annual variability in predicted fuel savings . . . . .	67
Figure 5.7	The relationship between simulation start time during the year on mean predicted fuel savings and on inter-annual variability in predicted fuel savings . . . . .	68
Figure 5.8	RMSE of fuel savings versus duration of simulated operation . . . . .	69
Figure 5.9	Relationship between solar irradiance variation (CVRMSE) and predicted fuel savings variation (CVRMSE) relative to duration . . . . .	70
Figure 5.10	Relationship between season of simulation and variation in HOMER predictions of fuel savings . . . . .	71
Figure 5.11	Relationship between season of simulation and variation in Surface Solar Radiation . . . . .	72

Figure 5.12	Seasonal fluctuation in power loads were provided to the HOMER model . . . . .	72
Figure 5.13	Relationship between season of simulation and variation in HOMER predictions of fuel savings, for 15-day and 1-month scenario durations . . . . .	73
Figure 5.14	Effects of climate on inter-annual variability across the seasons, shown for 10kW and 15 day scenarios . . . . .	74
Figure 5.15	Visualization of how inter-annual variability in HOMER fuel savings predictions varies across the four different 10kW micropower system generator compositions for the seven duration levels . . . . .	76
Figure 5.16	Fuel consumed (liters) when micropower system includes GREENS and TMY3 solar irradiance profiles (top) compared to fuel consumed (liters) when using no GREENS systems (bottom) . . . . .	77
Figure 5.17	HOMER predictions of fuel savings to be gained from employing GREENS systems, with savings specified as a percentage of fuel consumed when no GREENS are employed. Graph separates HOMER predictions by duration of scenarios and by scenario generator compositions . . . . .	78
Figure 5.18	Graph shows the difference between fuel savings predictions from employing HOMER with TMY3 solar irradiance profiles and mean fuel savings predictions from employing HOMER with the 50 (1961-2010) annual measured NREL solar irradiance profiles as solar resource inputs. . . . .	79
Figure 5.19	Graph shows the difference between fuel savings predictions from employing HOMER with TMY3 solar irradiance profiles and mean fuel savings predictions from employing HOMER with the 10 annual measured NREL solar irradiance profiles for the years 2001-2010 as solar resource inputs. . . . .	81

Figure 5.20	Graph shows the difference between fuel savings predictions derived from employing HOMER with TMY3 solar irradiance profiles and mean fuel savings predictions from employing HOMER with the 10 annual measured NREL solar irradiance profiles for the years 2001-2010 as solar resource inputs. Graph also shows the difference between fuel savings predictions from employing HOMER with TMY3 solar irradiance profiles and mean fuel savings predictions from employing HOMER with the 50 (1961-2010) annual measured NREL solar irradiance profiles as solar resource inputs. . . . .	82
Figure 5.21	Partition tree with one split identifying scenario peak load level as the most influential factor for inter-annual HOMER fuel savings prediction variability caused by inter-annual mean temperature variability . . . . .	84
Figure 5.22	Graphical representation of the impact of scenario peak load on variability in HOMER percent fuel savings predictions (RMSE) . . .	85
Figure 5.23	Graph shows strong linear relationship between mean predicted fuel savings and variability in predicted fuel savings for 5kW, 30kW and 60kW scenarios for HOMER prediction variability resulting from inter-annual scenario temperature variability . . . . .	86
Figure 5.24	Partition tree showing duration of the scenario to be the second most influential factor on the inter-annual variability of HOMER fuel savings predictions when that variability is due to inter-annual temperature variability . . . . .	87
Figure 5.25	The first split in partition trees associated with each peak load level, identifying duration as the second most influential factor for inter-annual variability in HOMER fuel savings predictions when variability is due to inter-annual temperature variability . . . . .	88
Figure 5.26	Visualization of the relationship between duration and inter-annual variability of HOMER model fuel savings predictions when variability is due to inter-annual temperature variability . . . . .	89
Figure 5.27	The first split in the partition tree identifying start time as the third most influential factor for inter-annual variability in HOMER fuel savings predictions when variability is due to inter-annual temperature variability . . . . .	89

Figure 5.28	Effects of climate on inter-annual variability of HOMER fuel savings predictions due to temperature variability, shown across the seasons for 10kW and 15-day scenarios . . . . .	91
Figure 5.29	Visualization of how inter-annual variability (RMSE) of percent fuel savings differ between HOMER simulations that utilize measured temperature profiles and measured annual solar irradiance profiles ("R" graph) and HOMER simulations that utilize measured temperature profiles and TMY3 solar irradiance profiles ("TMY" graph)	92
Figure 5.30	Visualization of how inter-annual variability (RMSE) of percent fuel savings differ between HOMER simulations that utilize measured temperature profiles and measured annual solar irradiance profiles ("Temp Only"), HOMER simulations that utilize measured temperature profiles and TMY3 solar irradiance profiles ("TempAndSolar"), and HOMER simulations that utilize measured annual solar irradiance files and don't consider temperature effects ("SolarOnly") .	93
Figure 5.31	Mean fuel savings derived from employing the GREENS PV arrays and batteries with the existing standalone converter and without the controller decreasing power provided by the PV arrays . . . . .	94
Figure 5.32	Comparison of mean fuel savings derived from employing the GREENS PV arrays and batteries with a grid-tie capable versus using a standalone converter . . . . .	95
Figure 6.1	Quantifying the variability in HOMER Fuel Savings predictions associated with different duration and peak load levels, when the variability is due to inter-annual solar irradiance variability . . . . .	99
Figure 6.2	Quantifying the variability in HOMER Fuel Savings predictions associated with different duration and peak load levels, when the variability is due to inter-annual temperature profile variability . . . .	100

---

## List of Acronyms and Abbreviations

---

<b>AC</b>	alternating current
<b>AMMPS</b>	advanced medium mobile power sources
<b>AOA</b>	analysis of alternatives
<b>API</b>	application programming interface
<b>C4I</b>	command, control, communications, computers and intelligence
<b>COC</b>	company operations center
<b>COP</b>	company outpost
<b>CSV</b>	comma separated value
<b>CV</b>	coefficient of variation
<b>DC</b>	direct current
<b>DES</b>	discrete event simulation
<b>DHI</b>	diffuse horizontal irradiance
<b>DNI</b>	direct normal irradiance
<b>DOE</b>	design of experiments
<b>DTS</b>	discrete time simulation
<b>E2O</b>	Expeditionary Energy Office
<b>EXFOB</b>	experimental forward operating base
<b>FOB</b>	forward operating base
<b>GHI</b>	global horizontal irradiance
<b>GREENS</b>	Ground Renewable Expeditionary Energy System
<b>HOMER</b>	Hybrid Optimization Model for Electric Renewables
<b>HELB</b>	high energy lithium battery
<b>IED</b>	improvised explosive device
<b>IEEE</b>	Institute of Electrical and Electronics Engineers
<b>ISD</b>	integrated surface data
<b>kW</b>	kilowatt
<b>LED</b>	light emitting diode
<b>LLC</b>	limited liability company
<b>MAGTF</b>	Marine air ground task force
<b>MOP</b>	measure of performance

**MEB** Marine expeditionary brigade  
**MEHPS** Mobile Electric Hybrid Power Source  
**MEM** mobile electric microgrid  
**NASA** National Aeronautics and Space Administration  
**NCDC** National Climatic Data Center  
**NOCT** nominal operating cell temperature  
**NPS** Naval Postgraduate School  
**NREL** National Renewable Energy Laboratory  
**NSRDB** national solar radiation database  
**NTE** nominal terrestrial environment  
**OEF** Operation Enduring Freedom  
**OIF** Operation Iraqi Freedom  
**ONR** Office of Naval Research  
**PV** photo-voltaic  
**RFI** request for information  
**SEED Center** Simulation, Experiment and Efficient Designs Center for Data Farming  
**SPACES** Space Portable Alternative Communications System  
**TAM** time-advance mechanism  
**TMY** typical meteorological year  
**TQG** tactical quiet generator  
**USMC** United States Marine Corps

---

---

## Acknowledgments

---

I would first and foremost like to thank my lovely wife, Melisa, for all her support throughout our time at the Naval Postgraduate School. Her generous support for my thesis research efforts over the last 18 months, even through the workup to our wedding, was invaluable. I would also like to thank the rest of my family, especially my parents, Maureen and Kevin, for enduring and encouraging my constant discussion of Marine Corps logistics and energy concerns.

None of this research would have been possible without the technical expertise of Steve Upton or the statistical analysis insights of Mary McDonald. Steve and Mary, both from the NPS SEED Center, generously donated their time to assist me in executing millions of simulations, organizing and evaluating the simulation outputs, and then rerunning the simulations every time something went wrong. I do not know how they both remained so positive and helpful throughout the process. Their assistance over the last year has been instrumental to the completion of this thesis and has been greatly appreciated.

Lastly, I would like to thank my thesis advisor Dr. Daniel Nussbaum, whose guidance kept me on track while still giving me free rein to focus my efforts where I felt they were needed. He made this thesis research experience positive, fulfilling, and productive.

THIS PAGE INTENTIONALLY LEFT BLANK



---

# CHAPTER 1:

## Thesis Introduction and Discussion of Marine Corps Energy

---

### **1.1 Introduction**

This research provides analysis of the Hybrid Optimization Model for Electric Renewables' (HOMER) robustness and potential application for Marine Corps expeditionary operations. HOMER is one of the few models in existence for the modeling of micropower systems that include both conventional and renewable energy resources. The model is a time-step model developed to analyze long-term life-cycle performance of different micropower systems. This research will investigate areas of concern in the modeling of renewable energy power planning, with an emphasis on solar power. The research will include consideration of the impact of inter-annual variability in solar irradiance and temperature profiles on the robustness of the deterministic HOMER model. HOMER's having been developed and used primarily for evaluation of micropower system long-term performance brings into question whether the model and simulation software is robust enough for simulating relatively short-term Marine Corps expeditionary operations. Through analysis of these areas, this research will assist the Marine Corps in its validation of the HOMER model as a tool for power planning in expeditionary operations.

#### **1.1.1 Scope**

The purpose of this research is to conduct a formal study of the HOMER model as it is tailored for the Marine Corps, to analyze components of the model, and evaluate the robustness of the model. Variability over solar irradiance and temperature profile estimates are expected to be influential on the performance of HOMER supporting expeditionary operations. This research assesses the usefulness of HOMER for Marine logisticians, engineers, and acquisition professionals alike by evaluating the model's robustness with regard to inter-annual solar irradiance and temperature profile variability across multiple factors. These factors include varying the duration, season, and location of simulated micropower systems, where the term "micropower system" refers to "a system that generates electric-

ity...to serve a nearby load [1]." The factors also include varying the size of the electric loads being powered and the composition of generators powering the loads. Along with this analysis of model robustness, this thesis provides recommendations on Marine Corps power planning doctrine. These additional recommendations provide unique insights on the benefits of grid-tie capable converters and the benefits of using multiple generators of different sizes to power a load.

The scope of this research can be more specifically understood by reviewing the research questions for which it provides answers. These research questions are:

1. Is the HOMER software robust enough for modeling and simulating micropower system performance for Marine Corps expeditionary operations, given its primary use for the simulation of long-term micropower system performance?
2. How does inter-annual variability of solar irradiance for a specified location and time frame impact the HOMER model's effectiveness? How do each of the five factors previously mentioned influence the relationship between variability in HOMER estimates and inter-annual solar irradiance variability?
3. How does the variation between National Renewable Laboratory typical meteorological year solar irradiance profiles and measured annual solar irradiance profiles influence the fidelity of HOMER simulations?
4. How does inter-annual variability of the temperature for a specified location and time frame impact the HOMER model's effectiveness? How do each of the five factors influence the relationship between variability in HOMER estimates and inter-annual temperature variability?
5. Does a micropower system composed of multiple generators of different sizes consume less fuel than a micropower system composed of a single peak load capable generator when powering the same load? Does this change when a renewable energy power system is added to the micropower system?
6. Does a grid-tie capable renewable energy power system provide greater fuel savings than a renewable energy power system that is not grid-tie capable?

### **1.1.2 Methodology**

As will be discussed further in Chapter 4, this research was conducted through the execution of two designs of experiments (DOE), utilizing the NPS SEED Center capabilities to support analysis. The first DOE focused on analyzing the robustness of HOMER with regard to solar irradiance values. For this DOE, solar irradiance profiles from 10 locations across the United States were acquired and included as inputs to the HOMER model as varying levels of the "location" factor. Different load profiles were built for each of the load size factor levels and, through the use of the SEED Center, HOMER simulations were conducted for the completion of a full factorial analysis.

The second design of experiments focused on identifying HOMER's robustness with regard to temperature profile robustness. For this analysis, inter-annual variability of temperature profiles was analyzed similar to how the solar irradiance variability was analyzed in the first DOE. Following this DOE, the results of the two DOEs were combined to identify the influence of inter-annual variability of solar irradiance temperature profiles on the variability of renewable energy-derived fuel savings estimates, estimated through HOMER simulations.

Following analysis of the influence of inter-annual variability of solar irradiance and temperature profiles on the HOMER model, analysis was conducted on benefits of grid-tie capable converters and the benefits of using multiple different sized generators to power a load. This additional analysis was conducted through the execution of additional HOMER simulations with an added "generator composition" factor level and comparison of previous DOE simulation output. Now that an introduction to this research has been provided, background information on the Marine Corps energy requirements and the modeling and simulation challenge must be explained before the methodology, analysis, and findings of this research can be presented in detail.

## **1.2 Marine Corps Energy Challenges**

Operation Enduring Freedom (OEF) and Operation Iraqi Freedom (OIF) demonstrated to the Marine Corps that increased employment of technology on the battlefield is paired with a serious challenge to expeditionary capabilities. This challenge comes in the form of an over-reliance on fuel, which shortens the tether between a unit's mobility and its fuel resupply requirements.

At the beginning of OEF and OIF, Marine Corps units deployed to expeditionary combat zones employed Marine Corps generators to meet all base power requirements. These power requirements ranged from lights and computers in Combat Operation Centers (COC) to camera systems and floodlights employed in support of base security. Over the course of the Iraq and Afghanistan wars, the Marine Corps saw an increased energy consumption by Marine Corps units. In 2011, the Marine Corps Expeditionary Energy Office (E2O) stated that the amount of fuel required for an average Marine company to execute a three-day patrol had increased from 160 Watts in 2001 to 1255 Watts in 2011, an increase of 684 percent [2]. This increased energy requirement resulted in a subsequent increased reliance on internal combustion generators and diesel fuel. The increased energy consumption was due to increases in warfighting capabilities with "enhancements to command, control, communications, computers, and intelligence (C4I) technologies; hardened vehicles, and weapon systems [3]." From 2001 to 2011, the Marine Air Ground Task Force (MAGTF) number of radios, computers, and vehicles increased by 250, 300, and 200 percent, respectively [3]. In the extreme Afghanistan climates 60 percent of Marine Corps power production was dedicated to just keeping these C4I systems cool enough to operate [3].

To support the energy requirements for these technology advances and equipment increases, the number of internal-combustion generators in the Marine Corps tripled between 2001 and 2013, rising from 4,000 to more than 13,000 [4]. The amount of fuel consumed by deployed Marine Corps units also increased linearly as the dependency on generators increased.

Increased fuel consumption needs of a given unit can be met either by increasing the fuel capacity of the unit or by increasing the number of fuel resupply missions executed by supporting units. Increasing capacity can decrease the unit's maneuverability and is often an untenable solution due to manning and equipment limitations. That is, battlefield mobility requirements limit the fuel capacity of individual Marine Corps unit positions. Units that require a capability of being mobile can only store as much fuel as they can carry with them on fuel transport trucks when it comes time to move. The amount of fuel consumed by a unit, therefore, directly relates to the number of logistics convoys required for support. To give perspective to the transport requirements for fuel, one 7-ton truck can carry 800 gallons of fuel and requires two to three Marines to man.

Increasing the number of fuel resupply missions required can tether the unit more to the supporting units and similarly decrease maneuverability. Increasing the number of fuel resupply missions to support a unit also increases force protection risks. In the recent Afghanistan and Iraq wars, this force protection risk was manifested in the improvised explosive devices (IED) employed by insurgents against coalition convoys. In 2012, the Secretary of the Navy reported to Congress that "for every 50 fuel convoys in theater, there is one Marine casualty [5]." Recognizing the importance of the energy issue, the Commandant of the Marine Corps, General James T. Conway, stood up the Expeditionary Energy Office in 2009 to "analyze, develop, and direct the Marine Corps' energy strategy in order to optimize expeditionary capabilities across all warfighting functions [6]." Two years later General Conway's successor, General James F. Amos, presented a Marine Corps strategy to tackle the challenges fossil-fuel dependency brings to the Marine Corps' expeditionary nature.

### **1.3 The Marine Corps Expeditionary Energy Strategy**

General Amos published the Marine Corps Expeditionary Energy Strategy on March 21, 2011. In this energy strategy, the Commandant of the Marine Corps set an objective of making 50 percent of Marine Corps bases "net-zero energy consumers" by 2020 [7]. In 2011, fuel consumption in Afghanistan was estimated at 8 gallons per Marine per day [8]. In the Expeditionary Energy Strategy, General Amos focused on the deployed environment and called for a 50 percent reduction in fuel consumption per Marine down to 4 gallons per Marine per day [3]. The Marine Corps reduction in fuel consumption will result not only in increased maneuverability and sustainability, but also a reduction in fuel-supply related casualties.

To accomplish this reduction in fuel consumption, the Marine Corps first focused on reducing the fuel consumption of forward operating bases (FOB). The Marine Energy Assessment team identified that 32 percent of fuel consumed by the Marine Expeditionary Brigade (MEB) deployed to Afghanistan in 2009 was used for electric power generation [9].

#### **1.3.1 EXFOB and Marine Corps Renewable Energy Technology**

Through the efforts of E2O, the Office of Naval Research (ONR), and their interaction with industry, the Marine Corps has developed robust, renewable technologies to meet the

energy objectives laid out in the Commandant's energy strategy. Through E2O, the Marine Corps has investigated energy solutions in such areas as photo-voltaic (PV) arrays for power harvesting, light emitting diodes (LED) for decreased energy consumption, and improved battery and smart power controller technologies for better energy management.

One forum that has been particularly useful in advancing Marine Corps renewable energy research and development has been the Marine Corps' Experimental Forward Operating Base (EXFOB). The EXFOB is an annual event established by the Commandant of the Marine Corps in 2009 that "brings together stakeholders from across the Marine Corps requirements, acquisition, and technology development communities in a dynamic process to quickly evaluate and deploy technologies that reduce our need for 'liquid logistics' today, and to establish requirements for tomorrow [10]." In the annual EXFOB Request For Information (RFI) document, E2O identifies for industry the particular area(s) of interest for a given year's EXFOB. The 2014 EXFOB was announced as focusing on tactical energy harvesting. In 2009 the first EXFOB immediately began yielding renewable energy technologies that were rapidly and successfully pushed through development, testing, and fielding to the war fighter. Two of the E2O's most notable and widely deployed technologies, the Ground Renewable Expeditionary Energy System (GREENS) and Space Portable Alternative Communications Energy System (SPACES) systems, were part of this first EXFOB.

### **1.3.2 Marine Corps PV Systems**

One of the most successful renewable energy assets developed by the Marine Corps is the GREENS. The GREENS is a power generation and conversion system that allows Marines to power systems with solar energy. Each GREENS is composed of eight PV array panels, four High Energy Lithium Batteries (HELB), and a central controller. Figure 1.1 shows how all components of a GREENS are combined to harvest solar power, receive alternating current (AC) and direct current (DC) power, employ the HELB batteries, and to provide DC output for a load. While a single GREENS can provide 300 watts of power for 24 hours or 1000 watts of peak power, GREENS systems are modular and can be combined into as large as a five GREENS system, providing up to 1500 watts of continuous power [11]. The GREENS' modular design also allows the user to employ fewer than the full 8 solar panels and fewer than the full four HELB batteries if desired, to configure the GREENS to meet

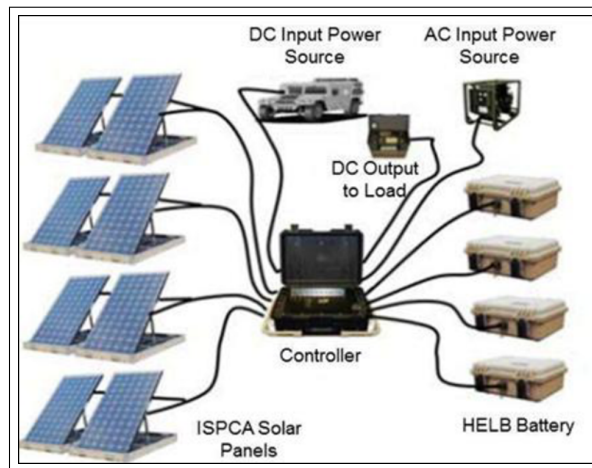


Figure 1.1: GREENS employed with all PV arrays and HELBs, from [11].

smaller load requirements. The first GREENS unit was tested in July 2009 and fielded by 2012 [12].

Another solar power generation asset developed by the Marine Corps at the same time as the GREENS was the SPACES. The SPACES is much smaller, lighter, and less powerful than the GREENS. Powered by two (12) volt folding portable solar panels a single SPACES is designed to recharge two BB-2590 lithium batteries or power battery operated devices such as laptops or radios [13]. Some basic specifications for the SPACES and GREENS can be found in the Marine Corps Technical Manual TM 12359A-OD: Principal Technical Characteristics of Expeditionary Power Systems Equipment; more detailed specifications can be requested from the ONR or E2O [14].

### 1.3.3 Fielding of the GREENS and SPACES Systems

The rapid development and fielding of the GREENS and SPACES demonstrated the Marine Corps' drive to leverage cutting edge renewable energy technology on the battlefield. One of the near-term materiel incentives specified in the United States Marine Corps (USMC) Expeditionary Energy Strategy and Implementation Plan's Implementation Planning Guidance is the initiative to "lead in deploying innovative energy solutions [3]." This initiative represents the Marine Corps objective of not only developing energy technologies but rapidly fielding them to the warfighter. The GREENS and SPACES systems exemplify

Equipment	Average Hourly Power Required (W)	Peak Power Required (W)
Motorola Battery Charger	50	200
VRC-110 w/Blue Force Tracker	165	440
PRC-150	57	375
Coffee Pot	45	975

Figure 1.2: Examples of common Marine Corps equipment the GREENS system can power with associated power requirements, after [11].

this rapid development and fielding approach. Fielding began in 2012 and only four years after the Commandant of the Marine Corps announced the Marine Corps Energy Initiative, Colonel Roberto Charette, former director of the E2O, asserted in 2013 that both the GREENS and SPACES systems were "available to all Marines in the Marine Corps [15]."

## 1.4 Changing How the Marine Corps Decreases Fuel Consumption

There are two general approaches for employing renewable energy technologies to reduce fuel consumption. The first technique includes decreasing the peak levels of a load by removing components of that load and powering them separately with renewable energy technology such as PV arrays, batteries and wind turbines. To ensure reliable availability of power, this will usually also include using a conventional generator as a backup to supply power in times of poor weather. The Marine Corps currently employs the GREENS in this way. The GREENS controller, which limits output from the PV arrays to 1kW, helps to ensure that Marines employing the system do not over extend the system by expecting a consistent provision of 1.76 kW from the arrays, which is the peak amount of energy the eight PV panels are capable of producing. With the GREENS limited by the controller to providing 1 kilowatt (kW) of power, the system is capable of powering common Marine Corps equipment such as those shown in Figure 1.2.

The second approach for employing renewable energy to decrease fuel consumption includes employing the renewable energy technologies to decrease the operating time of



an AC generator(s) covering the load. This combines the generator and renewable energy source into a hybrid system that passes the load between renewable power source and diesel generator depending on load size and renewable power production. In many situations, this method of employing a renewable energy technology can do more to decrease fuel consumption and allow for higher generator operating efficiency than the first technique described. Recognizing the efficiency of this method of renewable energy employment approach, the Marine Corps made hybrid systems the focus of the 2013 EXFOB. This investigation of the potential for hybrids was referred to as the Mobile Electric Hybrid Power Sources (MEHPS) Analysis of Alternatives (AOA) and sparked the pursuit of MEHPS technologies for the Marine Corps.

#### **1.4.1 EXFOB 2013: MEHPS AOA**

Following the Marine Corps' success in the fielding of the GREENS and SPACES system, the Corps continued to push forward to exploit tactical and logistic opportunities available in renewable energy technology development. While the early EXFOBs succeeded in developing renewable technologies for powering small loads of up to 1kW, with EXFOB 2013 the Marine Corps began its pursuit of hybrid systems capable of powering 3kW to 300kW loads [16]. The U.S. Army and Marine Corps teamed up to develop the hybrid systems and divided the task of developing the systems between the two services. While the Army has the lead in development of the 10 to 300kW systems, referred to as Mobile Electric Microgrids (MEM), the Marine Corps has the lead in the development of the "smaller hybrid systems (up to 10kW) [17]." It should be noted that while this thesis refers to stand-alone systems composed of power generation assets meeting a load as micropower systems, the Marine Corps classifies these systems differently, depending on the size of the system's peak load capability. Systems supporting an electric load less than 10kW are classified within the Marine Corps as hybrid power systems. Systems supporting an electric load greater than 10kW are classified as microgrids. For this thesis, to avoid confusion, all hybrid power systems and microgrids are referred to simply as micropower systems.

These hybrid systems, or MEHPS, will provide the next step for decreasing fossil fuel consumption by forces in an expeditionary environment. MEHPS hybrid systems also have potential for decreasing generator maintenance issues that result from generators operating with too low of power loads. One such maintenance issue, called "wet-stacking," is

seen when generators operate with loads well below optimum levels and results in "coke formation and gumming of the engine [18]." To meet larger loads of 3kW to 10kW while leveraging renewable energy, the MEHPS systems take the approach of passing the load between the renewable power source and diesel generator depending on the load size and renewable power available at a given time. This passing of the load automatically between power sources is accomplished through the use of smart grid technology. By combining "smart controls, energy storage, and solar PV with traditional diesel generators," these MEHPS systems can significantly decrease generator run time, preventing generator wet-stacking and decreasing fuel consumption [17]. Following EXFOB 2013, reductions in generator run time through the use of MEHPS systems were seen as high as 80 percent and fuel consumption reductions were seen as high 50 percent [17].

## **1.5 Marine Corps Employment of HOMER**

Beyond the renewable technologies and hybrid systems themselves, another renewable energy tool the Marine Corps has pursued as part of its energy strategy is the HOMER model. While several expeditionary, renewable energy assets have been developed, the users lack a capability for predicting the fuel consumption rates associated with the renewable energy hybrid systems. What is now needed to decrease fuel consumption is a tool that will assist Marine Corps power planners and logisticians in anticipating the fuel consumption savings to be gleaned from employing hybrid systems to support a given load requirement for a particular location and time frame. Understanding how to optimize renewable energy power production is necessary for Marine Corps logisticians and engineers to optimally design micropower systems with hybrid power generation technologies and modular renewable technologies. As a hybrid optimization model for electric renewable technologies, HOMER has the potential to fulfill this need for the Marine Corps. In order to understand the potential benefits and uncertainties associated with employing the HOMER model in support of expeditionary operations, the inner workings of the HOMER model must be understood. Chapter 2 will provide insight into how HOMER models micropower systems and the performance PV arrays as well as the model's origin and general applications.

---

## CHAPTER 2:

## HOMER

---

### **2.1 HOMER and Its Potential Marine Corps Application**

HOMER is a deterministic, time-step model that models micropower systems. It can model systems including both conventional, diesel powered generators and renewable power sources such as photovoltaic arrays and wind turbines.

HOMER has been utilized for years by organizations and companies across the globe to assist them in their cost-effective employment of renewable energy sources and appropriately sizing generators for the long-term powering of facilities. There is potential for HOMER to serve as a useful Marine Corps Modeling and Simulation tool for optimizing expeditionary micropower systems. To be useful for modeling expeditionary micropower systems, HOMER must provide system fuel consumption estimates with relatively low variability across a wide range of locations, micropower system compositions, and load profiles for short-term operations.

#### **2.1.1 HOMER's Origin**

The U.S. National Renewable Energy Laboratory (NREL) developed HOMER in 1993 as a part of its Village Power Program. The model was designed to assist users in designing micropower systems and modeling their performance under specific conditions. Although originally built only for consideration of off-the-grid micropower systems, the model was updated in 2000 to accommodate the modeling of grid-tied systems as well. The HOMER application simulates and measures the performance of each power generation asset, whether available individually or in hybrid configurations. In this way, the model is used to identify the most cost-efficient micropower system design for meeting long term electric load requirements.

#### **2.1.2 Discrete Time Simulations**

HOMER is a type of model known as a Discrete Time Simulation (DTS) model, meaning it employs a time-advance mechanism (TAM) driven by time-steps. Understanding TAMs,

and DTS models in particular, will assist in understanding potential strengths and weaknesses of the HOMER model. TAMs are methods used in modeling and simulation for representing time and its effects in the system being simulated. Three primary components employed for the representation of time advance: the states of variables or entities, the events that change those states, and the methods for timing those events. By using these components for the representation of time, models using TAMs can represent complex, dynamic systems. While DTS models use the time-step driven TAM, another type of model known as the Discrete Event Simulation (DES) uses an "event-driven" TAM method [19].

For the timing of events, DES models use an "event list," where future scheduled events are populated on the event list as they are scheduled by state changes (events). In DTS, or time-step, simulations, events are not scheduled by using events to populate future events on event lists. Instead, states are evaluated on a recurring basis at a specified time intervals, with events depending on the status of the states at those times. The "time step" is the interval of time between evaluating states and executing appropriate events. While both DTS and DES models are valid modeling and simulation tools, modeling and simulation professionals must be careful in determining which technique to employ and in what way. There are potential problems with both TAM methods that must be considered to prevent or mitigate particularly detrimental effects.

An example of a well-known issue seen with the time-step method is the "bullet through paper" problem, an issue referred to as "skipping" in the Naval Postgraduate School (NPS) thesis "The Effect of Time Advance Mechanism in Modeling and Simulation [19]." As the name implies, this issue refers to the problems associated with modeling a bullet hitting a piece of paper using a time-step model. The "impact" of the bullet hitting the paper can easily be modeled by a non-time step DES model because the event list assigns the event to occur at that specific time calculated for impact. When representing this event through time step, however, the model will represent two states, the state with the bullet on one side of the paper and a following state with the bullet on the other side of the paper, not represent the impact. This example may be confused as applicable only to physics models, but this "bullet through paper" problem can apply to non-physics modeling tasks as well.

Another concern with employing the time-step technique is that there is no consideration for the ordering of events for those events occurring within the same time step. One way

that time-step models are often evaluated, and a way in which this particular concern could be addressed, is the analysis of the simulation time-step interval size. Researchers vary the size of the time-step and analyze how those changes affect the output of the model. The time step selected for a model is an important consideration because "too large a time step introduces errors in the model, while too small a time step may cause extremely large run times [20]." The HOMER model graphical user interface (GUI) allows users to change the size of the time-step in terms of minutes. As will be seen in later sections of this thesis, limitations on the fidelity of solar irradiance data and input profiles makes time steps of less than an hour impractical with regard to reflecting changes in solar irradiance and temperature values. That being said, future analysis of the HOMER model could be useful in identifying how changes to the time-step size affect simulations' representation of generator operating times and the duration battery charging/discharging.

Statistician George Box once famously stated that "all models are wrong, but some are useful [21]." It is the responsibility of the modeling and simulation professionals to understand how the models they employ are wrong. This leads to considerations of model classifications as being either stochastic or deterministic. This is of particular importance when considering the HOMER model because although the HOMER model evaluates solar power on the basis of stochastic solar irradiance inputs, the model itself is deterministic. This is a third area requiring greater research, and is a primary focus of this research.

## **2.2 How HOMER Models Micropower Systems**

The HOMER engine is the component of the software that models the performance of a given micropower system with a particular scenario including a set of inputs, such as load, temperature, and solar irradiance profiles. The model engine is separate from the optimization software which iterates through the different power generation assets and identifies all possible combinations for analysis.

### **2.2.1 Micropower Systems and Load Profiles**

In many situations a "micropower system" refers to a power generator, such as a diesel generator, that is smaller than the average scale. In the context of the HOMER model and this thesis, the term "micropower" refers to the provision of power to electric devices using local power generation assets, that is to say, off the grid. A micropower system,

therefore, refers to the system of power generation devices (solar arrays, generators, wind turbines, etc.), energy storage apparatuses (batteries), and connective wiring that provides the required energy for that load in the form of electricity.

A load profile is a representation of the energy consumed by a piece or pieces of equipment in specified increments of time over a specified amount of time. In the HOMER model, load profiles of micropower systems are input by the user in one-hour increments, matching the one-hour time steps of the discrete event simulation. Each value in a load profile is the sum of energy, in kW that is drawn from the power sources (generators, batteries, PV arrays, etc.) during the specified hour.

Load profiles can be loaded in one of two ways in HOMER. First, the user can specify a generic one-day load profile for weekdays and weekend days of a given month. In using this option of load profile specification, the user can either keep weekday and weekend daily load profiles the same, or can account for some difference in micropower system operation over the weekend by making the daily load profiles unique. When the user specifies the weekday/weekend daily load profiles for each month the HOMER GUI assigns that daily load profile to every weekday/weekend day in the month. The second option, and the option used to support this research, is loading a single Comma Separated Value (CSV) file consisting of 8760 values. These 8760 values provide the micropower system's load, in kW, for every hour of a year.

If the HOMER model is run in a retrospective study of a system's performance, the actual load profile of the micropower system can be measured during the experiment and then loaded into the HOMER model in the form of a CSV file. Often this is not the case though, and HOMER is employed to analyze expected future micropower system performance. To conduct this analysis, the user must provide the model with a load profile that represents anticipated future load requirements of the micropower system in question. This research falls into the second category, HOMER's employment to analyze expectations of future performance across multiple factors. Because of this, the load profiles used in this research are not measured values but are instead extrapolations based on historical data. To analyze HOMER's capabilities for to the Marine Corps' needs, I utilized a modification of the load profile design used in the E2O's MEHPS AOA [16]. This load profile design is meant to represent the load profile of a typical Marine Corps unit of a specified peak power capacity.

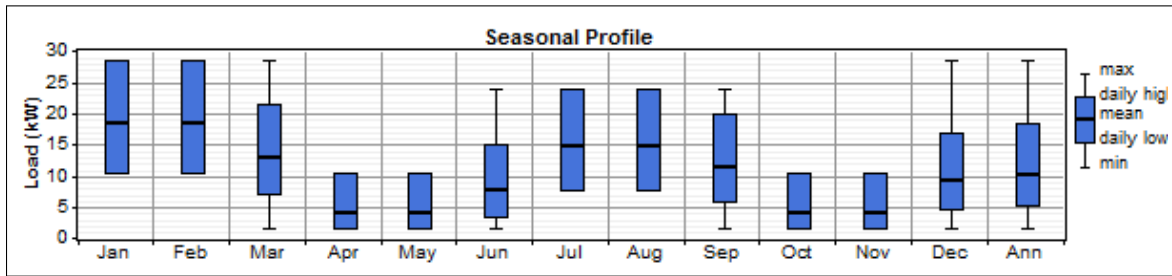


Figure 2.1: 30kW modified seasonal profile

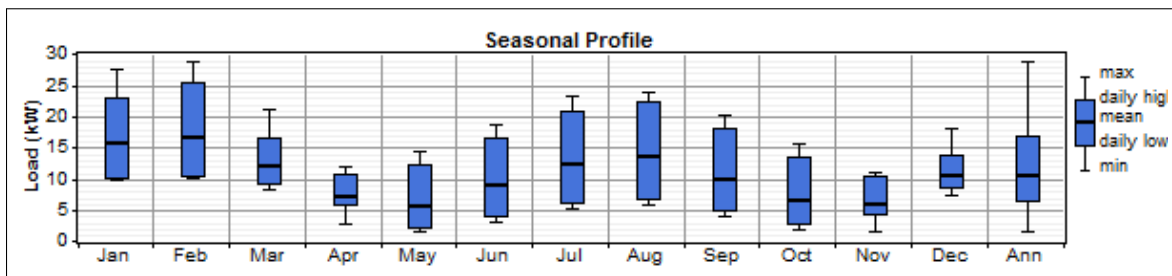


Figure 2.2: 30kW standard seasonal profile

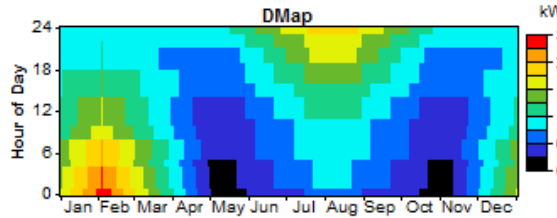


Figure 2.3: 30kW standard profile data map

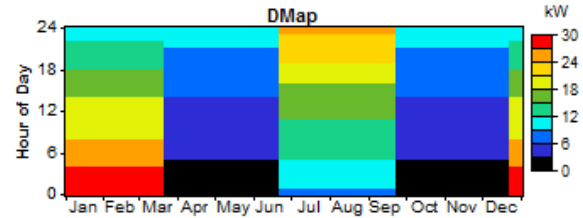


Figure 2.4: 30kW modified profile data map

The profile used in the MEHPS AOA, shown in Figure 2.1, splits the year up into four seasons and assigns a set load profile for each day of the season. The load profile is specified as a percentage of peak power. The above visualization of a standard load profile, Figure 2.1, was created using the HOMER GUI and represents the projected annual load profile of a 30kW peak power. This load profile, utilized by the Marine Corps for the MEHPS AOA, allocates the same load profile values to every day of the season, with an immediate change in the load profile values upon reaching the next season. These changes in load profiles show how power demands change for different seasons throughout the year, but they show

the shift in load profiles as occurring instantaneously. The winter and spring load profiles, for example, suggest that the day the season shifts from winter to spring the first hour of the load profile will shift from a load of approximately 82 percent to a load of 5 percent. This is not a realistic representation of how load profiles change throughout the year; season changes and their associated effects on load profiles are not immediate, but gradual.

For this research, the MEHPS load profile product was modified to reflect the gradual nature with which seasons change. This modified load profile was created by interpolating daily load profiles between the seasons. Season midpoints were set as the dates equidistant between the summer and winter solstices, and the autumnal and vernal equinoxes for the respective seasons [22]. For instance, load profiles constructed throughout the month of April, which lies between the vernal equinox and summer solstice, were constructed by combining varying percentages of spring and summer load profile levels. These four season midpoints were set to have load profiles equal to the MEHPS load profiles. The load profiles for the rest of the 361 days of the year were calculated by combining the load profiles for the season midpoints before and after the selected date. The season midpoints were combined with weights relative to the given date's distance from each season midpoint date. The modified load profile is shown in Figure 2.2. While the two seasonal profiles, Figure 2.1 and Figure 2.2, show very similar annual profiles by month, the Data Maps, Figure 2.3 and Figure 2.4, demonstrate how blending the load profile values provides a more realistic representation of a load profile's progression through the seasons.

### **2.2.2 Defining Micropower Component Specifications**

Modeling of micropower systems with the HOMER model includes not only quantifying the load profile, but also identifying the number and characteristics of power generation and storage equipment that comprise the system. These pieces of equipment can include internal combustion generators, battery banks, power converters, PV arrays, and other types of renewable energy equipment. The technical specifications for each piece of equipment are either pre-loaded into the HOMER GUI, if it is a common piece of equipment, or are specified by the user building the scenario for simulation. The technical specifications allow the HOMER model to determine the amount of power different pieces of equipment can generate, store, or convert for each time-step of the simulation. Specifications for the internal combustion generator include generator size (kW), minimum load ratio (percent),



and whether it is an AC or DC generator. Generator specifications also include the fuel type utilized and values necessary for demonstrating the efficiency curve of the fuel, including the fuel curve intercept coefficient and slope.

Modeling a PV array in the HOMER model requires specifying the size of the array (kW), the array output current (AC or DC), and the expected lifetime of the array. The HOMER model also requires users to specify properties related to the employment of the PV array. These include a derating factor (percent) associated with the panel, the slope (degrees) and azimuth with which the PV array is employed. A solar panel's derating value is defined by HOMER as "a scaling factor meant to account for effects of dust on the panel, wire losses, elevated temperature, or anything else that would cause the output of the PV array to deviate from that expected under ideal conditions [1]." If the user decides to include the effects of temperature on the PV array in the model, PV array technical specifications also include the temperature coefficient of power, NOCT, and efficiency at standard test conditions for the array. The importance of each of these values and how they assist the model in forecasting PV energy production will be discussed in the next section as the inner workings of PV cells are explained. Further information on the modeling of micropower components in the HOMER model and their technical specifications can be found in chapter 15 of the book *Integration of Alternative Sources of Energy*, titled "Micropower System Modeling with HOMER [1]."

## **2.3 Modeling Solar Energy**

### **2.3.1 Solar Energy Modeling in the Solar Industry**

Anticipating the performance of solar energy systems requires an ability to anticipate the solar resource available. For years the solar industry has relied upon NREL's Typical Meteorological Year (TMY) data set for modeling the performance of solar power systems [23]. A TMY is a statistically derived profile of a typical meteorological year for certain locations across the United States. NREL's TMY data consists of hourly measurements of solar irradiance and certain meteorological elements and has been updated three times since its establishment in 1978 by Sandia National Laboratories [24]. The current TMY, TMY3, was created with measurements acquired from 1976 to 2005. TMY3 data is meant to be used for simulation of solar power systems over "a longer period of time, such as 30 years [24]."

In fact, the first page of the TMY3 User Manual warns in italics: "The TMY should not be used to predict weather for a particular period of time [24]."

If the user inputs solar irradiance profiles in terms of average monthly irradiance values, the HOMER model uses the Graham-Hollands algorithm to produce a synthetic hourly solar irradiance profile based on the average solar irradiance value. The Graham-Hollands algorithm, developed in 1990, allows HOMER to create a synthetic solar irradiance profile that estimates the "likely magnitudes of random fluctuations" in solar irradiance [25]. This algorithm allows the HOMER model to be used even when the user cannot obtain a TMY solar irradiance profile or measured hourly solar irradiance profile.

### **2.3.2 The Basics of PV Cells**

To understand how PV arrays produce power, and the effects of solar irradiance and temperature on them, one must first understand some basics of semiconductors, the process of doping, and the structure of PV cells. The following descriptions are abridged explanations providing only so much insight as is necessary for the purposes of this thesis.

PV cells can be made of either specific elements, such as silicon, or compounds, but the material must be a semiconductor. Semiconductors are materials with lower electrical conductivity than conductors and higher conductivity than insulators. Conductivity is determined by the material's number of free electrons and its number of holes, where a hole is simply "the absence of an electron [26]." A high level of conductivity means having a high number of free electrons or a high number of holes. A pure semiconductor has a relatively low conductivity due to the absence of naturally occurring free electrons or holes.

Free electrons are established in a semiconductor, creating a potential for current flow, by applying energy, which breaks covalent bonds between the semiconductor's atoms or molecules. The amount of energy required to achieve this break is known as the band gap energy. Breaking the covalent bonds also creates a hole for every electron that is freed. While the breaking of covalent bonds must occur for increasing potential current flow, semiconductors must also undergo a process called doping to be used in PV cells.

Doping is the application of an element or compound to a PV cell's semiconductor that increases either the number of holes or the number of free electrons in the semiconductor.

To do this, the applied material must have either greater or fewer electrons in its valence level than does the PV cell's semiconductor. Semiconductors doped with a material having fewer electrons in its valence level than the semiconductor have an increased number of holes and are known as p-type semiconductors. Similarly, those semiconductors doped with materials having more electrons in its valence level than the semiconductor have a higher number of free electrons and are known as n-type semiconductors. This distinction is particularly important for understanding the construct and operation of PV cells.

Having identified the construct of semiconductors, the concept of how PV cells generate electricity is relatively easy to explain. When sunlight strikes a PV cell, power is generated through photogeneration. Brian Sullivan explains how the process of photogeneration works in his NPS thesis addressing temperature effects on PV cells:

Photons from the source of light enter the semiconductor material when they contain energy equal to or greater than the band gap of the material and transfer enough energy to electrons in the valence band to cause them to move to the conduction band. This transfer of energy, therefore, creates electron-hole pairs...as electron pairs appear, the electric field of the depletion region causes the carriers to separate to opposite ends of the material...The flow of carriers to opposite ends of the device creates a current in the material and a voltage differential on the two ends [26].

Greater detail on the construct of PV cells and the semiconductors that they are composed of can be found in the 2010 thesis, "The Effect of Temperature on the Optimization of Photovoltaic Cells Using Silvaco ATLAS Modeling," by Sullivan [26]. Sullivan's thesis also provides insight into the effects of ambient temperature levels on the performance of PV cells, a relationship which will now be discussed in this thesis as well.

### **2.3.3 Temperature Effects on PV Cell Performance**

Changes in a PV cell's operating temperature affect the power production of the PV cell, with increases in PV cell temperature resulting in a net decrease in cell power production. This relationship can be explained in terms of current and voltage changes relative to cell temperature, with temperature increases resulting in a slight increase in current and a much

larger relative decrease in voltage. In order to understand the HOMER model's representation of temperature effects, this relationship between temperature and PV cell performance will be explained in this section.

Between current and voltage effects, the less significant effect of temperature change is the impact on current. Several different elements, or compounds, can be used for constructing PV cells, and these different materials have different band gap energy levels. Increases in operating cell temperatures increase the thermal energy provided to the semiconductor and decrease the amount of radiant energy required to reach the band gap level. The addition of this thermal energy due to increased cell temperature is what increases short-circuit current flow in the PV cell, given a constant solar irradiance, "but only slightly [27]." The increase in current is minimal when compared to the effects temperature has on PV cell open-circuit voltage [27].

While increases in cell operating temperature slightly increase the cell's short-circuit current, increases in cell temperature also increase the resistivity of components within the PV array and thereby decrease the voltage produced by the PV cell [26]. The decrease in PV cell voltage due to temperature increases is much greater than the relative increase in current. This disparity between temperature effects on current and voltage results in a negative linear relationship between PV cell operating temperature and PV cell power production. Figure 2.5 provides a graphical representation of the relationship between PV cell temperature, current and voltage [28].

The relationship between temperature and PV cell power production is quantified through the specification of a nominal operating cell temperature (NOCT) and a temperature coefficient of power for every PV cell. The NOCT specifies the "temperature of [the PV cell] at the conditions of the nominal terrestrial environment (NTE)," which includes  $800 \text{ W/m}^2$  for solar irradiance, an ambient temperature of 20 degrees Celsius, and an average wind speed of  $1 \text{ m/s}$  [29]. The temperature coefficient of power specifies "how strongly the PV array power output depends on the cell temperature" and is a negative value due to the negative linear relationship between operating temperature and power production for PV cells [30].

The HOMER model simulates the effects of temperature on a PV cell's performance at

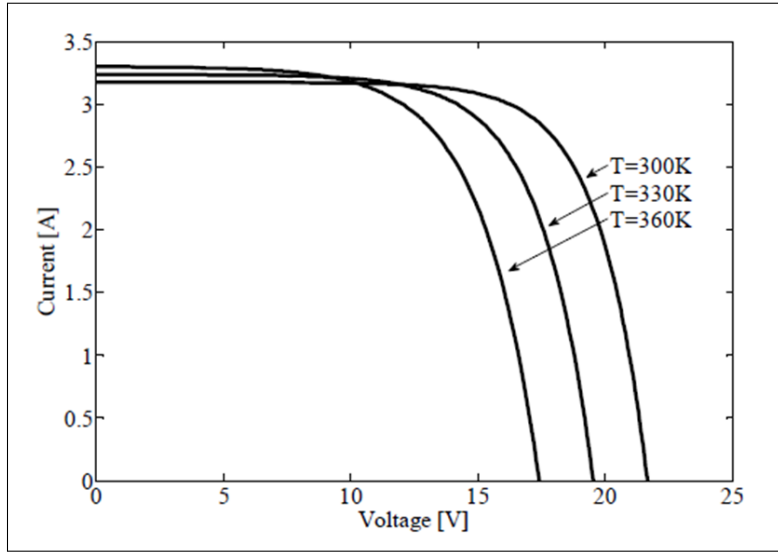


Figure 2.5: Representation of temperature effects on current and voltage in a PV cell

PV Cell Power Production: 
$$P_{PV} = Y_{PV} f_{PV} \left( \frac{\bar{G}_T}{\bar{G}_{T,STC}} \right) [1 + \alpha_p (T_c - T_{c,STC})]$$

where:

- $Y_{PV}$  is the rated capacity of the PV array, meaning its power output under **standard test conditions** [kW]
- $f_{PV}$  is the **PV derating factor** [%]
- $\bar{G}_T$  is the **solar radiation incident on the PV array** in the current time step [kW/m<sup>2</sup>]
- $\bar{G}_{T,STC}$  is the incident radiation at **standard test conditions** [1 kW/m<sup>2</sup>]
- $\alpha_p$  is the **temperature coefficient of power** [%/°C]
- $T_c$  is the **PV cell temperature** in the current time step [°C]
- $T_{c,STC}$  is the PV cell temperature under **standard test conditions** [25 °C]

Figure 2.6: HOMER model equation for calculating PV cell power output

each time step of the simulation. The model calculates PV cell temperature and models the effects of this temperature on the cell's power production for each time step. The model uses user-specified NOCT and temperature coefficient of power specifications for the given PV cell to calculate the temperature effects on power production. The HOMER GUI identifies Figure 2.6 as the equation used by the model to determine the power production for a given PV cell.

The PV cell temperature in this equation includes the temperature effects of both ambient temperature and the increased temperature derived from solar radiation striking the cell. Figure 2.7 shows the HOMER GUI-provided equation showing how the HOMER model

PV Cell Temperature:	$T_c = T_a + G_T \left( \frac{\tau \alpha}{U_L} \right) \left( 1 - \frac{\eta_c}{\tau \alpha} \right)$
where:	
$\tau$ is the <b>solar transmittance</b> of any cover over the PV array [%]	
$\alpha$ is the <b>solar absorptance</b> of the PV array [%]	
$G_T$ is the solar radiation striking the PV array [kW/m <sup>2</sup> ]	
$\eta_c$ is the electrical conversion efficiency of the PV array [%]	
$U_L$ is the coefficient of heat transfer to the surroundings [kW/m <sup>2</sup> °C]	
$T_c$ is the PV cell temperature [°C]	
$T_a$ is the ambient temperature [°C]	

Figure 2.7: HOMER model equation for calculating PV cell temperature

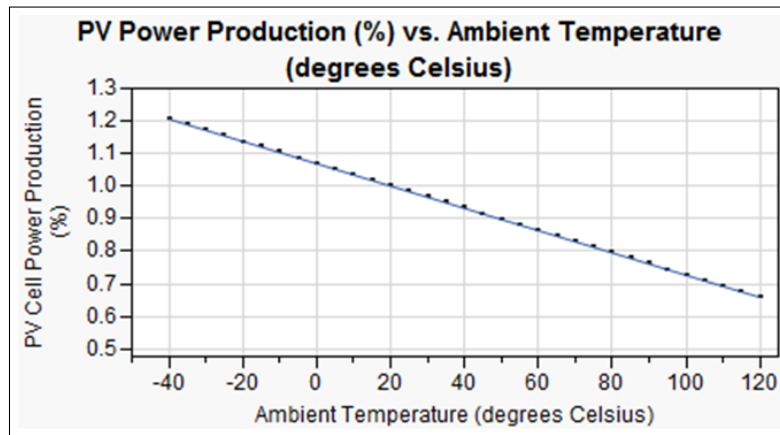


Figure 2.8: PV percent power production change for a PV cell with a temperature coefficient of power of -0.336

calculates the PV cell temperature based on ambient temperature and the temperature effects of solar irradiance. When considering the effects of ambient temperature changes alone, a PV cell's power production percent change that results from ambient temperature change can be determined by multiplying the temperature delta by the temperature coefficient of power. An example of how ambient temperature affects percent power production can be seen in Figure 2.8. This figure shows how a PV cell with a temperature coefficient of power of -0.00336 has a PV power production decrease of .336 percent for every degree Celsius that ambient temperature increases and an increase in power of 0.336 percent for every degree Celsius that ambient temperature decreases.

## **2.4 HOMER Model Resource Inputs**

### **2.4.1 Solar Resource Input**

"Solar resource" refers to the amount of global horizontal solar irradiance (GHI) that the specified location receives, per hour, over the operation's time period. GHI is defined by NREL as the sum of Direct Normal Irradiance (DNI) and Diffuse Horizontal Irradiance (DHI) for all practical purposes. DNI, which will be discussed later, is defined as "the amount of solar radiation from the direction of the sun [31]." Similar to a load profile, the solar resource can be loaded by the user in one of two ways. First, the user can provide an average daily GHI value for each month. The second method, and the method used in this research, is to load an 8760-value CSV file containing a GHI value for every hour of the year. Also similar to the load profile, the user can either input historically measured solar irradiance data, or estimated solar irradiance data. A common practice while using HOMER is to use the NREL's TMY3 data as the input. When the user cannot provide solar irradiance data for the given location and time frame, the HOMER GUI obtains the required solar irradiance values from either NASA or NREL databases.

### **2.4.2 Temperature Profile Input**

In order for the HOMER model to simulate the effects of temperature on PV cell performance, temperature data must be provided to the model for the location and time frame of the simulation. Once the user has selected to include temperature effects in the simulation, temperature input data is loaded by selecting the "Temperature" resource button on the HOMER GUI [30]. The temperature input data can be provided in the form of either an annual temperature profile with unique hourly temperature values or monthly average temperature values. If the user enters monthly temperature averages, the model uses those average values for every time step of the simulation for the respective month. If the user imports an hourly time series data file, in an 8760-value CSV file form, then the HOMER model uses each of the unique hourly values for the associated hour of the time step simulation.

THIS PAGE INTENTIONALLY LEFT BLANK



---

## CHAPTER 3:

# HOMER in Expeditionary Operations

---

### 3.1 HOMER Robustness for Expeditionary Operations

The Marine Corps boasts an ability to deploy to any clime or place. Due to the unpredictable nature of combat and humanitarian operations, the Marine Corps does not have the luxury of being able to gather data on the solar irradiance and weather patterns of a location for months (or years) prior to deploying there. To be useful for deployment to unanticipated locations, HOMER must be robust enough to handle the solar irradiance and temperature variability for those locations. Of particular concern when considering the use of HOMER for Marine Corps power planning is how HOMER simulates micropower system performance for the short-term durations associated with Marine Corps expeditionary operations. HOMER was designed for "simulating the long-term operation of a micropower system [1]." While modifications will be required to be made to HOMER to simplify the simulation of shorter time periods, this modification is expected to impact the GUI and not the model engine itself. This research assists in determining whether the HOMER engine is compatible with the simulation of short duration micropower simulations or if the inter-annual variability of environmental inputs induce unacceptable variability in HOMER simulation output.

For this research, it is assumed that when employing HOMER the Marine Corps will depend on the historical solar irradiance data gathered by NASA and NREL. This is a standard practice in the solar industry for performance simulation and is a preferred option, when possible, for using the HOMER model. A typical solar irradiance profile is utilized as the solar resource input for HOMER because the model was originally designed to analyze the long-term performance of micropower systems, specifically for 30 years. This solar irradiance profile can be derived either from the NREL TMY database or built using the Graham-Hollands algorithm and a value for the location's average monthly solar irradiance. Over the long term of 30 years, the effects of interannual solar irradiance and temperature variability are expected to be negligible. This assumption is based on the predicted profiles' errors above and below the actual measured solar irradiance and temperature profiles

of each year averaging out over the thirty years. With the Marine Corps likely employing the HOMER model for planning power generation in operations as short as 15 days, this variability can no longer be assumed to have a negligible impact and must be investigated.

In 2010, Newell conducted an experiment where he assessed the capabilities of the HOMER model in forecasting the power output of a solar panel at NPS [32]. In his experiment Newell utilized the Graham-Hollands algorithm and average monthly solar irradiance measurements from the NASA Surface Solar Energy data set to build a synthetic solar profile which served as the solar resource input for the HOMER model. He also utilized average monthly temperature measurements as the temperature input for running the model. Newell's research initially found the HOMER model to perform with unacceptably poor fidelity, with HOMER estimating "an energy production level that was over 25 percent higher than the actual measured energy [32]." Newell associated this overestimate of power production to three factors: a disparity between measured and anticipated surface solar irradiance, a disparity between measured and anticipated ambient temperature, and an underestimate of the derating value for the solar panels.

As discussed earlier, in order for the HOMER model to simulate the performance of the solar panels, the user must load the solar resource and temperature profile into the model. The 25 percent overestimate in energy production, identified in Newell's thesis work, was predicted with resource inputs based on average monthly solar irradiance and temperature values and the generation of a solar irradiance profile with the Graham-Hollands algorithm. To identify the impact of discrepancies between the inputted and the real temperature and solar irradiance profiles, Newell reran the model with the measured temperature and solar irradiance profiles for that period of time. Figure 3.1 shows the results of Newell's analysis. These HOMER runs showed that the differences between real world and originally inputted temperature and solar irradiance profiles accounted for 10 percent of the HOMER model's 25 percent overestimate in PV power production for Newell's experiment. Six percent of the overestimate in power production was due to differences between real and original temperature profiles. Four percent of the overestimate in PV power production was due to differences between real and Graham-Hollands-generated solar irradiance profiles.

Newell concluded that the model performed satisfactorily if the derating factor for the array was assumed to have decreased below the standard 80 percent, based on the weathered and

	PV Usable Energy (kwh)	Accuracy
<b>Measured Data</b>	<b>1270</b>	
<b>HOMER Model</b>	<b>1612</b>	<b>+27%</b>
<b>Add Temp Effects</b>	<b>1539</b>	<b>+21%</b>
<b>Add True Solar Irradiance</b>	<b>1483</b>	<b>+17%</b>

Figure 3.1: Effects of solar irradiance and temperature discrepancies in Major Brandon Newell's 2010 solar panel and HOMER model experiment, from [32].

unclean status of the particular array [32]. While the effects of solar irradiance and temperature discrepancies were clearly presented in Newell's thesis, the question of identifying the correct derating factor is less justified. Without the support of follow-on experiments to validate the derating factor Newell applied, the conclusion of subscribing the remaining 17 percent inaccuracy to derating of the solar panel is dangerously close to assuming the conclusion. That being said, this research, which focuses on the effects of input variability, assumes Newell's assessment of the HOMER model's accuracy to be correct. In order for this research to be better grounded future research would need to be conducted to validate the derating factor laid out in Newell's assessment of the HOMER model.

## 3.2 Solar Irradiance Variability

Marine Corps expeditionary operations depend on robust, space and weight efficient sources of power. An important component of expeditionary operations is the relatively

small size of the units conducting fast paced and short duration operations. Logistics planners and commanders must be able to rely on their energy source, and solar irradiance variability is one element of solar irradiance that brings that reliability into question. Solar irradiance variability can be caused by multiple factors, including varying cloud cover and pollution.

Newell's 2010 thesis research demonstrated that solar irradiance and temperature variability from the provided solar irradiance and temperature model resources will result in inaccurate power production predictions by the HOMER model. He also demonstrated that the percentage of solar irradiance disparity does not account for the percentage of inaccuracy created in predicted power output. While the original user-provided solar irradiance profile overestimated actual solar irradiance by 9.35 percent, this did not equate to the model overestimating PV power production by 9.35 percent. As Newell pointed out, this is "due to the nature of the comparison, which only compared the total kW per m squared for the month and disregarded when the disparities occurred [32]." The amount of solar irradiance variability that occurs for a given scenario does not necessarily equate to an equivalent amount PV power production variability, but there is a direct relationship between solar irradiance and PV production variability that must be identified. In the previous chapter, it was mentioned that HOMER uses the Graham-Holland method to handle solar irradiance profiles provided in terms of average monthly irradiance. While the use of Graham-Holland provides for the generation of "synthetic sets of hourly solar irradiation values," utilizing such a synthetic solar irradiance profile does not account for inter-annual variability [25]. Even the TMY solar irradiance profiles provided by NREL, which may be expected to exhibit higher fidelity than the Graham-Hollands derived profiles, can not diminish the effects of real-world inter-annual solar irradiance variability. For these reasons, an appreciation of the relationship between solar irradiance variability and HOMER model power estimate variability must be acquired through a DOE leveraging the model itself.

### **3.2.1 NREL Report on Temporal and Spatial Solar Irradiance Variability**

In a 2010 NREL report on the variability of solar irradiance, researchers analyzed eight years worth of measurements from the National Solar Radiation Database (NSRDB) in terms of temporal and spatial variability [33]. Temporal variability refers to the interannual

variability of solar irradiance measurements for set locations and times of the year. Spatial variability refers to the variability faced when a solar irradiance profile is acquired at a given measurement site and the profile is attempted to be utilized for locations of increasing distance from the measurement site. Both of these types of solar irradiance variability influence decision making on where and when to employ solar power systems in the solar industry.

In this report, researchers Wilcox and Gueymard quantified temporal variability as the inter-annual variability of mean monthly DNI coefficient of variation (CV) (percent) across the eight years, 1998-2005. When considered across the full year, the DNI CV values range from 0.49 percent to 15.8 percent. Figure 3.2 shows how temporal solar irradiance variability is affected substantially by both climate and season. This graphic shows that the winter seasons have substantially higher inter-annual solar irradiance variability than the summer months. The West Coast and northern regions of the United States similarly display higher degrees of inter-annual solar irradiance variability than the other parts of the country. These findings are useful to the Marine Corps and other institutions that employ solar power assets as users can see that solar irradiance profile forecasts for the winter and west coast/northern regions of the United States are more susceptible to profile variability due to temporal solar irradiance variability than are profile forecasts for regions in the summer and midwest or southwest regions of the United States.

For these and other reasons, temporal solar irradiance variability, or inter-annual solar irradiance variability, is a primary focus of this research. While Wilcox and Gueymard provide valuable insight into the relationship between temporal solar irradiance variability and the factors of climate and season, their study was limited in scope to eight years and did not directly identify the effects of temporal variability on the HOMER model. Spatial solar irradiance variability was not included in this research's experiments. That being said, understanding spatial variability provides valuable context for evaluating the options for Marine Corps employment of NREL TMY solar irradiance profiles.

By quantifying spatial solar irradiance variability the Marine Corps, and other institutions interested in forecasting solar irradiance, can identify the number of solar irradiance measuring stations required to characterize and quantify a region's solar irradiance profiles. This knowledge can assist in determining the degree of confidence with which users can

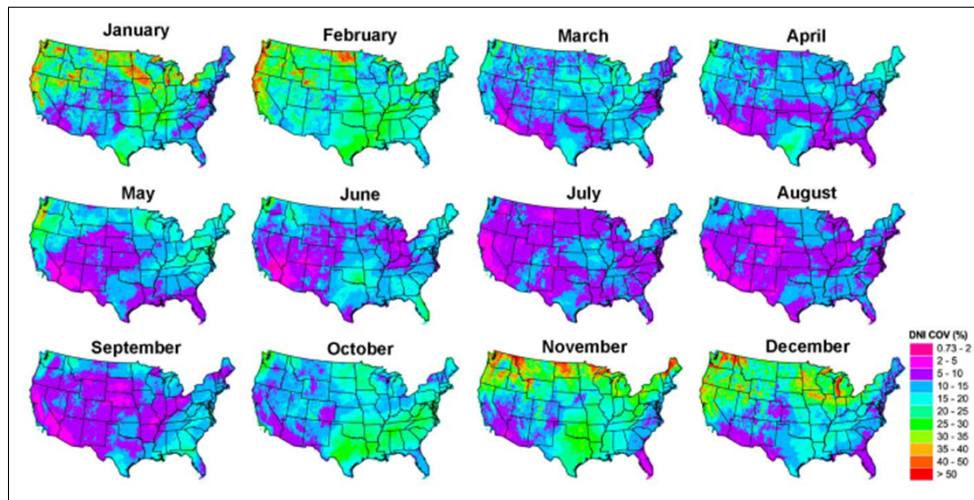


Figure 3.2: Monthly temporal CV (percent) of DNI across the United States, 1998-2005, from [33].

utilize existing data for modeling solar irradiance and the associated performance of photovoltaics. Wilcox and Gueymard found that spatial variability varies across the United States with climates and is particularly sensitive to a location's proximity to the west coast. The degree of spatial variability across the United States can be seen in Figure 3.3. In Figure 3.3 variability is quantified as CV of solar irradiance in terms DNI, for which solar irradiance is "always substantially more variable than that in GHI [33]." This CV measures inter-annual variability of daily mean DNI measures in 50x50 km areas over eight years. The results therefore "roughly represent an area within...25km of a measurement site [33]." A more detailed description of the methodology can be seen in [33].

The analysis conducted by Wilcox and Gueymard shows that spatial variability of solar irradiance data depends on season and climate. Figure 3.2 shows that spatial variability across the United States is at its lowest in July and August, with most DNI CV values in the 2-10 percent range, and at its highest in November and December, with most DNI CV values in the 15-50 percent range. Figure 3.2 also demonstrates that climate affects spatial variability and temporal variability similarly, with the West Coast and northern regions of the United States displaying higher spatial variability than other regions.

The take away from the Wilcox and Gueymard study on spatial variability of DNI is that

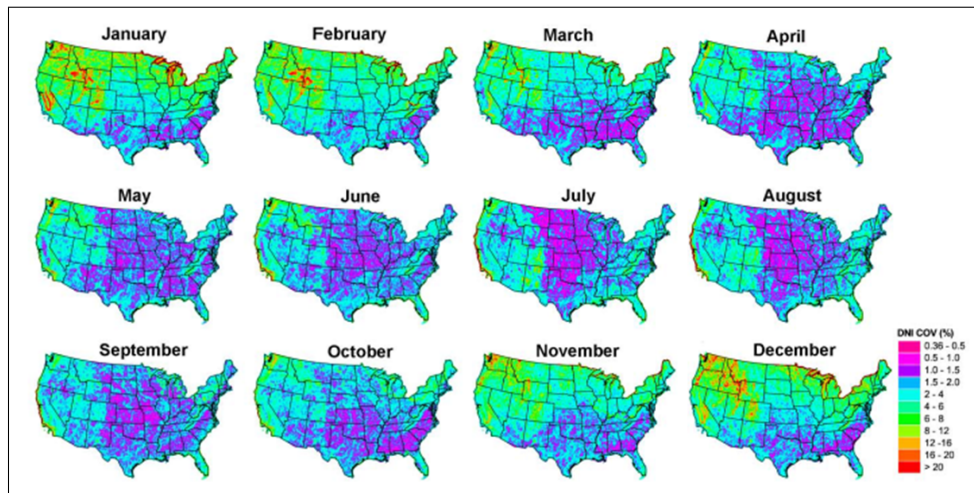


Figure 3.3: Monthly spatial CV (percent) of DNI across the United States, 1998-2005. Seasonal effects are visibly similar to changes in mean temporal DNI CV seen across the seasons and climates of the United States in Figure 3.2, from [33].

users can estimate spatial variability of solar irradiance data to determine the usefulness of measurement sites in forecasting solar irradiance profiles of nearby locations. Solar irradiance data for locations in much of Southern California in August, for example, can expect locations within 25km of a measurement site to have variability (CV) of approximately 2-5 percent from the DNI at the measurement site. For Washington in November or December locations within 25km of a measurement site can expect to have variability of approximately 30-50 percent from to DNI at the measurement site. This knowledge provides some context to the discussion of Marine Corps employment of the HOMER model and the NREL TMY3 database.

The nature of Marine Corps expeditionary operations makes the effects of temporal and spatial solar irradiance variability even more important than in the commercial settings of the solar industry. The short term duration of expeditionary operations makes the Marine Corps-employed PV systems more susceptible to the effects of temporal solar irradiance variability. Although the NREL research was conducted using DNI rather than GHI, which is the measurement used for this research, the variations in variability are assumed to be proportional.

Spatial variability of solar irradiance is particularly important because the Marine Corps

units must select where to position themselves based on tactical concerns rather than where solar irradiance measurements were taken. While this research focuses on the effects of temporal solar irradiance variability, the spatial variability findings of the NREL study provide a context for understanding the scope and range of temporal solar irradiance variability. Understanding spatial solar irradiance variability will help the Marine Corps better understand the applicability of solar irradiance measurements for regional analysis of the solar resource.

### **3.3 Temperature Variability**

The previous chapter explained the effects of temperature on PV array performance. The effects of interannual temperature variability can be inferred from that discussion of temperature effects, but Newell's previous research provides a more specific example of the effects of temperature variability. Newell's research demonstrated a 9.35 percent discrepancy in total solar irradiance input resulting in a 4 percent overestimation in the HOMER model's prediction of power production. In that experiment, the effect of temperature on the model's overestimation of power was even greater. The inclusion of the measured temperature profile for the simulation demonstrated that employing the synthetic TMY temperature profile accounted for a 6 percent HOMER model overestimate in PV power production. Temperature effects on a PV cell's ability to produce power were discussed in Chapter 2, and this experiment provides an example of why the ability to model the effect of temperature on PV cells was included in the HOMER model. The experiment also exemplifies the importance of understanding the effects of temperature variability on HOMER model power predictions.

### **3.4 Effects of Load Profile Variability on HOMER**

Uncertainty in the HOMER model's predictions of fuel savings comes both from the user's inability to predict exact profiles for solar irradiance and ambient environmental temperature and from the inability of the user to anticipate their exact load profile. Marine Corps logisticians and engineers currently build unit power plans based on peak load capacities of the unit's equipment. Load profiles are not employed because it is difficult to project load profiles from one operation to another. This concern over variability between user specified load profiles and reality was highlighted in a 2007 Institute of Electrical and Electronics



Engineers (IEEE) report assessing the HOMER model's performance with regard to wind turbine power planning [34]. In this report, Zdenko Simic identified three modeling assumptions requiring follow-on research to "verify sensitivity of presented results on some modeling assumptions [34]." One of those modeling assumptions Simic cited as requiring verification was the potential for variation from "assumed load schedule [34]." The lack of requisite measured experimental load profiles prevented this research from analyzing the HOMER model's robustness with regard to load profile variability. All analysis conducted during this research employed synthetic load profiles which will be described in the next chapter.

THIS PAGE INTENTIONALLY LEFT BLANK

---

## CHAPTER 4:

### Methodology

---

#### **4.1 Experiment Design**

To analyze the effects of solar irradiance variability and temperature variability on the robustness of the HOMER model, a DOE was constructed that analyzes the HOMER outputs for different scenarios simulated for each year of up to 50 years. This was accomplished through the synthesis of 50 years' worth of NREL's NSRDB data. While an analysis of the effects of variability in load profile input was originally intended, a lack of historical data that could represent the accurate depiction of load profile variability prevented its inclusion in the experiments. The DOE instead focuses on quantifying the robustness of HOMER with regard to the inter-annual variability of solar irradiance and temperature profiles as resources for the model. This DOE employs a variety of factors that could reasonably be expected to impact the solar power produced by a PV array. By including these factors, this DOE supports an analysis of which scenarios are more affected by increased inter-annual fluctuations in solar irradiance or temperature. Understanding how different scenarios are influenced by these variations will assist the Marine Corps in determining not only the general robustness of the HOMER model but also how best to employ the model across the range of expeditionary operations.

Factors included in this DOE can be classified as either micropower system design factors or environment design factors. Micropower system factors include the size of the unit (represented by peak power level), the number and size of diesel generators in the micropower system, and the number of solar power assets utilized. Environmental factors include the physical location of the micropower system, the duration of the micropower system run evaluated, and the season, represented by the starting date of the micropower system run evaluated. Figure 4.1 shows each of the DOE factors and the levels across which each is varied. The sections below describe each factor's levels and how these levels were selected.

DOE Factor	Number of Factor Levels	Factor Description
Location	10	Locations were identified across the United States based on dispersion and completeness of data
Duration	7	Duration effects are assessed by running simulations with durations of 15 days, and 1,2,3,4,5, and 6 months
Season	24	Season is accounted for by utilizing scenario start times evenly distributed across the year
Unit Size	5	Unit size is represented by varying the size of the simulated microgrid peak load levels between scenarios
Generator Compositions	4	Numbers and sizes of generators are varied for scenarios to investigate the effects of pairing large and small generators
Solar/Temperature Input Profiles	3	1/3 of scenarios input TMY3 solar profiles and measured temperature profiles, 1/3 input measured yearly solar profiles and no temperature, and 1/3 input correlated annual measured solar irradiance and temperature profiles

Figure 4.1: The 6 DOE factors, number of levels for each factor, and a brief description of each factor

#### 4.1.1 Size of the Unit

Marine Corps units are modular, with larger units being composed of smaller, standard sized units. An artillery battalion, for example, is comprised of a headquarters company and three artillery companies. Each of the artillery companies are in turn comprised of three platoons. The Marine Corps generally employs its forces in these modular configurations, with the size and composition depending on the mission. In Afghanistan, battalion-level bases direct dispersed company-level bases and these companies often command dispersed platoon and squad-sized outposts. Each of these dispersed bases and outposts have some level of energy consumption that has to be met, and somewhere along the way a leader made the decision on what energy equipment was provided to support the unit. The HOMER model would be employed to assist those leaders in determining how to most efficiently allocate their power equipment between their outposts and bases. Because the HOMER model would be used across this variety of unit sizes and power requirements, the size of the unit is included as a factor in this DOE.

The different unit sizes are represented by varying the peak power requirements. This method was employed in the E2O's MEHPS AOA which was briefed to industry on 31 January 2013 [16]. Unit sizes utilized for the MEHPS AOA and discussed in the brief include a platoon outpost, a company COC, and a battalion COC. Replicating the load peak power specifications used by E2O, this research will represent a platoon's load profile as

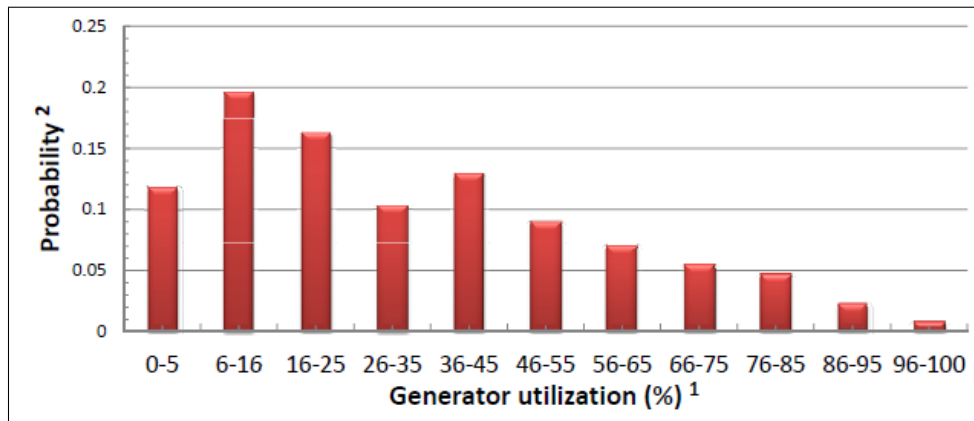


Figure 4.2: Generator usage chart, based on 767 historical records of real world 10kW, 30kW, 60kW and 100kW tactical quiet generators. Probability refers to the likelihood of the load equaling the given percentage of peak power, from [16].

having a peak power of 3kW, a company's load profile with 5kW or 10kW peak powers values, and a battalion's load profile with 30kW or 60kW peak power values. For an identification of the equipment used to derive these peak power levels, the user should refer to the MEHPS AOA brief. The load profile for each unit size is created using the modified load profile percentages described in the previous chapter.

### 4.1.2 Diesel Generators

Units that employ a single generator rated to their peak power can often be expected to consume more fuel than units with the multiple smaller generators summing to the same peak power level. This is due to how the fuel efficiency of internal combustion generators decreases as the size of the load decreases [35]. Employing multiple smaller generators rather than a single large capacity generator often "allows the use of one or two units at full load rather than a larger unit at reduced load [35]." Figure 4.2 shows the probability (y-axis) for 10kW, 30kW, 60kW and 100kW Tactical Quiet Generators (TQG) to be utilized with various loads, with loads specified as a percentage of generator peak power capacity. This figure shows that micropower system loads rarely reach the peak power level. Indeed, Figure 4.2 shows that generators have a higher probability of being run at load levels less than half their peak load capacity levels than they have of being run at load levels above half their peak load capacity levels.

Peak Power level (kW)	# 60kW Diesel Generators	# 30kW Diesel Generators	# 15kW Diesel Generators	# 10kW Diesel Generators	# 5kW Diesel Generators	# 3kW Diesel Generators	# GREENS/ # SPACES
3	-	-	-	-	-	1	1 GREENS
5	-	-	-	-	1	1	1 GREENS
	-	-	-	-	0	2	1 GREENS
10	-	-	-	1	1	0	3 GREENS
	-	-	-	0	2	0	3 GREENS
	-	-	-	1	0	2	3 GREENS
30	-	1	0	1	0	0	5 GREENS
	-	0	2	0	0	0	5 GREENS
	-	0	0	3	0	0	5 GREENS
60	1	1	0	0	0	0	5 GREENS
	0	2	0	1	0	0	5 GREENS

Figure 4.3: Composition of diesel generator and GREENS/SPACES systems factors for DOE energy generation scenarios. "Diesel Generators" refers number of Marine Corps TQGs included in each scenario design.

Units with multiple smaller generators can run only those generators needed to meet their current power requirements at any given time and no more. This was seen in the MEHPS AOA consideration of fuel consumption for three micropower systems with peak power levels of 60kW over a 120 day period. The system powered by a single 60kW generator consumed 170 gallons more than the system powered by two 30kW generators and 683 gallons more than the system powered by one 30kW generator and two 15kW generators [16]. To account for these effects in the DOE, the number and type of diesel generators in each micropower system is included as another design factor, with each of the units having three unique compositions. The 3kW platoon sized unit is the only unit that only includes two diesel generator composition options, because of the small size of the load. The generator profiles can be seen in Figure 4.3.

Including a generator within the HOMER model requires an accurate representation of

certain specifications. The fuel curve intercept and slope are of particular interest as they dictate the speed at which the generator will consume fuel at different loads. The technical characteristics for each of the 3, 5, 10, 15, 30 and 60kW generators was represented in the HOMER model through the use of fuel consumption data measured at Aberdeen Proving Ground and provided by Harold Scott Coombe of ONR on 27 June 2013. All generators are Marine Corps Advanced Medium Mobile Power Sources (AMMPS) generators, except for the 3kW, which is a TQG generator due to the current absence of a 3kW AMMPS generator and a need to simulate load profiles and generators below 5kW.

### **4.1.3 Solar Power Assets**

As discussed earlier, the Marine Corps has developed and fielded two solar power generation assets; the GREENS and SPACES systems. The GREENS and SPACES PV array and component battery technical specifications were provided by ONR to support this research. Both the GREENS and SPACES systems were designed to be employed for stand-alone rather than grid-tie functions. While the GREENS system generates enough power that it can offer significant fuel savings when employed in a micropower system, the SPACES system does not provide enough energy to provide noticeable savings relative to the fuel consumption of micropower systems supporting loads of 3kW to 60kW. The SPACES system, with its provision of up to 320W of continuous power, is usually employed to power communications equipment and charge batteries for smaller units. An additional key difference between the GREENS and SPACES systems, mentioned in the Marine Corps Warfighting Lab guide for employing renewable technologies, is that "the GREENS is not as sensitive to optimal conditions as SPACES; as it can harvest energy in less ideal conditions" than SPACES can [11]. Early analysis of the fuel savings in micropower systems derived from employing the SPACES system also showed that its limited power capabilities made it much less useful in directly supporting a micropower system load. For these reasons, the SPACES was not included in this research's investigation of the HOMER model's robustness regarding inter-annual variations in solar irradiance and temperature.

For this DOE, the number of GREENS systems employed per unit size are shown in Figure 4.3. With its capability of providing 300W of continuous power, and up to 1000W in peak power, a single GREENS system can be used to significantly support the load requirements of platoon (3kW) or company-size (5kW) units [11]. The GREENS system's mod-

ular design allows for its employment in supporting larger company, company-reinforced (10-30kW) and battalion-size (60kW) load requirements as well. For these larger units the number of GREENS systems was selected to, as much as possible, maintain the GREENS power production to load peak power ratio seen in the MEHPS medium system in the MEHPS AOA brief [16]. Additionally, GREENS system is currently capable of combining only five GREENS units under one converter/inverter, limiting the number of GREENS allocated to the larger 30kW and 60kW sized units to only five.

Adjusting the GREENS system size across the range of unit sizes decreases concerns of having the micropower system size act as a confounding variable in the analysis of solar irradiance variability effects relative to unit size. As the Marine Corps would be using the HOMER model for all unit sizes assessing such a variety of unit micropower system sizes with HOMER is essential for assessing the robustness of the HOMER model.

#### **4.1.4 GREENS Converter**

Modeling the GREENS system included not just the modeling of the PV arrays for each system, but also their batteries and converters. While specifications needed for the modeling of these components were provided by ONR, questions regarding the simulated quantity of GREENS systems and certain component specifications required additional steps. In terms of quantities of GREENS systems simulated, the assumption was made for this research that the GREENS system is employed as a complete individual unit or as a combination of complete individual units. Although the individual GREENS system is modular, it is not represented as such for the purposes of this study. The only modular capability that is reflected is the ability of multiple GREENS systems to be employed to support one load. Following this representation of GREENS systems as being employed as complete units, the proportion of batteries and converters to PV arrays was kept constant as the number of GREENS systems was changed for different scenarios.

Modeling the GREENS converter demanded the acquisition of more detailed converter specifications. Specifically, the inability of the converter, when acting as an inverter, to "operate simultaneously with an AC generator" proved to be an important specification to clarify [30]. Although the specifications provided by ONR dictated that the GREENS converter is not currently capable of operating simultaneously with AC generators, they



suggested that such a capability could soon be developed. Scenarios simulated through the use of the HOMER GUI showed that changes in the grid-tie capability of the inverter had a noticeable impact on the system's ability to decrease fuel consumption for certain scenarios. After consultation with Scott Coombe, Program Officer Code 331, the decision was made to conduct this analysis with the converters modeled in accordance with the current specifications, that is to say with the converters specified as not capable of operating simultaneously with AC generators.

Following analysis of the HOMER model's robustness concerning variability of inputs, the opportunity was taken to compare the HOMER model's representation of standalone and grid-tie capable PV arrays. The simulations which included annual measured solar irradiance input profiles were replicated with the only change being that the GREENS system converter was represented as being capable of operating simultaneously with AC generators (grid-tie capable). In one scenario, for example, if the converter was simulated as being grid-tie capable the system was able to save 2,580 liters of fuel. The GREENS system simulated as not being grid-tie capable represented a savings of only 17 liters of fuel under the same circumstances.

By executing these additional grid-tie system experiments, this research provides an understanding of how the HOMER model will benefit the Marine Corps in assessing the performance of the current GREENS system as assessing a grid-tie capable GREENS system. This analysis provides the Marine Corps with an opportunity not only to assess the HOMER model, but also to assess the benefits of shifting to grid-tie capable solar power systems. As the Marine Corps continues its shift toward MEHPS systems, it will be helpful to understand how analysis tools such as the HOMER model perform when assessing the performance of grid-tie capable systems. The findings of this standalone versus grid-tie system analysis will be presented in the analysis chapter following analysis of temperature and solar irradiance inter-annual variability effects on the HOMER model.

#### **4.1.5 Location**

The location of the micropower system being simulated is an important environmental factor because it dictates the climate of the environment. Identifying how the effects of solar irradiance variability associated with different climates will help the Marine Corps

anticipate the robustness of HOMER for expeditionary operations relative to the theater of operations and the climate of the target location. While this research focuses on the United States because of the high quality data, future research focusing on the impact of climate can be used to identify the robustness of the HOMER model across regions of the world where the Marine Corps has a high likelihood of deploying.

The solar irradiance variability visualization of the 2010 NREL solar irradiance variability report, Figure 4.4, demonstrate how interannual solar irradiance variability is affected by climate. The 2012 Locus Energy researchers who evaluated the characteristics of solar irradiance variability at five locations across the United States recommended that "the quantity of sites be expanded to better comprehend the impact of locations and climates upon solar variability [23]." To ensure this research includes the effects of discussed by the Locus Energy researchers, this DOE includes 10 locations selected from across the United States. The 10 cities, superimposed on the 2010 NREL report's irradiance variability graphic in Figure 4.4, were selected based on the completeness of their NSRDB data and their dispersion in distance and climate across the United States.

To identify the effects of climate on the inter-annual variability in HOMER fuel savings predictions the 10 locations assessed in this research were classified and grouped by climate. The classification system used was the Koppen-Geiger climate classification system. The Koppen-Geiger system classifies climates by their main climate which is determined by vegetation group (arid, warm temperate, snow, etc.), precipitation, and temperature [36]. A map of the Koppen-Geiger climate classification for the U.S. is shown in Figure 4.5.

Although there are climate variations across almost all locations used in this research, the 10 locations were able to be grouped into 3 general climate groups: steppe climates, snow-fully humid climates, and warm-temperate climates. The steppe climate group includes Albuquerque, El Paso, TX, and Boulder. The snow-fully humid climate includes Bismarck, ND, Madison, WI, and Salt Lake City. The warm-temperate climate includes Seattle, Sterling, VA, Tallahassee, and Eugene, OR.

#### **4.1.6 Starting Date**

Starting dates are included as an environmental factor in this DOE to support the analysis of seasonal solar irradiance variability effects on the HOMER model's performance. The

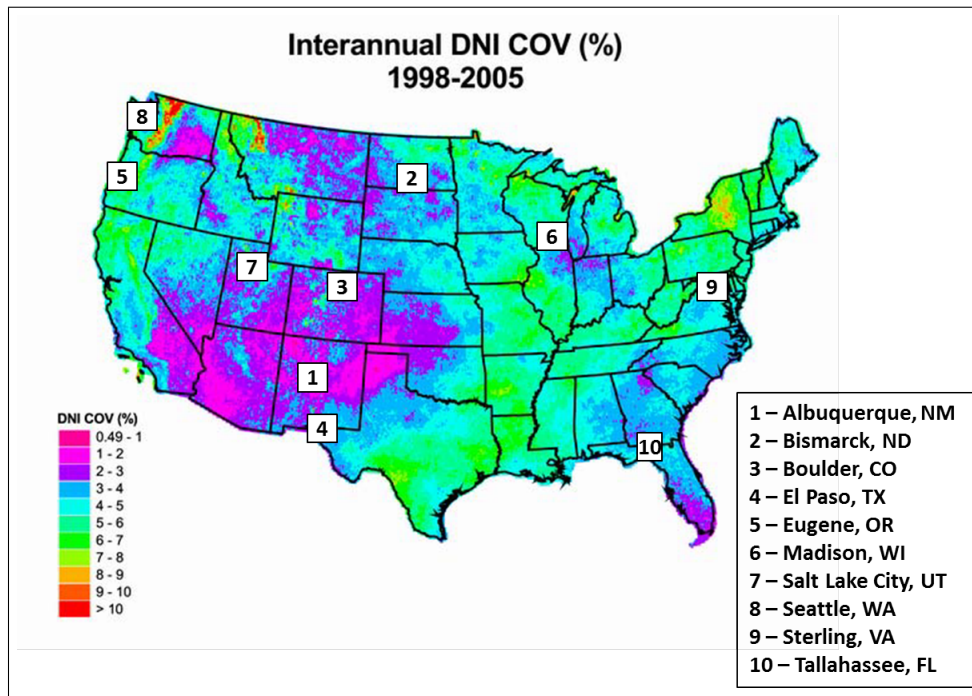


Figure 4.4: 2010 NREL solar irradiance variability report visualization of 1998-2005 solar irradiance variability, adjusted to show the ten locations selected as location factor levels for this research, from [33].

NREL solar irradiance variability report that demonstrated the impact of climate on solar irradiance variability also demonstrated the importance of considering the season relative to the location [33]. Just as 10 locations across the U.S. are used in this DOE to evaluate the effects of spatial solar irradiance variability, the starting dates of the simulations were selected for this DOE for evaluating the effects of variability across the seasons as well. To ensure all seasons are considered, the levels for this factor are the first and fifteenth day of every month of the year.

#### 4.1.7 Duration of Operation

The final environmental factor, the duration of the simulated operation, is composed of seven levels. The seven levels included in this DOE are time periods of either 15 days or one, two, three, four, five or six months for simulated expeditionary operations. Varying the duration of the simulated operations (micropower system run times) in this way represents the wide range of time frames of Marine Corps expeditionary operations. The levels them-

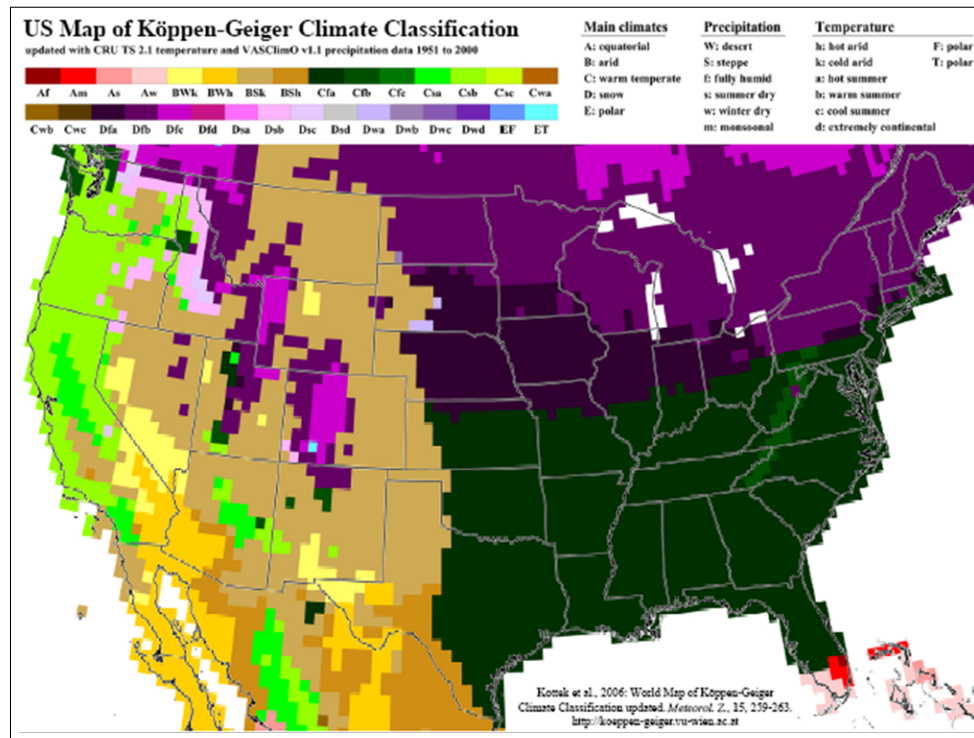


Figure 4.5: Köppen-Geiger climate classification system applied to the continental United States, from [36].

selves were selected based on the way that E2O defines expeditionary time periods for analysis of expeditionary technologies, defining them as those missions lasting less than 120 days [37].

The longer time periods allow for considering how HOMER's projections adjust as the operation moves between seasons of greater or lesser solar irradiance variability. Shorter time periods are expected to demonstrate the effects seen in locations containing seasons with particularly large interannual variability. To simplify the process of data and the manipulation of the HOMER model in support of this DOE, operations are not included that would link data of different calendar years. This means, for example, that there are no two month operations simulated as occurring from 1 December to 1 February.

## **4.2 Assessing HOMER Robustness with Regard to Solar Irradiance Variation**

One key question asked by this research is how critical is it that inter-annual variation in solar irradiance is not reflected in the HOMER model, which typically relies on TMY data to provide the solar resource. It was anticipated that the short-term duration of Marine Corps expeditionary operations, for which the HOMER model would be employed by the USMC, would represent greater risk of variability in the HOMER fuel savings prediction than the variability seen in the long-term scenarios for which HOMER is usually employed. To answer this question the research methodology needed to identify a measure of variation in solar irradiance over the 50 years of data as well as a measure of variation in the associated fuel savings predicted by the HOMER model for each of those years.

### **4.2.1 Acquisition and Synthesis of Solar Irradiance Data**

The solar resource used in the HOMER model must be loaded into the model in the form of a list of 8760 quantifications of solar irradiance in kilowatt-hours. A source of solar irradiance data was found in the NREL's NSRDB. The NSRDB provides a variety of meteorological data sets for locations across the United States. The locations previously specified in the DOE were selected from the list of solar irradiance measurement sites in the NSRDB based on the high quality and completeness of their associated data.

All ten data collection sites that were selected provided solar irradiance data from 1961 to 2010. The NSRDB data sets were acquired from the NSRDB website. After acquiring the 500 files, a java script was written to synthesize the .txt files, parsing out only the hourly values for solar irradiance in terms of GHI and creating (500) 8760 value CSV files.

### **4.2.2 Quantifying Variability in HOMER's Predicted Fuel Savings**

Quantifying the variability in HOMER's fuel savings predictions first required a quantification of HOMER's fuel savings predictions. To determine the fuel savings reaped from employing the GREENS, each scenario was run twice for each year, once with the GREENS included in the micropower system and once without the GREENS system. The difference in the micropower system's fuel consumption between these two runs was calculated as the fuel savings reaped from employing the specified number of GREENS. Because of the dif-

ferences in quantities of fuel consumption between the different micropower system sizes (3, 5, 10, 30, and 60kW) the percent fuel saved (fuel saved by employing GREENS divided by fuel consumed without GREENS) was selected as the metric for quantifying and comparing fuel savings. The analysis of variation in HOMER fuel savings predictions was therefore conducted using percent fuel savings in this research. To identify the relationship between inter-annual variability in HOMER's predicted fuel savings and the inter-annual variability in solar irradiance variability, a similar metric had to be selected for quantifying variability for both. The root mean square error (RMSE) would eventually be selected as the measure of variability, but the first consideration was the CV. While checking the assumptions needed to employ the CV a trend was found in the solar irradiance data that disqualified the CV and introduced a new concern for the robustness of the HOMER model with regard to the fidelity of its solar resource input data. This trend and its impact on this research's analysis of the HOMER model's robustness with regard to inter-annual solar irradiance will be discussed over the next 5 sections.

### **4.2.3 Inter-Annual Solar Irradiance Trend**

One well known tenet in the modeling and simulation community is the "trash-in-trash-out" understanding of modeling. Avoiding the input of "trash" into a model is important for model researchers and users alike to ensure there are no confounding factors or trends in the input data. To check for any confounding effects in the solar irradiance input files, the irradiance files for each city were analyzed across the 50 years for each scenario location, season (start date), and duration across all 50 years. The results of this check identified a significant confounding effect in the solar irradiance input files. For nine of the ten locations used in this research, the majority of the scenarios demonstrated a linear decline in surface solar irradiance over the 50-year period from 1961 to 2010. This trend was seen in scenarios ranging across all seasons and across all durations that were investigated. The linear regression was significant in the majority of cases for these locations. The origin of this trend and the way it is accounted for in this research will be discussed over the next four sections.

### **4.2.4 Global Dimming**

After further research to identify the source of this long term trend of declining solar irradiance over the 50 years of available data, the trend was found to be a manifestation

Station	1951 - 1983		1984 - 2010	
	W/(m <sup>2</sup> decade)	%/decade	W/(m <sup>2</sup> decade)	%/decade
Braunschweig	3.2 ± 3.2	2.8 ± 2.8	4.3 ± 2.4	3.8 ± 2.1
Fichtelberg	-3.7 ± 4.6	-3.3 ± 4.2	4.5 ± 3.2	4.0 ± 2.9
Hamburg	-0.6 ± 1.7	-0.5 ± 1.6	4.5 ± 2.6	4.1 ± 2.4
Hohenpeissenberg	-4.3 ± 2.5	-3.1 ± 1.8	3.6 ± 2.7	2.6 ± 1.9
Potsdam	-1.8 ± 1.8	-1.6 ± 1.5	4.7 ± 2.2	4.1 ± 1.9
Trier	-4.1 ± 6.0	-3.3 ± 4.9	2.7 ± 2.9	2.2 ± 2.4
Weihenstephan	-3.3 ± 3.1	-2.4 ± 2.3	4.9 ± 2.7	3.7 ± 2.0
Wuerzburg	-0.4 ± 3.4	-0.3 ± 2.7	3.2 ± 2.2	2.6 ± 1.7
Mean Anomalies	-2.1 ± 1.6	-1.7 ± 1.3	4.0 ± 2.0	3.3 ± 1.6

Figure 4.6: Measurements of long-term GHI that suggest a shift in Europe's solar irradiance trend from global dimming to global brightening, from [38].

of a phenomenon known as "global dimming [38]." Global dimming is described as the "decadal decrease of surface solar radiation [39]." The name "global dimming" was coined by Stanhill and Cohen in their 2001 article, "Global Dimming: A Review of the Evidence for a Widespread and Significant Reduction in Global Radiation [40]." The "global" portion of the name does not refer to the phenomenon having a universal effect across the world but instead refers to "the sum of diffuse and direct solar radiation," that is to say global radiation [39]. The dimming refers to a decrease in that global radiation which was measured as occurring at different rates across the world. In the 1980s and '90s, climate modelers began to distinguish a trend of decreasing surface solar radiation in available surface solar radiation records dating back to the 1950s. The rates of the decrease differed by location but were mostly seen as occurring from the 1950s up to the 1980s [38]. Figure 4.6 shows some examples of global dimming rates, in terms of Watts per meter squared per decade, from 1951 to 1983, that were identified across Germany in the 2014 paper "Rethinking Solar Resource Assessments in the Context of Global Dimming and Brightening."

Figure 4.6 also identifies an apparent shift in the global dimming trend that was identified as having occurred in Europe in approximately 1985 with a shift from decreasing to increasing solar irradiance. This trend is referred to as "global brightening" as researchers found rates of increasing solar irradiance from the mid-1980s into the 21st century. The second column of Figure 4.6 shows the reversal of rates to increasing solar irradiance from 1984 to 2010, showing global dimming reversing to global brightening for the specified locations in Europe.

The decrease in surface solar radiation that characterizes global dimming is thought to be caused by increases in pollution and aerosols into the atmosphere where the decrease in solar irradiance is seen. This poses an interesting challenge for climate modelers regarding international trends in aerosol usage. Although one nation may decrease its usage of aerosols, a neighboring nation's continued or increased use of aerosols can have an effect of inducing global dimming across the region. The reversal in the solar irradiance trend from global dimming to global brightening in Europe during the 1980s-'90s is thought to be largely attributed to Europe's significant reduction of aerosol emissions [38]. This relationship shows that there is potential for modelers to utilize historical and predicted aerosol emissions by location to forecast global dimming and brightening.

#### **4.2.5 Accounting for Global Dimming in the Analysis Methodology**

The effects of global dimming on the surface solar radiation are notable and their effects on the HOMER model warrant further discussion in this research. That being said, the focus of this research is focused on the HOMER model's robustness concerning solar irradiance variation and not the effects of climate change. For this reason, the effects of global dimming were discounted from the total inter-annual solar radiation variation. The decision to hide the variation imposed by global dimming was made under assumptions regarding HOMER employment and climate modeling of global dimming which will be discussed later.

Recognition of global dimming as a confounding factor in the solar irradiance input data changed the way that the HOMER model's robustness with regard to solar irradiance variability could be assessed. The original intent was to assess the HOMER model's robustness using the CV in fuel savings across the 50 years, as seen in Figure 4.7, as the measure of performance to be compared with the CV in solar irradiance in the time frame across all 50 years. For calculating the solar irradiance CV, the standard deviation in cumulative measured GHI for a given scenario across the range of fifty years would be represented as sigma. In this equation  $n$  represents the number of years of complete data for the given scenario,  $E_m$  represents the mean sum of hourly measured GHI in kilowatt-hours per square meter ( $kWh/m^2$ ) for the scenario across the  $n$  available years, and  $E_i$  represents the measured solar irradiance for the given year  $i$ . This method of quantifying the interannual solar irradiance variability for the different scenarios is an extension of the method employed



$$\sigma_{scenario} = [\sum_{i=1}^{i=n} (E_m - E_i)^2 / n]^{1/2}$$

$$CV_{scenario} = \sigma_{scenario} / E_m$$

Figure 4.7: Modification of the Wilcox and Gueymard equation for calculating the cumulative GHI CV for each scenario across the available years of data, after [33].

by Wilcox and Gueymard in their analysis of solar irradiance variability across the United States [33]. The CV of percent fuel savings from employing the GREENS system in a given scenario would be calculated in a similar manner. Comparison of these two CVs, relative to the various DOE factors, would demonstrate the effects of solar irradiance inter-annual variations on the HOMER model's fuel savings predictions.

The CV would serve as a suitable measure of variability for this analysis only under the assumption that there is no trend in the solar irradiance data. The effects of global dimming, seen in Figure 4.8, required the utilization of a measure of variability that could account for the inter-annual trends associated with global dimming.

The linear regressions applied for each location in Figure 4.8 demonstrate a need to also account for the trends caused by global dimming relative to location. While the majority of locations and time periods assessed demonstrated a negative trend with a statistically significant linear relationship some locations, such as Tallahassee, did not demonstrate such a trend. Effects of global dimming on the variation in inter-annual surface solar radiation are therefore relative to the location from which the measurements were taken.

Figure 4.8 shows the cumulative solar irradiance, in GHI kilowatt-hours per meter squared, measured at each of the ten GHI measurement stations for the first 6 months of each year from 1961 to 2010. The line superimposed over each plot shows the linear regression for the given location across the 50 years for which measurements are held (1961-2010). As these figures show, for all locations except for Tallahassee, the variation around the mean for each location is much greater than the variation around the linear regression plot.

Taking out the effects of global dimming on inter-annual solar radiation variation was accomplished by quantifying solar radiation variation as the RMSE of the cumulative solar

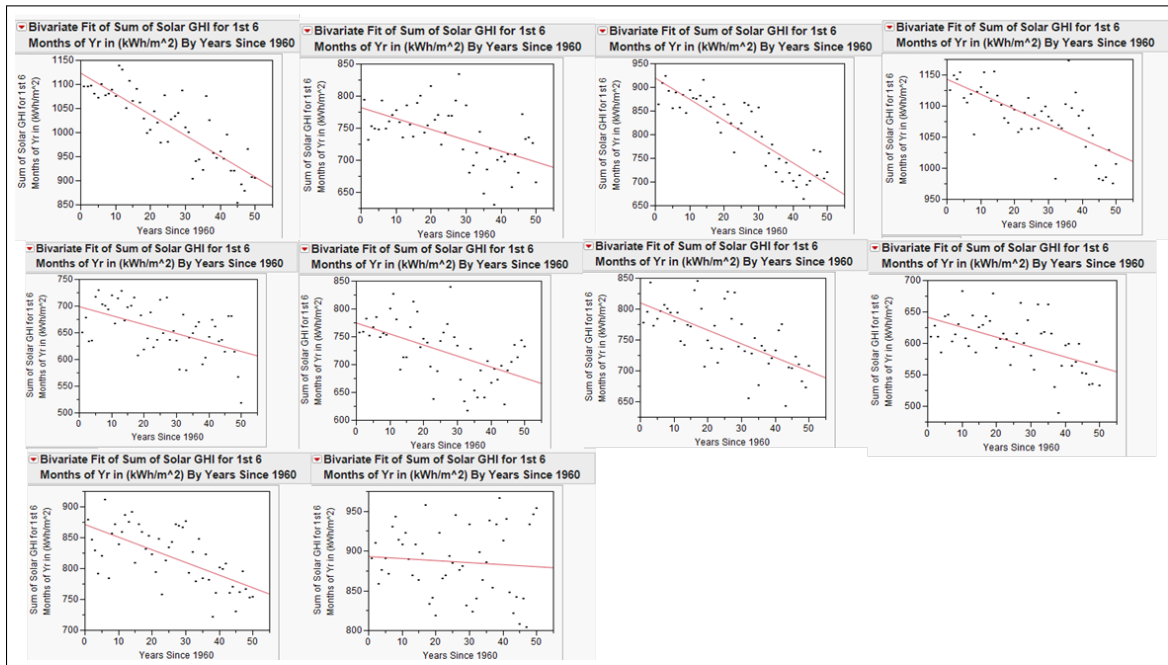


Figure 4.8: Linear regression plots show the negative linear relationship between years since 1961 and cumulative surface solar radiation for the first 6 months of each year per location. Top row: Albuquerque, Bismarck, Boulder, El Paso; Middle row: Eugene, Madison, Salt Lake City, Seattle; Bottom row: Sterling, Tallahassee

irradiance for each location, start time, and duration specified in the DOE. RMSE discounts the effects of global dimming on solar irradiance variability by calculating the variation of the 50 surface solar radiation measurements around the scenario's line of linear regression rather than around the mean of the 50 measurements. Later, when the variation in each micropower system's percent of fuel savings, the variation in the percent fuel savings was similarly quantified as the RMSE of percent fuel savings across the 50 years.

#### 4.2.6 Assumptions for Discounting GHI Variation Resulting from Global Dimming

Representing solar irradiance and fuel savings variation in RMSE downplays the variation in solar irradiance due to global dimming. Had the effects of global dimming not been accounted for and removed from the solar irradiance variation through RMSE, the variation of solar irradiance over the last 50 years would appear to be much greater. This variation caused by global dimming was taken out of the picture for this research under the

assumption that the effects of global dimming will be considered in the employment of the HOMER model for forecasting PV performance.

This representation of solar irradiance in RMSE also assumes that the trend in global dimming will either maintain its downward trend or that climate models will succeed in forecasting changes in global dimming. While the data in Figure 4.8 show a continuing decline in solar irradiance through 2010, several reports highlight a reversal of the global dimming trend in solar irradiance, referred to as "global brightening."

#### **4.2.7 Implications of Global Dimming in Modeling of PV Arrays**

A different, more significant implication of the global dimming trend is a concern over how to employ TMY3 data with the HOMER model to account for a decreasing supply of solar irradiance. NREL's TMY3 profiles are currently employed in HOMER in a manner that does not allow users of the HOMER model to account for inter-annual trends in solar irradiance for their location. This research is primarily concerned with analysis of the HOMER model's robustness with regard to expeditionary operations. That being said, the performance of the model with regard to long-term solar irradiance trends is important because of its effect on each solar power systems' performance over its life cycle. GREENS performance estimates based off of ten-year-old TMY data, for example, will overestimate the solar irradiance available to power the system where there is a negative linear relationship between time and solar irradiance. This concern will be discussed later in the thesis, after the impact of interannual solar irradiance variability is evaluated.

#### **4.2.8 Quantifying Inter-annual Solar Irradiance Variability: Coefficient of Variation of RMSE (CVRMSE)**

Before discussing the variation in HOMER model's power predictions due to solar irradiance variation, the variation seen in the latter must first be discussed and quantified. The units of a RMSE analysis are the same as the units of the values being assessed. For variability in predicted fuel savings this means RMSE values are in terms of the percent difference of a given prediction from the mean fuel savings predicted by the linear regression. More specifically, the RMSE value identifies the percent of inter-annual variation for 68 percent of residuals, while 95 percent of residuals can be expected to fall within twice the RMSE value from the mean fuel savings.

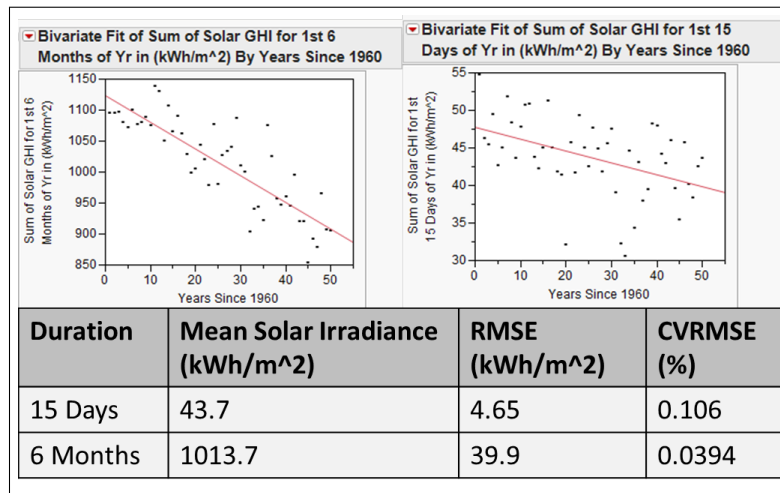


Figure 4.9: Example demonstrating the effect of different cumulative solar irradiance means on RMSE representation of variability and how CVRMSE removes the effects of different quantities of cumulative solar radiation

The measure of predicted fuel savings was set to be a percentage in order to remove the effects of varying levels of cumulative fuel savings on the fuel savings variation. A similar concern is seen in quantifying how the degrees of solar irradiance variability change for different scenarios.

When comparing RMSE between scenarios of different durations, locations, and seasons, the differences in cumulative solar irradiance make the RMSE less useful because its value is relative to the mean cumulative solar irradiance of the given scenario. To assess the effects of duration, location, and start time on solar irradiance variability the effect of varying cumulative solar irradiance must be removed. This is accomplished by employing the CVRMSE as the measure of inter-annual variability in solar irradiance. CVRMSE removes the effects of varying cumulative solar irradiance means by dividing the RMSE by the solar irradiance for the respective scenario. The Figure 4.9 example demonstrates the benefits of this approach by comparing representations of variability for the first fifteen days and for the first six months of each year in Albuquerque, New Mexico.

The RMSE of inter-annual solar irradiance is expressed in units of kilowatt-hours per square meter. Comparing the RMSE measures of variability for the fifteen day and six month duration,  $4.65 \text{ kWh/m}^2$  vs  $39.9 \text{ kWh/m}^2$ , gives the impression of six month du-

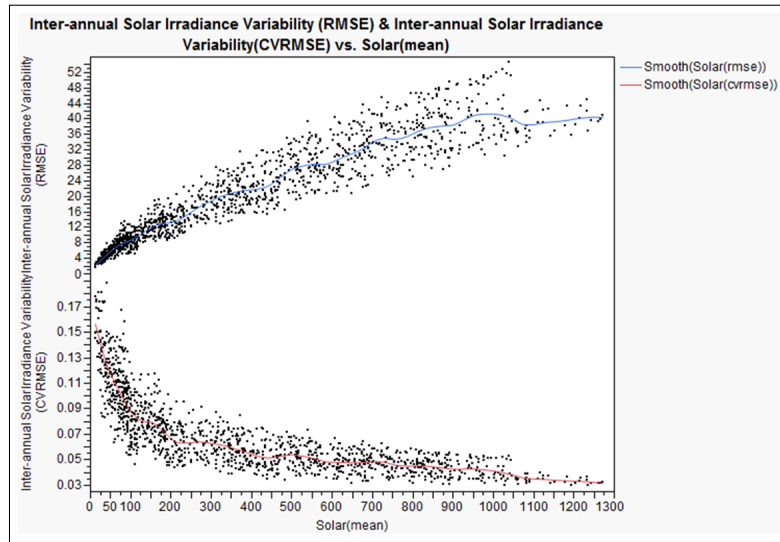


Figure 4.10: The effect of varying means on RMSE representation of variability and how CVRMSE removes these effects of varying means

ration having a higher degree of variability. The RMSE does not account for the different measures of mean solar irradiance though. The CVRMSE measures in Figure 4.9 show that the shorter duration scenario represents greater variability relative to the mean cumulative solar irradiance of the scenario. In fact, the shorter scenario's CVRMSE of .106 represents over twice the variability seen in the longer scenario's CVRMSE of .0394.

Expanding the scope of the analysis to evaluate the variability of all scenarios, Figure 4.10 shows how CVRMSE removes the effects of increasing cumulative solar irradiance from the measure of solar irradiance variation with regard to changing mean cumulative solar irradiance. The CVRMSE quantification of inter-annual variability in solar irradiance seen in Figure 4.10 removes the effects of the increased cumulative solar irradiance and allows the user to identify interesting relationships. For the remainder of this thesis, while inter-annual variability in HOMER-predicted fuel savings will be quantified as RMSE in units of percent fuel savings, the inter-annual variability of measured solar irradiance will be quantified as the CVRMSE of measured cumulative solar irradiance.

### **4.3 Assessing HOMER Robustness with Regard to Temperature Variability**

The HOMER model allows users to include the effects of ambient temperature in their simulations. Just as with solar irradiance the use of typical meteorological data for temperature profiles provides additional uncertainty associated with inter-annual variability. In Chapter 2 the effects of temperature on PV cell performance were discussed, and it was identified that temperature effects come not only from ambient temperature but also from the temperature changes associated with solar irradiance striking the PV cell. The option for including ambient temperature in the model accounts for both of these temperature influences. For this thesis, because the solar irradiance effects of temperature cannot be disassociated from the power effects of varying solar irradiance, analysis of "temperature variation" on the HOMER model refers to the effect of ambient temperature variation. To accomplish this focus on temperature variation, solar irradiance profiles are derived from the TMY3 solar irradiance values for the specific scenarios across all years. In these temperature focused simulations inputted temperature profiles are derived from the NSRDB temperature profiles for the specific year being simulated for each scenario.

#### **4.3.1 Quantifying Inter-annual Temperature Variability: RMSE**

With temperature means ranging above and below zero degrees Celsius, CVRMSE cannot be employed for quantifying temperature variation. This is because CVRMSE cannot be calculated when the values that are measured can be either positive or negative. Because of this, and the minimal linear relationship between scenario mean temperature and temperature variability, temperature variability is quantified in this thesis in terms of RMSE with units of degrees Celsius.

Figure 4.11 shows that an inverse linear relationship exists between scenarios' mean temperature values and temperature variability in RMSE. Figure 4.12 demonstrates that while the linear fit has a reasonably strong fit, with an RSquare of 0.380, the Polynomial fit shows a stronger fit with a RSquare of 0.534. This shows that scenarios' interannual temperature variability increases at a quadratic rather than linear rate as the mean temperature of a scenario decreases.

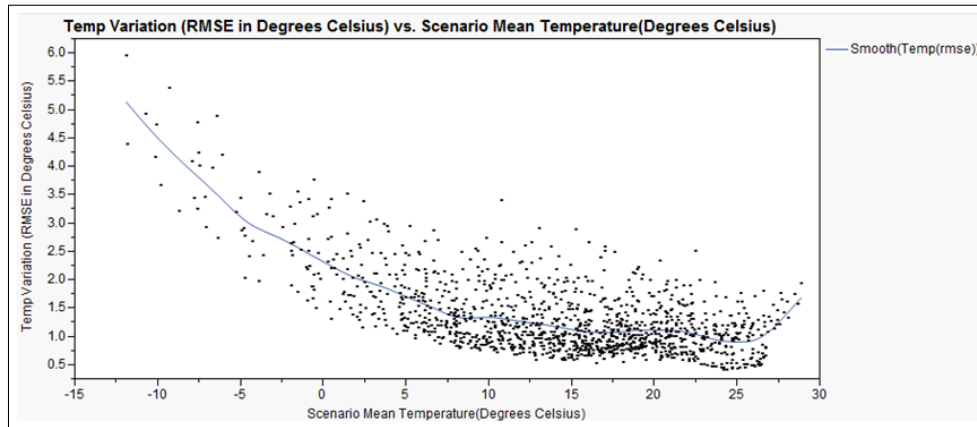


Figure 4.11: Relationship between scenarios' mean temperature values and variability in temperature in RMSE

For the purposes of this research, RMSE is considered sufficient for quantifying variability in temperature. Figure 4.12 shows the generally inverse relationship between temperature means and temperature variability in RMSE.

### 4.3.2 Acquisition and Synthesis of Temperature Data

In order to conduct an analysis of the HOMER model's robustness with regard to temperature variability, a source for hourly temperature data needed to be identified. To allow this research to also assess the relationship between temperature variability effects and solar irradiance variability effects, this source needed to provide temperature measurements for the same ten locations as seen in the solar irradiance data. The NSRDB contains the solar irradiance measurements, but it does not contain measured temperature data.

The National Climatic Data Center's (NCDC) Climate Data Online system does provide temperature data associated with those same 10 locations. This system provides Integrated Surface Data (ISD) that includes temperature in the meteorological data section of its measurements. Additionally, the system identifies the locations where data is collected by USAF number, latitude, and longitude, helping to ensure that the 10 locations used for temperature measurements collection match those used in the solar irradiance analysis. While the NCDC ISD provided the temperature profiles needed for this research, the data required significant synthesis before it could be used. The two flaws in the data were (1) a lack of consistent "on the hour" measurements and (2) gaps in data throughout the years of

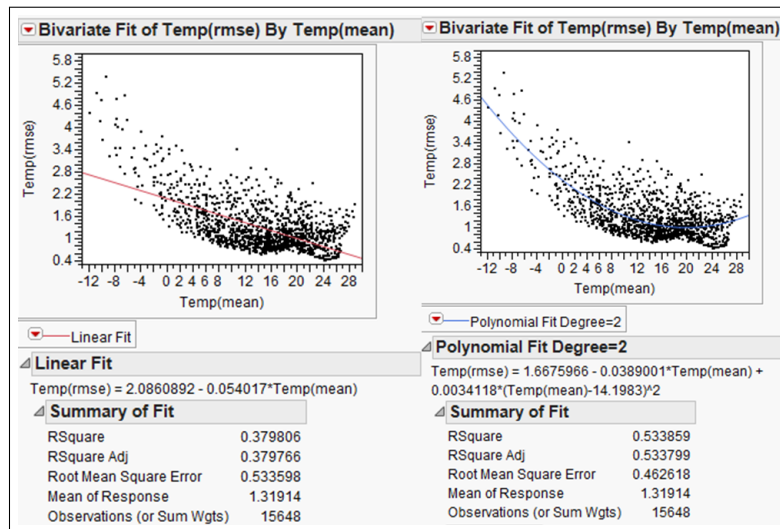


Figure 4.12: Relationship between scenarios' mean temperature values and variability in temperature in RMSE described with a linear fit (left) and described with a quadratic fit (right)

each location.

The required synthesis to fix and properly identify the extent of these flaws was accomplished using two java scripts. The first script accounted for missing temperature measurements and for those not measured on the hour. Like with solar irradiance profiles, temperature profiles loaded into the HOMER model must be provided with values for every hour on the hour for the entirety of the given time frame. Some of the ISD days provided measurements for every hour on the hour, but some days of measurements provided more or fewer values and values at times off the hours. To fix this, the first script iterated through every hour from 1961 to 2010 for the temperature data for each location, identifying the temperature measurement closest to the given hour that is within a half hour of that hour. This script also flagged all hours lacking a temperature measurement so that the absence of the measurement would be considered when building experimental runs later. This first script provided an adjusted CSV file to was used to facilitate later leap year and time zone corrections. The second script identified all missing data to allow support the creation of an experiment design considering only the full temperature files. This was done by reading in the adjusted CSV file mentioned above. The script accounted for leap years by bypassing all February 29 values and, since the ISD data is provided in Universal Time Code time,



changing the time to local time according to the location.

Due to this research including hourly data across 50 years and 10 locations, acquiring perfect data was not possible. This analysis was therefore conducted under the assumption that temperature measurements obtained within 30 minutes of the given hour have negligible fluctuations in value from that hour mark. All dates and locations that lacked a measurement within 30 minutes of any hour were not included in experiments. A HOMER input scenario file was written that dictated the scenario locations and time frames to be run as well as the particular years to be included in each scenario's simulations. To create this input scenario file, a java script was written to compile the input scenario file and only include scenarios where at least 30 years' worth of complete data were available for each time frame and location. In order to actually execute these experiments, an interface needed to be developed to provide access to the HOMER application programming interface (API).

## **4.4 Accessing the HOMER API**

HOMER LLC has continued to expand the models application and improve its GUI since the software the company was established in 1997. Over the course of these improvements the HOMER model software has been released in multiple versions. Version 2.0, released in 2001, increased the model's applicability to micropower systems that are connected to an electrical grid [41]. In the development of version 3, the company detached the HOMER model engine from the GUI. This means HOMER 3.0 modeling and simulation engine was left without a graphical interface for accessing the API. Part of the reason for this was that the HOMER team did not release HOMER 3.0 and instead progressed to developing HOMER 4.0. HOMER 4.0 was in beta development for the duration of this research's experiments.

In recent years, and in coordination with ONR and E2O, HOMER LLC has sought to modify the HOMER model to make it meet specific Marine Corps expeditionary power planning needs. This USMC version of the HOMER model was developed by combining and modifying capabilities of the HOMER Explorer and HOMER Professional versions [42]. Executing this research on HOMER 4.0 or the USMC version of HOMER was not feasible due to the status of both versions in beta development. This research was accordingly conducted using the HOMER 3.0 engine. HOMER 3.0 was sufficient for the purposes of this

research since the HOMER engine itself was not significantly affected in the modification of the modeling and simulation software in the development of the USMC version.

HOMER 3.0 met the requirements for analyzing the HOMER engine, but a user interface was needed for accessing the API and executing the DOE. Running a full factorial analysis of the HOMER model as specified requires the execution of several million HOMER simulations. Executing these millions of HOMER simulations would have taken approximately 771 computer hours, not including trouble shooting time requirements. This would not have been feasible for my lone laptop. Assistance was found with the computer cluster run by the Simulation, Experiment and Efficient Designs Center for Data Farming (SEED Center). The SEED Center's cluster was essential for executing the DOE as it provided for the executed of these simulations in a matter of hours rather than weeks. In order to utilize the SEED Center's cluster a user interface accessible through the command line was required. This java interface was built over a week in Boulder, CO, with the SEED Center's Steve Upton and HOMER LLC's John Glassmire.

During this week-long visit to the HOMER team offices in Boulder, Upton was instrumental in the identification of the HOMER 3.0 API methods required for manipulating all required factors. Upton then developed a java interface that accesses the API and provides it with the necessary factor specifications and the input files required to execute the model accordingly. Greater detail regarding the construction and design of the interface designed and built by Upton to support this research can be found in the "read me" document he wrote for the interface. This "read me" is provided in appendix 1.

Following a considerable amount of interface trouble shooting, the final interface was used to execute the previously described DOE. The HOMER output for each simulation was then combined into large CSV files. These simulation output files, containing the output of hundreds of thousands of scenarios, were used in the R and JMP analysis discussed in the previous sections of this chapter. SEED Center analyst Mary McDonald provided considerable assistance in combining these files and in calculating the several measures of performance and variability required for the conduct of this research.

---

## CHAPTER 5:

### Analysis and Findings

---

#### 5.1 Analysis Techniques

This analysis was conducted using JMP Statistical Discovery Software. JMP facilitated the analysis of inter-annual variability in fuel savings predictions, cumulative solar irradiance measurements, and average temperature measurements across the factors of location, length of operation, start date, size of the unit simulated, and the number and size of internal combustion generators included in the micropower system.

The primary JMP tools employed for this analysis included partition trees, linear regressions, and the wide variety of JMP visual data representation capabilities. For analysis of solar irradiance and temperature variability, partition trees were implemented first to identify which factors were most influential on the inter-annual variability of HOMER fuel savings predictions. After identifying the most influential factors, JMP graphical displays and linear regressions were employed to identify the nature of the relationships.

Where applicable, linear regressions were employed to quantify the linear relationship between individual factors and the variation being evaluated. To ensure the thoroughness of this analysis, multiple graphical depictions of the results were constructed for each factor and for combinations of factors to facilitate a visual exploration of the data. This visual exploration allowed for an identification of non-linear relationships between factors and the measures of variability in fuel savings, solar irradiance, and temperature.

The first section below will present analysis of the HOMER model's robustness in the way of fuel savings estimates' variability due to inter-annual solar irradiance variability. This analysis was accomplished by utilizing the unique fifty solar irradiance profiles for each location as described in the previous chapter, while deselecting the HOMER option of including temperature considerations. The second section compares fuel savings estimates derived using TMY3 solar irradiance profiles to those derived using the NREL measured annual profiles. The third section below presents analysis of the HOMER model's robustness in the way of fuel savings estimates' variability due to inter-annual temperature

variability. This analysis was accomplished by executing the HOMER model with TMY3 solar irradiance files, selecting the HOMER option of including temperature considerations, and inputting the unique temperature files for each year and location as discussed in the previous chapter. The fourth section below compares the variability in HOMER fuel savings estimates that is due to inter-annual solar irradiance variability and the variability of HOMER estimates that is due to inter-annual temperature variability. The fifth and final section below identifies how the inclusion of PV and battery bank systems similar to GREENS in a micropower system affects the benefits derived from using multiple different sized generators over a single, peak load capable generator.

## **5.2 Analysis of HOMER Robustness with Regard to Inter-annual Solar Irradiance Variability**

The HOMER model's output from each of the simulations was compiled into single measures of performance (MOP) quantifying fuel savings variability for every scenario across the range of complete years of data utilized. Each MOP quantifies the variation in fuel savings derived from employing the GREENS system for each scenario.

As mentioned in the previous chapter, the RMSE of cumulative percent fuel savings is the MOP used to assess the variability of HOMER's fuel savings predictions relative to the variability associated with the effects of global dimming for each location. Comparing the RMSE of each scenario allows this research to analyze the HOMER model's robustness given varying degrees of solar irradiance variability. Analyzing how the variation in fuel savings predictions is affected by each factor was conducted by first investigating the effects of each factor across all 50 years of the measured solar irradiance profiles for each location.

The factors being assessed, as outlined in Chapter 4, include the size of the simulated unit, composition of diesel generators in the system, physical location, duration of the simulated operation, and the season(s) of the simulated operation. Since the MOP for this analysis is the RMSE of fuel savings achieved through the use of the GREENS system for each scenario, there is only one data point (RMSE value) for each set of factor levels.

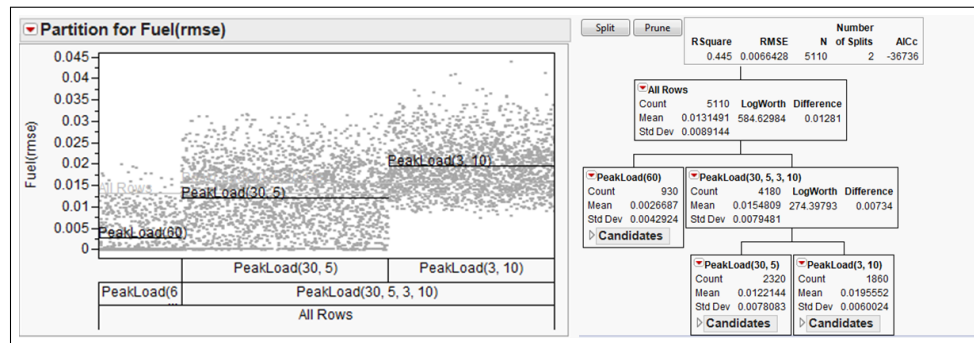


Figure 5.1: Partition tree showing peak load as the most influential factor in determining RMSE of percent fuel savings with regard to solar irradiance variation effects

## 5.2.1 Solar Irradiance Variability: Effects of Unit Size on HOMER Fuel Savings Estimates

A partition tree was employed with the RMSE of percent fuel saved as the Y value and with all factors of the DOE as the X variables. The factors included were peak load of the scenario load profile, duration, location, and operation start date. The partition tree is shown in Figure 5.1 with the two most influential splits. The results of this preliminary partition tree showed that the peak load of the micropower system has the greatest effect on the variability in HOMER predictions of percent fuel savings. After identifying this, additional graphics were utilized to facilitate visual exploration of the nature of the relationship between peak load and variability in fuel savings predictions.

Figure 5.2, which includes RMSE for only the 15-day and 1-month scenarios, shows that the peak load of the system has a strong influence on the variability of percent fuel savings in RMSE. The relationship between the systems of different peak loads shows that the predicted fuel savings of simulated 3kW and 10kW micropower systems are generally more affected by inter-annual solar irradiance variation than the simulated 5kW, 30kW and 60kW systems are, with the 60kW systems being the least affected by solar irradiance variation.

It was expected that scenarios with different peak loads, with their different generators meeting the loads and different numbers of GREENS systems providing renewable energy to help meet those loads, would have differing degrees of variability in percent fuel savings. The reason for including the different unit sizes, and representing them by different peak

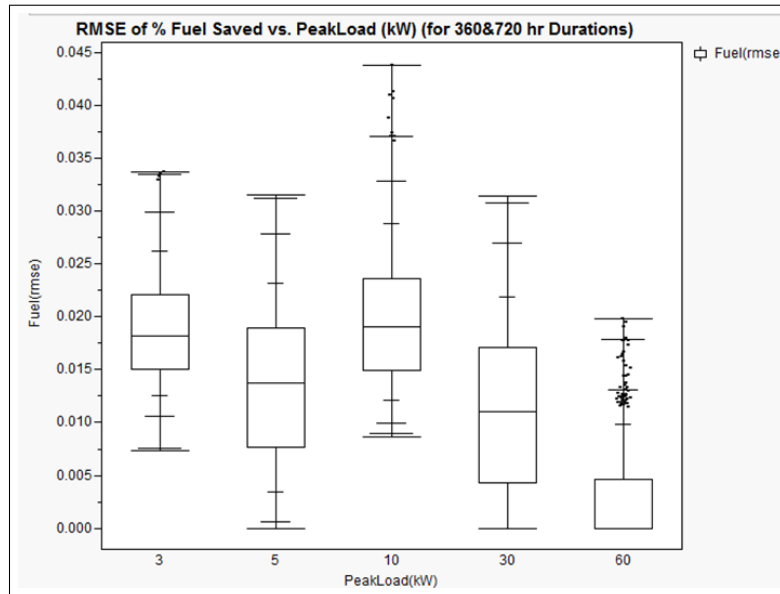


Figure 5.2: Graphical representation of the relationship between scenario peak load and inter-annual variability in predicted fuel savings

power loads and equipment compositions, was to identify how other factors' effects would differ between the different unit sizes. The fact that variability in predicted fuel savings was at its highest for the 3kW and 10kW scenarios, rather than increasing or decreasing relative to increasing or decreasing peak load levels of all scenarios, showed that some characteristic of the different scenarios other than peak load level was having the greatest impact on inter-annual variability of fuel savings predictions. After looking further into this relationship it was identified that those scenarios with the greatest inter-annual variability in predicted fuel savings were the scenarios with the highest ratio of PV power production capacity to peak load level.

Figure 5.3 shows how scenarios with different peak load levels differed in their ratio of PV power production capacity to peak load profile levels. Micropower systems with a higher ratio of PV production capacity to peak load are shown to be generally more capable of gaining fuel savings from employing PV-battery systems. Micropower systems with a lower ratio of PV production capacity to peak load are less capable of providing fuel savings because they provide less cumulative PV power relative to load requirements. A lower ratio also decreases the amount of the load that can be covered by the PV arrays

Peak Power level (kW)	Maximum Power Provision Capacity for PV Arrays of Associated Scenarios (kW)	Ratio of Peak Load Level to PV Power Production Capacity
3	1.76	0.59
5	1.76	0.35
10	5.28	0.53
30	8.8	0.29
60	8.8	0.15

Figure 5.3: Table shows the maximum PV power available for each scenario relative to the scenario's peak load level

in these scenarios because of the stand-alone converters used. When using a stand-alone (not grid-tie capable) converter, the PV array(s) can only provide power to the load when they can replace the generator(s) completely, this requires the PV power available is to equal or exceed the load for the given time steps. Because of this, the systems with a smaller ratio of PV power production capacity to peak load have a smaller trade space for employment of PV power which is where fuel savings variation can occur. The systems with the smaller ratio are therefore more likely to have scenarios with mean fuel savings of zero, and variability in fuel savings of zero will be zero. This is best seen with the 60kW scenario, which has the lowest ratio of PV power production capacity to peak load and for which 75 percent of scenarios have a mean fuel savings predictions below 3 percent. For all other peak load scenarios combined, 75 percent of mean fuel savings predictions are greater than 14 percent.

For the 5kW, 30kW and 60kW scenarios, which all had smaller ratios of PV power production capacity to peak power load than the 3kW and 10kW scenarios, a strong linear relationship between mean predicted fuel savings and variability in predicted fuel savings is seen. Figure 5.4 shows how this linear relationship is present for the 5kW, 30kW and 60kW scenarios, with RSquare values of .38, .52 and .71, respectively. Figure 5.4 also shows how variability in predicted fuel savings in the 3kW and 10kW scenarios is much less affected by mean predicted fuel savings, with RSquare values of .01 and .02, respectively. This identified how differences in the scenario ratios of peak load level to PV power production capacity affect PV array performance and fuel savings variability. This also pre-

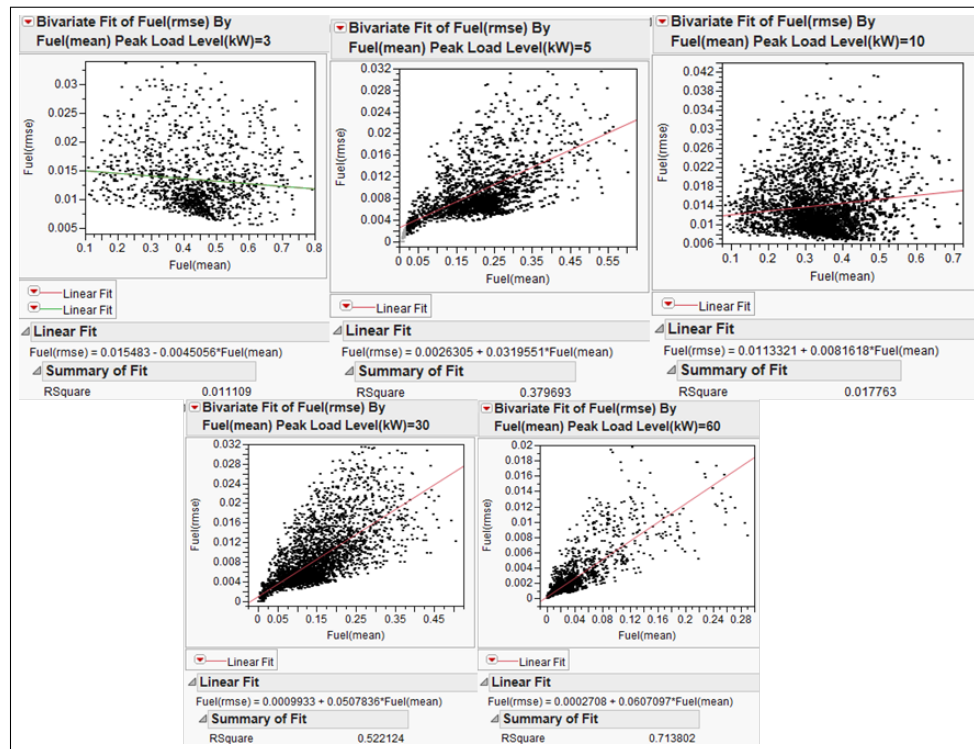


Figure 5.4: Graph shows strong linear relationship between mean predicted fuel savings and variability in predicted fuel savings for 5kW, 30kW and 60kW scenarios for HOMER prediction variability resulting from inter-annual solar irradiance variability

sented a concern for how to conduct the analysis of the other factors in the DOE, including duration, season and location.

For the analysis of the other DOE factors, analysis across the 5kW, 30kW, and 60kW scenarios would suffer from the confounding effects of the relationship between mean predicted fuel savings and variability of percent fuel savings. This confounding effect would influence the perceived relationship between the assessed DOE factor and variability in predicted fuel savings. In the end, it was decided to keep scenarios of all peak load levels in the analysis, with the recognition that the 3kW and 10kW scenarios would best represent the effects of the subsequent factors to be evaluated. Analysis of the other factors in the DOE was conducted separately for each of the 5 different peak power levels. This separation was done to remove the effects of different peak load levels and different PV power to load ratios between the scenarios, minimizing the confounding effects of both peak load



levels and mean predicted fuel savings levels in the analysis of other DOE factors.

It is important to clarify that while the load profiles and peak loads of these scenarios are based on ONR and E2O experiments, and while the equipment simulated for the experiments is Marine Corps equipment, the GREENS system simulated in these simulations is meant to provide a representation of solar power that would be provided by other PV hybrid power systems. These results therefore do not accurately represent, and are not meant to represent, the ability of Marine Corps solar power equipment as it currently exists to support the varying levels of load profiles. For these scenarios it is also worth reemphasizing that all variation is due solely to inter-annual differences in solar irradiation, which is the only factor changed in the model inputs across the fifty years of data for each design point.

### **5.2.2 Solar Irradiance Variability: Effects of the Duration of an Operation on HOMER Fuel Savings Estimates**

Having identified the high degree of influence of a micropower system's peak load level, as well as the influence of the PV power capacity to peak load ratio, on the variability of predicted fuel savings, partition tree analysis was used to determine the second most influential factor. This time a partition tree was used for the results of each peak load separately to determine what factor was most influential for scenarios of different peak load levels.

A partition tree, executed with scenarios of all peak load levels, showed that the most significant factor across all scenarios after peak load level was simulation duration, with an RSquare value of 0.165. Although duration was found to be the most influential factor in determining RSME of percent fuel savings, the degree of influence varied depending on the peak load of the micropower system. This can be seen in Figure 5.5, which shows that duration explains more about the RMSE variability of predicted fuel savings when the micropower system's peak load is 3kW or 10kW. The season, or start time, of a simulation provides more insight into the breakdown of RMSE values when the scenario peak load is 5kW, 30kW, or 60kW. As discussed in the previous section, the 5kW, 30kW, and 60kW scenarios are influenced by the confounding effects of mean predicted fuel savings. The confounding effect of mean predicted fuel savings can be seen through a visual exploration of the effects of simulation duration and start time, seen in Figure 5.6 and Figure 5.7,

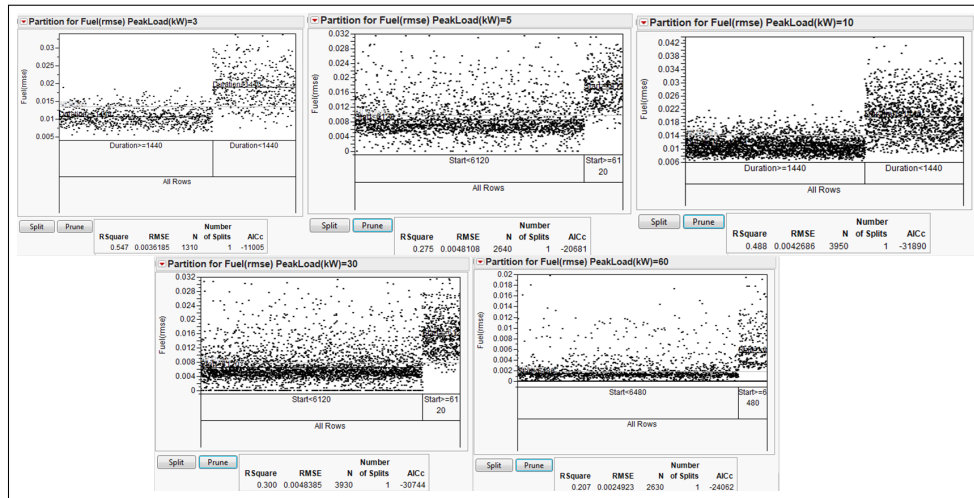


Figure 5.5: Partition tree showing differences between peak load scenarios in what qualifies as the second most influential factor in determining RMSE of percent fuel savings with regard to solar irradiance variation effects

respectively.

Figure 5.6 and Figure 5.7 visualize the effects of duration and season on mean HOMER fuel savings predictions as well as their effects on the variability of HOMER derived percent fuel savings predictions. By visually assessing Figure 5.7 across the simulation start dates it is seen that the HOMER variability associated with the season factor is confounded by the effects of varying mean predicted fuel savings across the seasons. The duration factor shows no such confounding relationship between inter-annual variability in predicted fuel savings and variation in mean predicted fuel savings.

Figure 5.7 shows that the season, or start date, of simulations has a noticeable effect on both the inter-annual variability of predicted fuel savings and on the mean predicted fuel savings of the simulations. The matching bi-modal shape between the HOMER predictions variability and HOMER mean fuel savings graphs in Figure 5.7 suggests that the changes in inter-annual variability are associated with the seasonal changes in mean predicted fuel savings levels. The relationship between the graphs can be seen to be stronger for the 5kW, 30kW, and 60kW scenarios, which can be ascribed to the previously discussed confounding effects of mean predicted fuel savings. The seasonal variability in HOMER's predicted fuel savings for the 5kW, 30kW, and 60kW scenarios can therefore be ascribed to seasonal

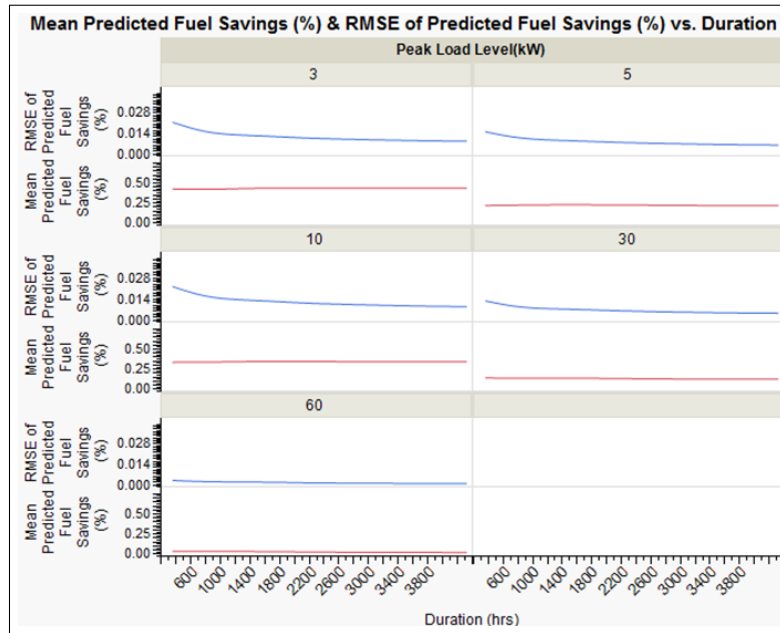


Figure 5.6: The relationship between simulation duration on mean predicted fuel savings and on inter-annual variability in predicted fuel savings

variations in load levels rather than seasonal differences in inter-annual solar irradiance variability.

While Figure 5.6 shows that duration exhibits a noticeable effect on the variability of predicted fuel savings between the years, it does not exhibit a noticeable effect on the mean predicted fuel savings. This suggests that the relationship between inter-annual variability of predicted fuel savings and simulation duration is not due to any relationship between duration and mean predicted fuel savings levels. Based on this, and the degree of influence duration exhibited on the 3kW and 10kW scenarios in the partition trees, the duration of the simulations is determined to be a more significant factor than seasonality in determining inter-annual variability of HOMER's predicted fuel savings.

As the duration of a scenario has been identified as the second most influential factor on the inter-annual variability of a scenario's HOMER fuel savings predictions, the nature of this factor's influence will now be discussed. Figure 5.8 shows that, when considering the effects of inter-annual solar irradiance variability on projected fuel savings variation, an increase in duration is associated with a decrease in the variability of HOMER percent

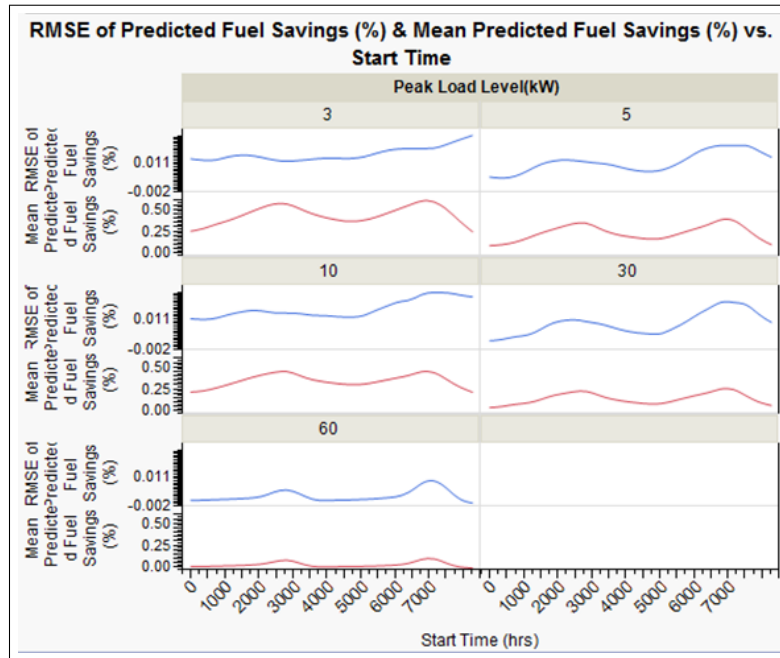


Figure 5.7: The relationship between simulation start time during the year on mean predicted fuel savings and on inter-annual variability in predicted fuel savings

fuel savings estimates. An increase in the duration of a scenario is also associated with a decrease in the range of predicted fuel savings variability.

Considering the RMSE values for the 3kW peak load scenarios helps to illustrate the variability of HOMER-generated fuel savings estimates to be expected for operations of different durations. The increase in the range of the RMSE box plots' first and third quartiles as durations of scenarios decrease in length, as seen in Figure 5.8, illustrates how operations of a longer duration have a more predictable degree of inter-annual variability. In the 3kW scenario, the RMSE first and third quartiles for percent fuel savings were 0.00946 and .0337, respectively for 15 day durations; these RMSE quartiles were .00565 and .01886 for 2 months durations; and these RMSE quartiles were .00665 and .0116 for 6 month durations. As seen in Figure 5.8, the decrease in the degree of variation (RMSE) and the decrease in the difference between first and third quartiles of the box plots is seen across scenarios of all peak loads as scenario duration increases. This analysis supports the hypothesis that shortening the duration of operations increases the variability of HOMER-generated fuel savings predictions due to increased inter-annual solar irradiance variability.

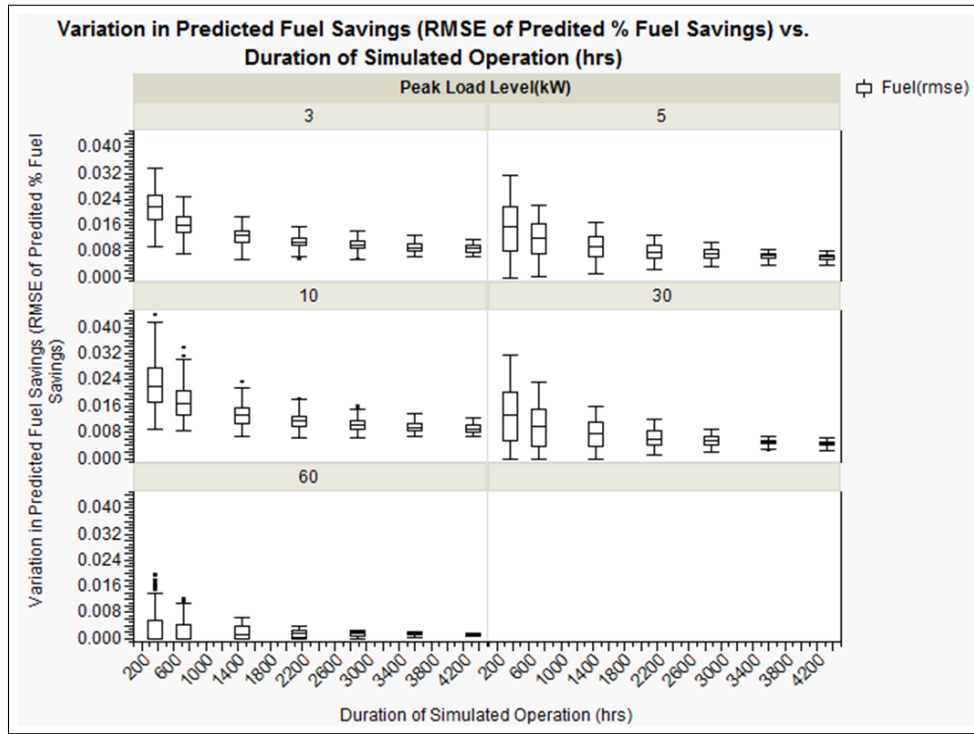


Figure 5.8: RMSE of fuel savings versus duration of simulated operation

The relationship between inter-annual surface solar radiation variability and duration mirrors the relationship between inter-annual variability in HOMER predicted fuel savings and duration, where the inter-annual variability in HOMER fuel savings predictions is due to inter-annual surface solar radiation variability. These relationships can be seen in Figure 5.9. As the duration of scenarios increase the variation in cumulative surface solar radiation decreases. The shorter duration simulations show higher degrees of variability in surface solar radiation just as they represent higher degrees of variability in HOMER-generated fuel savings predictions. Figure 5.9 shows this relationship between solar irradiance and duration, as well as predicted fuel savings and duration, in terms of CVRMSE. CVRMSE is utilized for this comparison due to the need to account for increased solar irradiance variation in RMSE that is due to increased quantities of cumulative solar irradiance from longer durations. CVRMSE provides a better representation of variability relative to the amount of cumulative solar irradiance per scenario. This relationship suggests that, by identifying the inter-annual variability of surface solar radiation associated with different

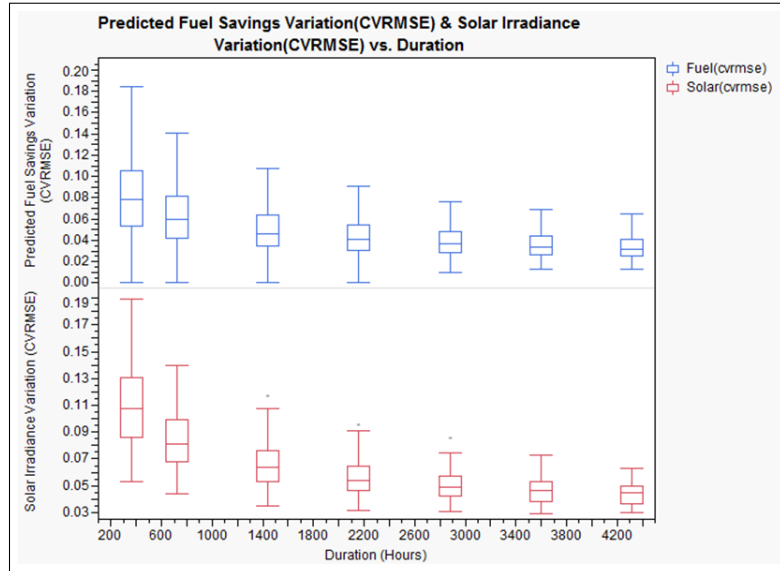


Figure 5.9: Relationship between solar irradiance variation (CVRMSE) and predicted fuel savings variation (CVRMSE) relative to duration

durations of time, for a given micropower system, location, and season, a user can estimate the inter-annual variability of HOMER fuel savings predictions associated with the simulated operation duration.

### 5.2.3 Solar Irradiance Variability: Effects of the Season of an Operation on HOMER Fuel Savings Estimates

The season of simulated operations demonstrates a minor influence on the inter-annual variability of HOMER model fuel savings predictions. As is seen in Figure 5.10, the season of a simulated operation has an increasing effect on the inter-annual variability of HOMER model predicted fuel savings as the duration of the simulation is shortened. This can be explained by noting that simulated operations of longer durations increasingly include more than one season, which can cause the results to smooth out the perceived effects of the different seasons. Analysis of seasonal effects on the inter-annual variability of HOMER fuel savings predictions will therefore focus on the fifteen day and one month scenarios. This allows for a clearer identification of seasonal effects on inter-annual variability of HOMER fuel savings predictions.

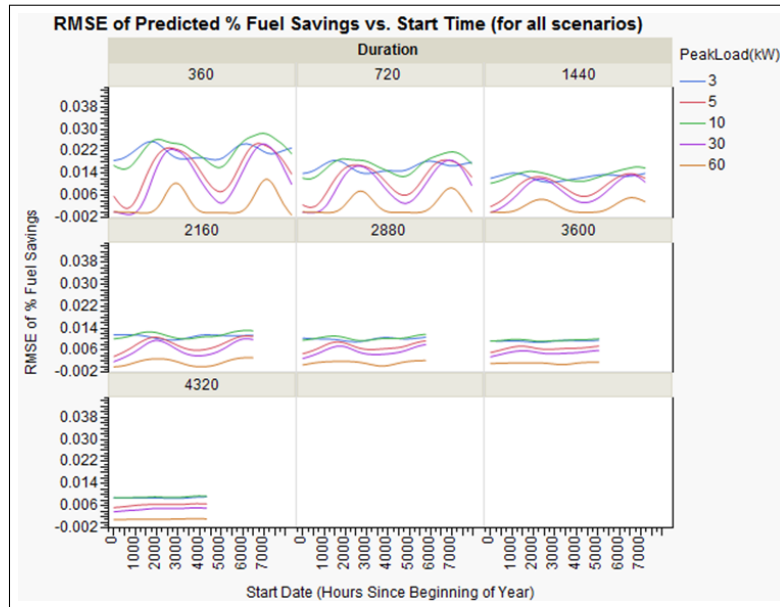


Figure 5.10: Relationship between season of simulation and variation in HOMER predictions of fuel savings

Figure 5.10 shows the degree to which inter-annual variability in predicted fuel savings fluctuates with the seasons. These fluctuations in RMSE of fuel savings predictions do not relate to the seasonal fluctuations in solar irradiance variability. While Figure 5.10 shows the seasonal fluctuations in fuel savings variability to be bimodal, Figure 5.11 shows the seasonal fluctuations in solar irradiance variability to be unimodal. Instead, the fluctuations seen in predicted fuel savings variability mirror the seasonal fluctuations in micropower system load that is specified by the user in the model. The bimodal nature of inter-annual variability in HOMER model fuel savings predictions reflects the bimodal nature of the load profiles used as model inputs.

Figure 5.12 shows the seasonal fluctuations in the power loads that were provided to the HOMER model. For the 15-day and 1-month scenarios in particular, fluctuations in the inter-annual variability of HOMER-generated fuel savings estimates mirror the seasonal fluctuations in micropower system loads and the subsequent fluctuations in mean predicted fuel savings that come from seasonal changes in the load profile. Figure 5.13 highlights this relationship between seasons and mean predicted fuel savings. Figure 5.13 also shows that this relationship is strongest for the 5kW, 30kW, and 60kW scenarios. As discussed in the

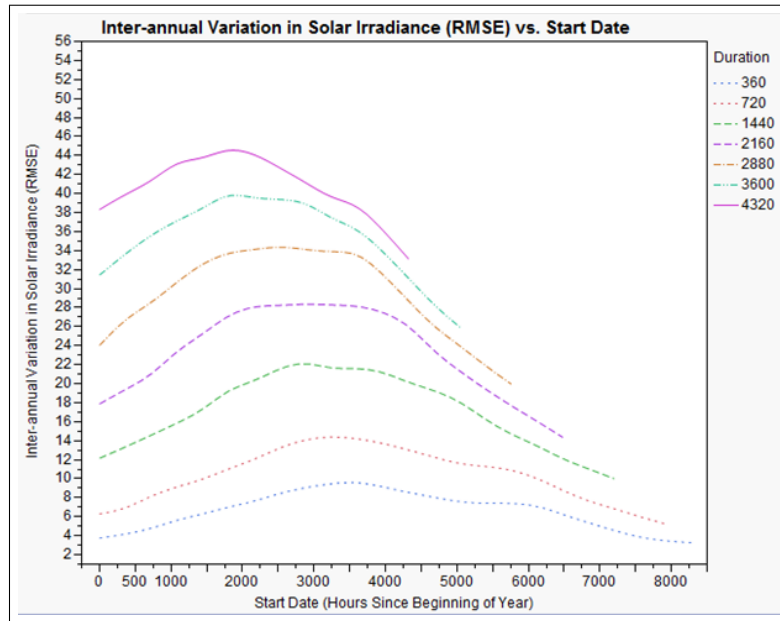


Figure 5.11: Relationship between season of simulation and variation in Surface Solar Radiation

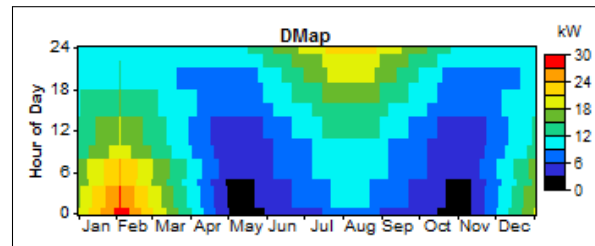


Figure 5.12: Seasonal fluctuation in power loads were provided to the HOMER model

previous section, the 5kW, 30kW, and 60kW scenarios are more affected by the load levels due to their lower ratio of PV power production capacity to peak load levels. This suggests that seasonal changes in the variability of HOMER-generated fuel savings estimates are the result of seasonal changes in load profiles more than they are the result of seasonal changes in inter-annual solar irradiance variability.

The take away from this analysis is that seasonal effects on load profile fluctuation have a greater impact on HOMER model inter-annual variability than seasonal effects have on inter-annual solar irradiance variability. Seasonal effects on inter-annual solar irradiance variability demonstrate minimal effects on the inter-annual variability of the HOMER



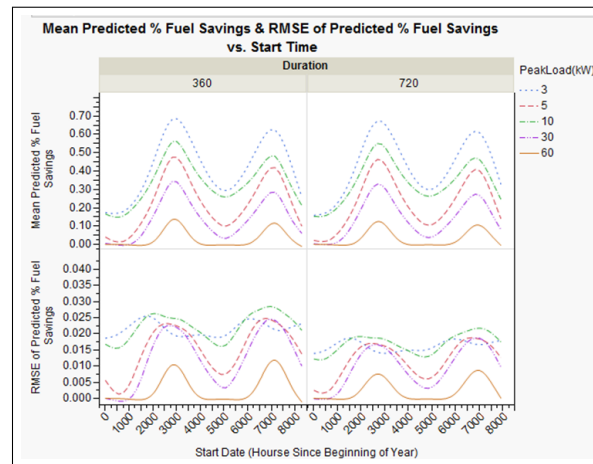


Figure 5.13: Relationship between season of simulation and variation in HOMER predictions of fuel savings, for 15-day and 1-month scenario durations

model's fuel savings predictions. For the 5kW, 30kW, and 60kW scenarios, this analysis demonstrates a relationship between seasonal load profile changes and changes in the inter-annual variability of HOMER model fuel savings predictions. These findings show that seasonal effects of inter-annual solar irradiance variability are negligible for the purposes of the Marine Corps, at least for environments such as those to be found across the continental United States. It is worth noting that the climates assessed in these simulations, which will be discussed in the following section, only allow for identification of seasonal effects of inter-annual solar irradiance for United States climates. These results are not representative of seasonal effects on inter-annual solar irradiance variability that may be seen in climates outside the continental United States. With the identification of how load profiles affect variability in HOMER fuel savings predictions, it is also worth reminding the reader that the load profiles used in these simulations were derived from an adaption to the Marine Corps' seasonal load profile template. The demonstrated influence of load profile seasonal changes on inter-annual variability of HOMER fuel savings predictions provides an additional incentive for improving the fidelity of load profiles for HOMER simulations.

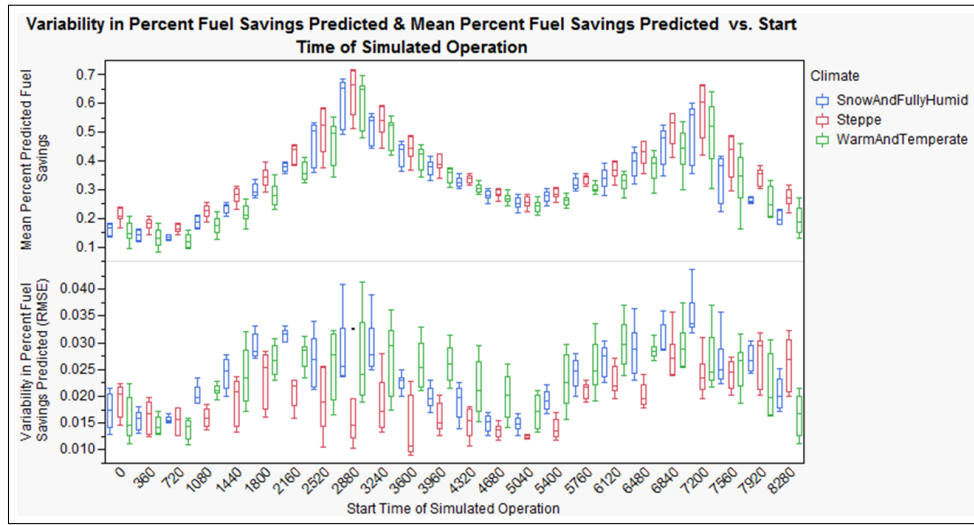


Figure 5.14: Effects of climate on inter-annual variability across the seasons, shown for 10kW and 15 day scenarios

## 5.2.4 Solar Irradiance Variability: Effects of Location on HOMER Fuel Savings Estimates

After having identified the most influential three factors of the DOE to be the size of the load supported by the micropower system, the duration of the simulation, and the season of the simulation, remaining factors included the scenario climate and the composition of diesel generators within a micropower system. The use of partition trees for this analysis was hampered due to the number of more significant factors influencing variability in HOMER model fuel savings predictions due to solar irradiance variability. Because of this, visual exploration was used as the method of analysis for identifying first the effects of climate and then the effects of different diesel generator compositions on the inter-annual variability of HOMER model predictions.

A subsection of the total data was selected for visual exploration of climate effects on inter-annual variability of HOMER fuel savings estimates due to inter-annual solar irradiance variability. Parameters for this subsection were selected, based on previous findings, to best illustrate the effects of climate on inter-annual variability by using the scenarios with the greatest inter-annual variability due to peak load and duration factor specifications. Figure 5.14 includes the scenarios with 10kW peak load levels and 15 day durations, this

included 720 data points, representing variability across 36,000 individual HOMER simulations. With the climate categories of "Snow and Fully Humid," "Steppe," and "Warm and Temperate" defined in the previous chapter, Figure 5.14 shows how the climate of a location relates to the level of inter-annual variability in HOMER model fuel savings estimates across the seasons.

While the bi-modal shape of the plots shows the confounding effects of load profile levels on the measures of mean percent fuel savings estimates and inter-annual fuel savings variability, the interesting information to pull from these graphs is how the climates' measures relate to each other. Figure 5.14 shows that the steppe climate simulations consistently have mean percent fuel savings predictions above those of the other two climate categories. This matches some expectations, as steppe climates are generally characterized by greater sunlight and fewer clouds throughout the year. Figure 5.14 also suggests that HOMER simulations for steppe climates have less inter-annual variability in fuel savings estimates for most times throughout the year. It is also interesting to note that the inter-annual fuel savings variability for the steppe climate does not follow the bi-modal shape as much as the other two climates do. This is particularly evident in the spring season, when the steppe climate demonstrates much less inter-annual variability in HOMER fuel savings predictions compared to the other climates. This is not the case for the winter season, when the mean inter-annual variability measures of the steppe climate rise above the mean inter-annual variability measures of both other climates. These findings are not surprising, but they do support the hypothesis that fuel savings estimates of HOMER simulations in steppe climates include less inter-annual variability than do estimates for the other two climates.

### **5.2.5 Solar Irradiance Variability: Effects of the Composition of Diesel Generators on HOMER Fuel Savings Estimates**

The final factor left to assess in considering how inter-annual solar irradiance variability affects the inter-annual variability of HOMER fuel savings predictions is the number and size of diesel generators used to power a given load. Analysis of this generator composition factor across each peak load level showed that the number and size of diesel generators utilized for supporting a load of a specified peak capacity had a negligible effect on the inter-annual variability of the systems for all peak load levels. To assist in focusing on factors aside from peak load, and given the similarity in HOMER results across the multiple

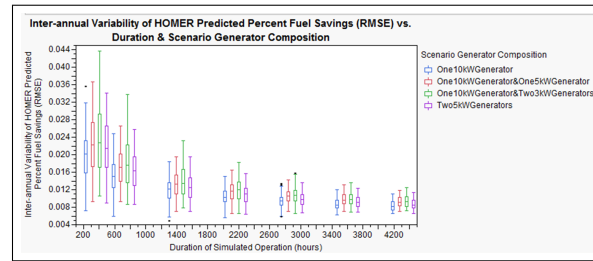


Figure 5.15: Visualization of how inter-annual variability in HOMER fuel savings predictions varies across the four different 10kW micropower system generator compositions for the seven duration levels

peak load levels, analysis of the generator composition factor was narrowed down to one peak load level for more specific analysis. It was identified earlier that the 3kW and 10kW scenarios are preferable for continued analysis, due to their higher ratio of load to solar power generation capacity. As the 10kW peak load level is the only load level, between the 3kW and 10kW scenarios, that was simulated with multiple diesel generator size and quantity configurations, the analysis of the 10kW peak load scenarios is presented here.

To support this analysis an additional generator composition was added for the analysis; a single 10kW generator scenario. Four different generator compositions were therefore simulated for scenarios with a peak load of 10kW. These included a scenario with one 10kW generator and one 5kW generator, a scenario with one 10kW generator and two 3kW generators, a scenario with two 5kW generators, and a scenario with one 10kW generator. In Figure 5.15, the different generator composition scenarios with a 10kW peak load level were further separated by duration levels. This improves the visualization of how generator composition affects inter-annual variability in HOMER fuel savings predictions. In Figure 5.15, only minimal relationship is seen between the generator composition scenarios and inter-annual variability of HOMER fuel savings predictions.

While generator composition does not provide any interesting findings with regard to inter-annual variability of HOMER predictions, this factor did provide an opportunity to investigate the relationship between the generator composition of a micropower system and fuel consumption for the given micropower system and load profile. In section 4.1.2, it was explained that scenarios including the use of multiple small generators have greater potential for decreased fuel consumption than do those scenarios that include only one large gen-

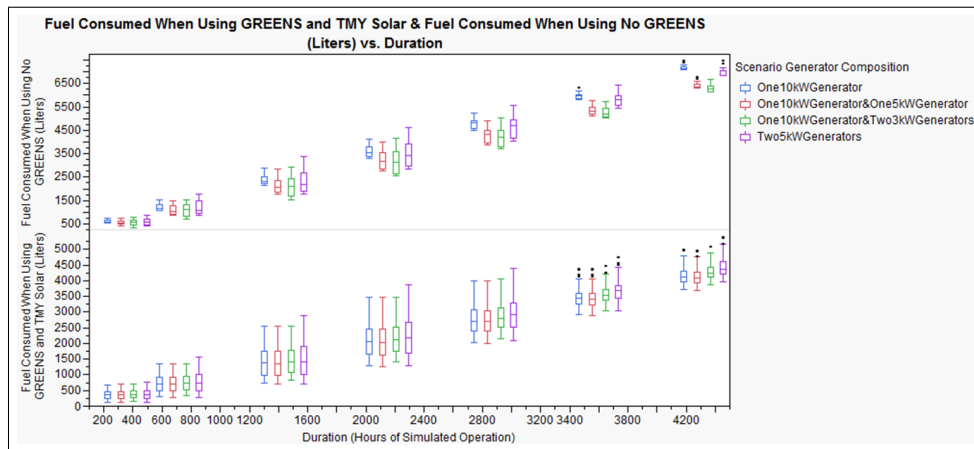


Figure 5.16: Fuel consumed (liters) when micropower system includes GREENS and TMY3 solar irradiance profiles (top) compared to fuel consumed (liters) when using no GREENS systems (bottom)

erator supporting the same load. Comparisons of fuel consumption levels across the fore mentioned scenario generator compositions have supported this hypothesis. Figure 5.16 shows how changing generator compositions for the 10kW scenarios impacted fuel consumption when GREENS systems were not included. In this figure it is seen that, when GREENS systems are not considered, greater fuel consumption is seen in the scenarios including a single large generator than in any of the other three options simulated. All scenarios included cumulative generator power production capacity capable of providing at least peak power for the load (10kW).

Having identified the benefit of providing a micropower system with more options than just a single peak power capable generator, it is next valuable to identify how inclusion of solar energy systems influences this relationship. Figure 5.17 shows that the fuel savings benefits of employing GREENS, in terms of percent fuel savings for the micropower system, differed between the different generator compositions. This figure shows that the scenario with a single 10kW generator benefited the most from employing a GREENS system.

The bottom half of Figure 5.16 shows that, when GREENS systems are included, the scenarios with only one peak power capable generator see the greatest decrease in fuel savings due to inclusion of a PV-battery system in the micropower system. In fact, the 6 month scenarios with only the one 10kW generator go from having a higher median fuel consumption

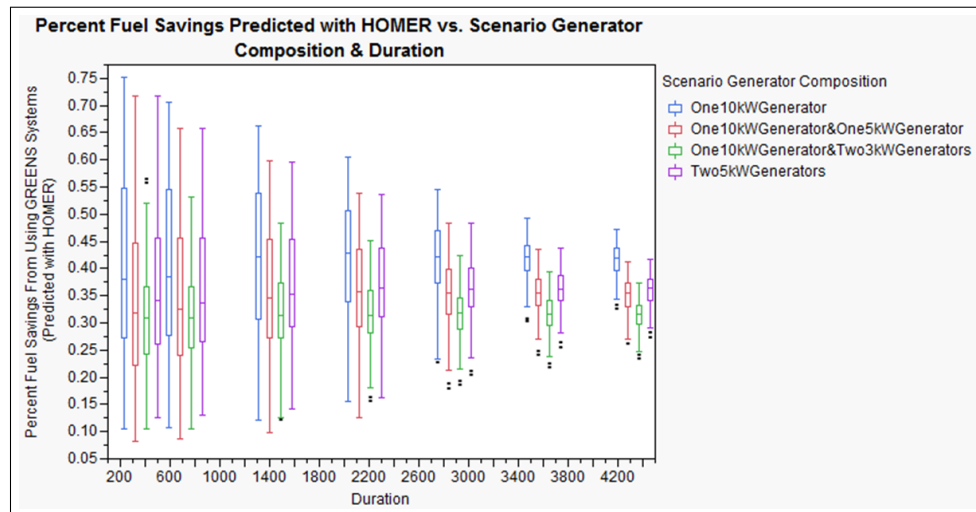


Figure 5.17: HOMER predictions of fuel savings to be gained from employing GREENS systems, with savings specified as a percentage of fuel consumed when no GREENS are employed. Graph separates HOMER predictions by duration of scenarios and by scenario generator compositions

than all other scenarios, to having lower median fuel consumption than two of the other three scenarios when GREENS systems are included. This is a counter-intuitive result, as one of those two other scenarios has a 10kW generator in its assets as well. Because of this, it was expected that the "One10kWGeneratorAndTwo3kWGenerators" scenario would be able to at least match the performance of the "One10kWGenerator" scenario. Instead, the presence of the GREENS systems reversed the relationship between the two generator composition scenarios, with the single peak power generator scenario becoming more fuel efficient than two of the three scenarios including multiple, different sized generators. This result shows that, when GREENS are present, multiple small generators can't be assumed to consume less fuel than a single peak power generator, as is seen when GREENS are not present in the micropower system.

John Glassmire of the HOMER Limited Liability Company (LLC) suggested that a possible explanation for these results is the way controllers are modeled to direct generator interaction with battery banks. A potential reason the micropower systems don't perform as expected is that the controller is operating without the "knowledge of the future" that the user has. He explained that "if you had perfect knowledge of the future, you could dispatch the generators in a way that maximized the utility of the battery, but that's not realistic [43]."

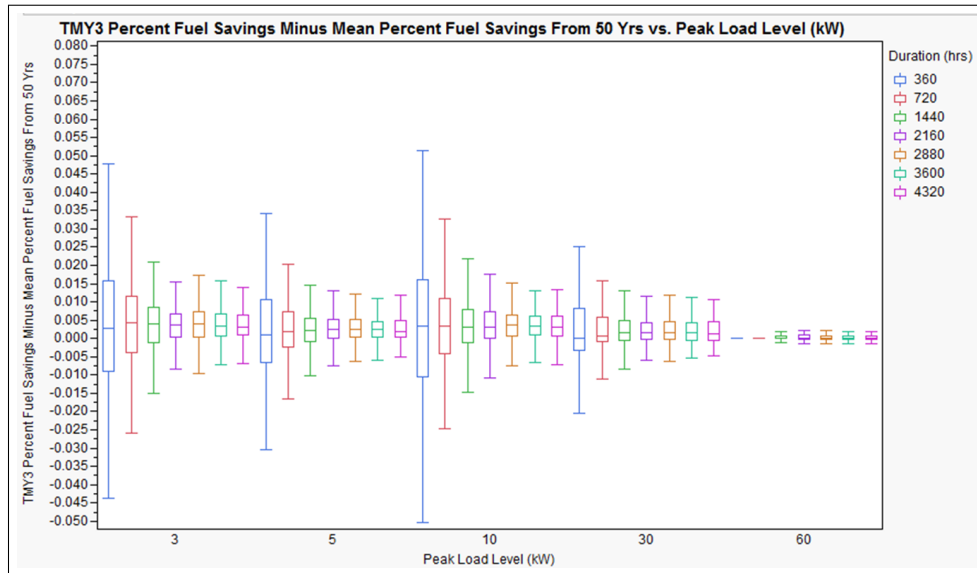


Figure 5.18: Graph shows the difference between fuel savings predictions from employing HOMER with TMY3 solar irradiance profiles and mean fuel savings predictions from employing HOMER with the 50 (1961-2010) annual measured NREL solar irradiance profiles as solar resource inputs.

Instead, controllers operate without an ability to anticipate the future load profiles or solar energy that will be available. This leaves the controllers unable to optimize the charging and discharging of battery banks or optimize the employment of different sized generators that are available.

It is unknown to the author whether smart grid controllers exist that could overcome this shortfall. Regardless of whether any do exist, it is valuable to understand how the addition of GREENS PV array and battery systems can decrease or reverse the fuel savings gained from employing multiple different sized generators instead of a single peak power capable generator.

### 5.3 HOMER Fuel Savings Predictions Using TMY3 Profiles Compared to Fuel Savings Predictions Using Measured Solar Irradiance Profiles

In the previous section, the effect of inter-annual solar irradiance variability on the inter-annual variability of HOMER predictions was quantified. This section will identify how

the fuel savings predicted with the use of TMY3 solar irradiance profiles relate to the mean fuel savings predicted with the use of the 50 annual solar irradiance profiles from 1961 to 2010. These 50 measured annual solar irradiance profiles are the NREL profiles which were used to evaluate the effects of inter-annual solar irradiance variability as discussed in the previous section. This section will also discuss how predictions achieved using the TMY3 profile solar inputs relate to predictions achieved using annual measured profiles from only the last 10 years of measured NREL data (2001-2010). This will provide some insight on how long-term trends in solar irradiance, namely global dimming, impact the use of TMY3 profiles as solar resource inputs for HOMER fuel saving predictions.

Comparison of the fuel savings estimates generated with TMY3 solar profiles and the fuel savings estimates generated with the 1961-2010 annual measured solar profiles was conducted, and is shown in Figure 5.18. For each individual scenario, Figure 5.18 shows a plot of the mean fuel savings predicted using HOMER across the 50 annual solar irradiance profiles and a plot of the fuel savings predicted using HOMER with TMY3 solar irradiance profiles for each individual scenario. The difference between estimates from TMY3 inputs and estimates from the 50 annual measured profiles was calculated for each individual scenario by subtracting the latter's percent fuel savings prediction from the TMY3-generated percent fuel savings estimate. The visualization of the differences in estimates is categorized both by scenario peak load and by scenario duration. As can be seen in Figure 5.18, the HOMER fuel savings estimated using TMY3 solar irradiance profiles had a median of variation of less than half a percent above the mean HOMER fuel savings estimated using the 50 measured annual profiles. This shows that there is a difference of less than a half of a percent between TMY3-generated fuel savings predictions and the mean fuel savings predictions generated derived from using the 50 measured annual solar profiles.

The second analysis mentioned at the beginning of this section, the identification of global dimming effects on the use of TMY3 profiles in HOMER, was conducted in a manner similar to this first analysis. The difference between TMY3-generated fuel savings estimates and estimates derived from using the 10 (2001-2010) annual profiles was calculated for each individual scenario by subtracting the latter mean percent fuel savings prediction from the TMY3-generated percent fuel savings estimate. The results of this analysis, again categorized by scenario peak load and by scenario duration, can be seen in Figure 5.19.



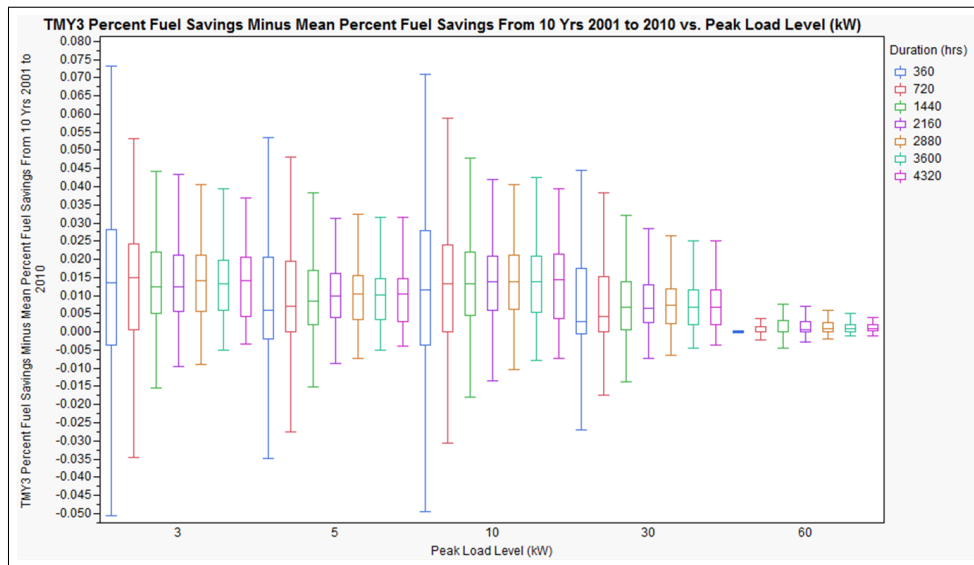


Figure 5.19: Graph shows the difference between fuel savings predictions from employing HOMER with TMY3 solar irradiance profiles and mean fuel savings predictions from employing HOMER with the 10 annual measured NREL solar irradiance profiles for the years 2001-2010 as solar resource inputs.

Figure 5.19 shows that the fuel savings estimated with the HOMER model using the most recent 10 years of annual solar irradiance profiles were lower than the TMY3-generated fuel savings estimates for the different scenarios.

Figure 5.20 shows the difference between TMY3-generated fuel savings estimates and fuel savings estimates generated using the 50 years of solar irradiance profiles. Figure 5.20 also shows the difference between TMY3-generated fuel savings estimates and the fuel savings estimates generated using the most recent 10 years of solar irradiance profiles. In Figure 5.20 it can be seen that the median difference between HOMER fuel savings predictions derived from using 2000-2010 annual solar irradiance profiles and HOMER fuel savings predictions derived from using TMY3 profiles is 1.36% and 1.35% for the 3kW and 10kW scenarios, respectively. The median difference between HOMER fuel savings predictions derived from using TMY3 solar profiles and the HOMER fuel savings predictions derived from using all 50 years of solar irradiance profiles is 0.37% and 0.33% for the 3kW and 10kW scenarios, respectively. This suggests that HOMER fuel savings predictions made with TMY3 solar irradiance input profiles can be expected to overestimate

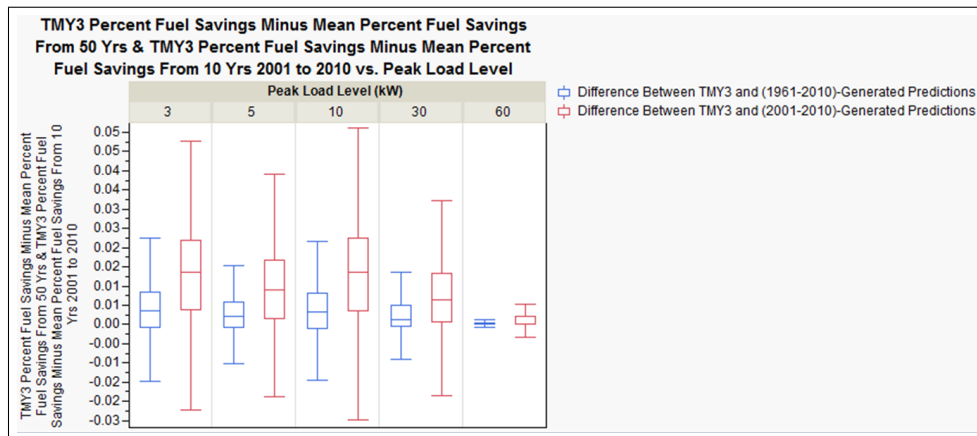


Figure 5.20: Graph shows the difference between fuel savings predictions derived from employing HOMER with TMY3 solar irradiance profiles and mean fuel savings predictions from employing HOMER with the 10 annual measured NREL solar irradiance profiles for the years 2001-2010 as solar resource inputs. Graph also shows the difference between fuel savings predictions from employing HOMER with TMY3 solar irradiance profiles and mean fuel savings predictions from employing HOMER with the 50 (1961-2010) annual measured NREL solar irradiance profiles as solar resource inputs.

fuel savings to be derived from using PV-battery systems by roughly one percentage point due to the effects of global dimming alone.

## 5.4 Analysis of HOMER Robustness With Regard to Inter-Annual Temperature Variability

Analysis of how inter-annual temperature variability affects the robustness of the HOMER model's fuel savings predictions was accomplished in a similar manner to the analysis demonstrated above, which investigated solar irradiance variability effects. RMSE is the MOP for inter-annual variability of percent fuel savings predicted by the HOMER to be achieved by employing GREENS systems. This is the same MOP for HOMER robustness as was used in the analysis of inter-annual solar irradiance variability effects on the model. While CVRMSE was utilized as the measure of inter-annual solar irradiance variability, RMSE is utilized as the measure of inter-annual temperature variability. By using an average temperature rather than cumulative temperature measure in this analysis, the effects of varying the duration of simulations is already accounted for. This allows RMSE to be employed rather than CVRMSE for identifying and comparing the inter-annual tem-

perature variability of the scenarios. The following subsections iterate through the factors of the DOE, identifying how inter-annual temperature variability affects the robustness of HOMER fuel savings predictions and identifying how each factor of the DOE affects that relationship. For analysis of temperature effects, generator composition was not included. The additional experiment with scenarios generator compositions consisting of one 10kW generator alone was only executed with variations in the solar irradiance input and not temperature input. Without this scenario, there is little that can be gleaned from the analysis of generator composition effects with regard to inter-annual temperature variability. The ordering of the factors considered (unit size, duration, season, and climate) is based on partition tree identification of decreasing influence on inter-annual variability of HOMER fuel savings predictions.

#### **5.4.1 Temperature Variability: Effects of Unit Size on Variability in HOMER Fuel Savings Estimates**

The first partition tree executed in this analysis found that the peak load of the scenario considered was the factor with the greatest influence on the relationship between inter-annual temperature variability and inter-annual variability in HOMER fuel savings predictions. Figure 5.21 shows the first split of this initial partition tree. This split shows that 24.5% of inter-annual variability in HOMER fuel savings predictions resulting from inter-annual temperature variability can be explained by identifying whether the peak load of the scenario is above or below 30kW. It should be recalled that the peak load factor was similarly identified as the most influential factor on the effects of inter-annual solar irradiance variability on HOMER fuel savings prediction variability.

As with the analysis of solar irradiance, the peak load factor was further evaluated through linear regression analysis and visual exploration of inter-annual HOMER fuel savings prediction variability across the five peak load levels. Box plots were utilized to identify the quantity and range of inter-annual variability in the HOMER fuel savings predictions for each of the five load profile peak load levels. Figure 5.22 shows that the quantity of inter-annual variability in HOMER fuel savings predictions is far less when due to temperature variability than it was when due to inter-annual solar irradiance variability, seen in Figure 5.2. The median inter-annual variability of HOMER predictions for the 3kW scenarios, for example, is approximately 1.7% when resulting from inter-annual solar irradiance vari-

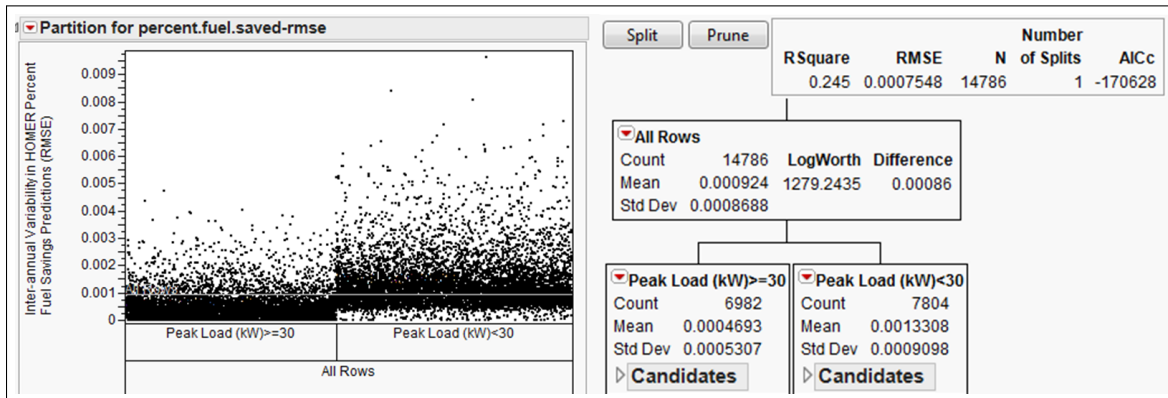


Figure 5.21: Partition tree with one split identifying scenario peak load level as the most influential factor for inter-annual HOMER fuel savings prediction variability caused by inter-annual mean temperature variability

ability and only approximately 0.13% when it is resulting from inter-annual temperature variability.

Although the inter-annual variability in HOMER fuel savings predictions resulting from temperature variability is close to a magnitude of ten less than the variability resulting from solar irradiance variability, the influence of scenario load profile peak load levels on variability of HOMER predictions is similar. Figure 5.22 shows how the relationship between inter-annual variability of HOMER fuel savings predictions and the different peak load levels of the scenarios is similar to what was seen when assessing the effects of solar irradiance inter-annual variability. Here again the 3kW and 10kW scenarios demonstrate a higher degree of inter-annual variability in HOMER fuel savings predictions than the 5kW, 30kW, or 60kW scenarios. Figure 5.23 helps to explain this relationship between peak load levels and inter-annual variability in HOMER fuel savings predictions. It shows that the ratio of peak load level to PV power production capacity once again appears to serve as a confounding factor on inter-annual variability in fuel savings predictions. The table showing the peak load level to PV power production capacity ratios can be reviewed in Figure 5.3.

Figure 5.23 visualizes the confounding effect of these ratios with the use of linear regression lines, as was done in the analysis of solar irradiance variability effects. Similar to what was seen in this previous solar irradiance analysis, when considering the effects of inter-

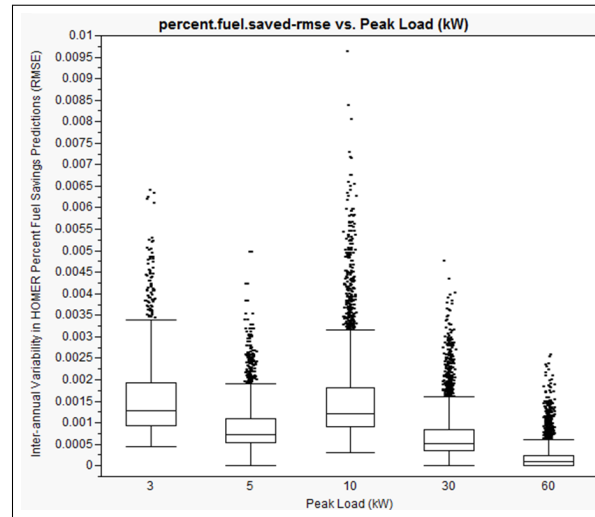


Figure 5.22: Graphical representation of the impact of scenario peak load on variability in HOMER percent fuel savings predictions (RMSE)

annual temperature variability the linear relationship between mean predicted fuel savings and variability in predicted fuel savings is more prevalent in the 5kW, 30kW, and 60kW scenarios. Figure 5.23 shows the linear regressions for the five peak load levels, with the 5kW, 30kW and 60kW scenarios having RSquare values of 0.401, 0.569 and 0.775, respectively. The 3kW and 10kW scenarios, as seen in Figure 5.23, demonstrate a weaker linear relationship between mean predicted fuel savings and inter-annual variability in HOMER fuel savings predictions, with RSquare values of 0.112 and 0.199, respectively. The difference seen in HOMER prediction variability between the two groups of peak load levels (3kW and 10kW versus 5kW, 30kW, and 60kW) is assumed here to be attributed to the different ratios of peak load to PV energy production capabilities between the two groups.

For consideration of the remaining factors in the analysis of variability in HOMER fuel savings estimates due to inter-annual temperature variability all five peak load levels are again included in the analysis. Also, the 3kW and 10kW peak load scenarios are again considered to be more representative of the effects of temperature inter-annual variability on inter-annual variability of HOMER fuel savings predictions. This is because of the higher ratio of PV power production capacity to system peak load levels in the 3kW and 10kW scenarios and the subsequently weaker linear relationship between HOMER's mean percent fuel savings predictions and inter-annual variability in HOMER percent fuel sav-

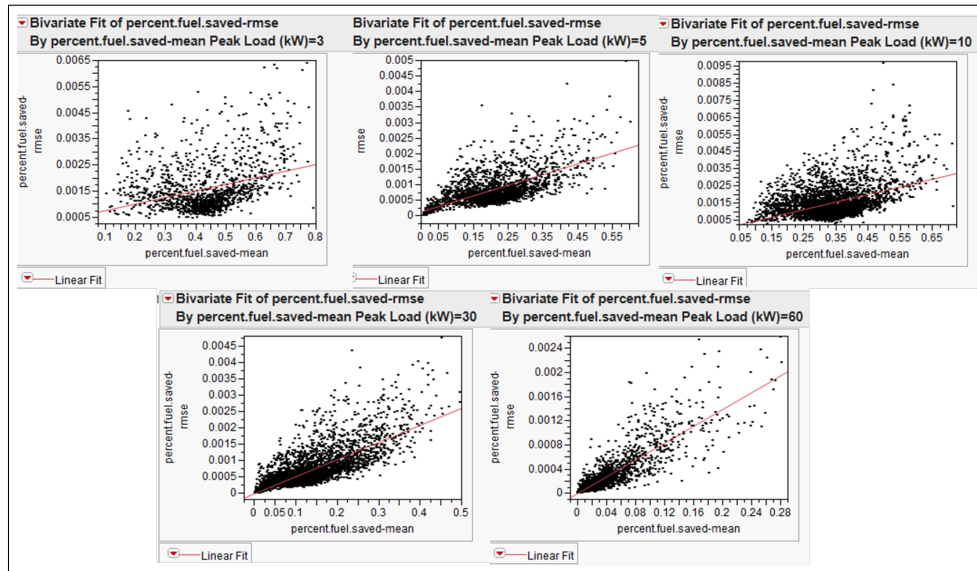


Figure 5.23: Graph shows strong linear relationship between mean predicted fuel savings and variability in predicted fuel savings for 5kW, 30kW and 60kW scenarios for HOMER prediction variability resulting from inter-annual scenario temperature variability

ings predictions.

## 5.4.2 Temperature Variability: Effects of Duration on Variability in HOMER Fuel Savings Estimates

The factor with the second greatest influence on HOMER fuel savings predictions inter-annual variability due to inter-annual temperature variability was identified through the use of a partition tree. This partition tree did not include peak load as a factor and instead considered the three factors location, start time (season), and duration as x variables. The RMSE variability of HOMER percent fuel savings predictions was set as the y variable for the partition tree. This partition tree, seen in Figure 5.24, shows that the duration of the scenario is the second most influential factor concerning how inter-annual temperature variability affects inter-annual variability of HOMER fuel savings estimates. The partition tree shows that 13.4% of inter-annual variability in HOMER fuel savings predictions can be explained by identifying whether a given scenario's duration is greater than or less than two months. This is of course given that the variability in HOMER fuel savings predictions are due to inter-annual temperature variability, with the solar irradiance resource kept constant

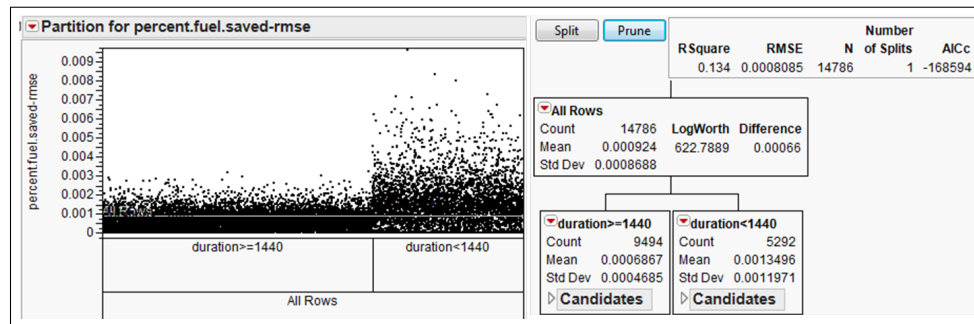


Figure 5.24: Partition tree showing duration of the scenario to be the second most influential factor on the inter-annual variability of HOMER fuel savings predictions when that variability is due to inter-annual temperature variability

for all years using the NREL TMY3 solar irradiance profiles.

To better quantify the effects of duration as a factor across each of the five peak load levels, five partition trees were reviewed, one for each peak load level. In Figure 5.25 the first split for these partition trees shows that duration proved to be the second most influential factor for four of the five peak load levels. The duration factor's influence is greatest for the 3kW and 10kW scenarios, with RSquare values of 0.443 and 0.354, respectively. That being said, even the 5kW and 30kW scenarios show duration to be their second most influential factor with RSquare values of 0.231 and 0.169, respectively. Only the 60kW scenarios show scenario start time to be the second most influential factor, with an RSquare of 0.051, for explaining inter-annual variability of HOMER fuel savings predictions when variability is due to inter-annual temperature variability. Even for the 60kW scenario, however, duration can be seen as an influential factor on the fourth split of the partition tree, when this factor increases the RSquare value from 0.261 to 0.501. It is notable that for all of the other four peak load level scenarios the important split occurs at the same level for the duration factor; the two month mark. As can be seen in Figure 5.25, there is a noticeable increase in both the average variability and range of variability in fuel savings predictions when duration values are less than two months, or 1440 hours.

Now that duration has been identified as the second most influential factor for explaining the relationship between inter-annual temperature variability and inter-annual variability in HOMER fuel savings predictions, a visual exploration of the relationship will support a

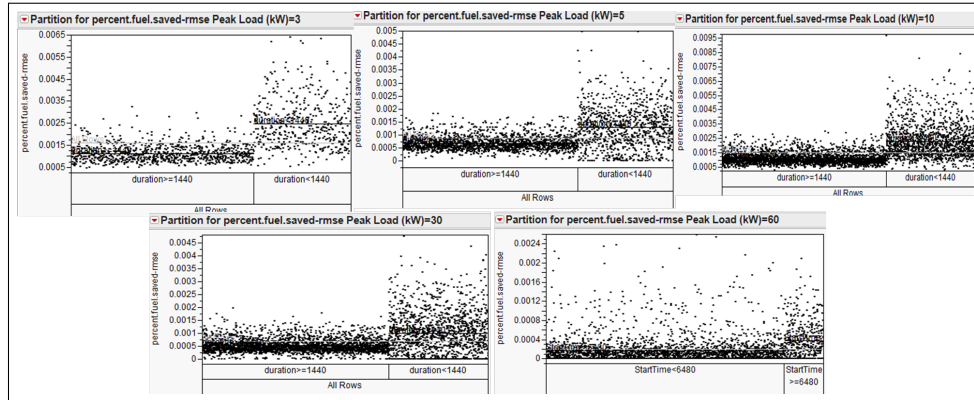


Figure 5.25: The first split in partition trees associated with each peak load level, identifying duration as the second most influential factor for inter-annual variability in HOMER fuel savings predictions when variability is due to inter-annual temperature variability

qualification of the relationship between HOMER variability and scenario duration. Figure 5.26 supports such a visual exploration of the relationship between duration and inter-annual variability of HOMER model fuel savings predictions when this variability is due to inter-annual temperature variability. This visualization shows that inter-annual variability of HOMER fuel savings predictions increases at a rate that increases substantially as duration of the scenario decreases below three months. The relationship between duration and variability predictions is the greatest for the scenarios with 3kW and 10kW peak load levels; this was anticipated, given the output of the previously discussed partition trees.

For the 3kW and 10kW peak load levels, approximately 75% of fifteen day scenarios show greater inter-annual variability than 50% of one month scenarios. For these same peak load levels, 50% of one month scenarios show greater inter-annual variability than 75% of all scenarios with larger duration levels. While the relationship is more prominent for scenarios with 3kW and 10kW peak load levels, the relationship seen between scenario duration and inter-annual variability in HOMER fuel savings predictions is seen across all peak load levels.



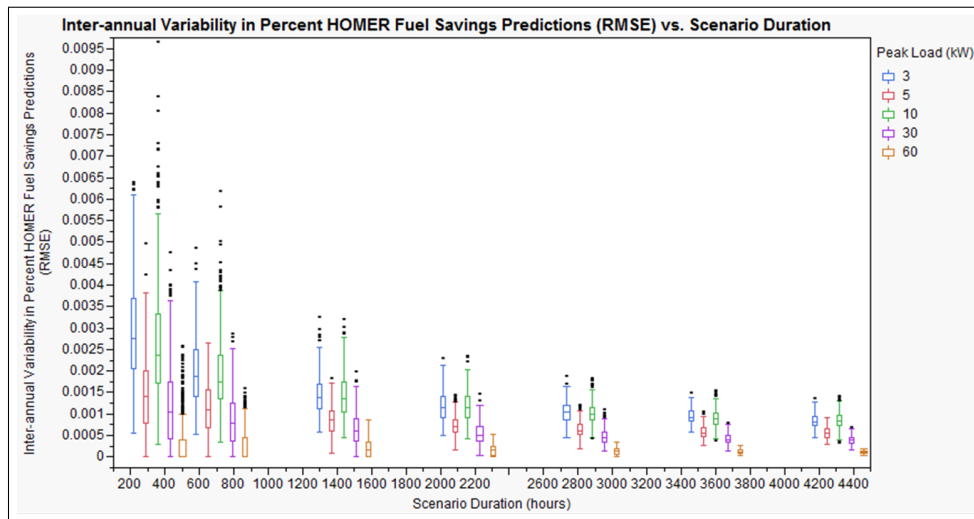


Figure 5.26: Visualization of the relationship between duration and inter-annual variability of HOMER model fuel savings predictions when variability is due to inter-annual temperature variability

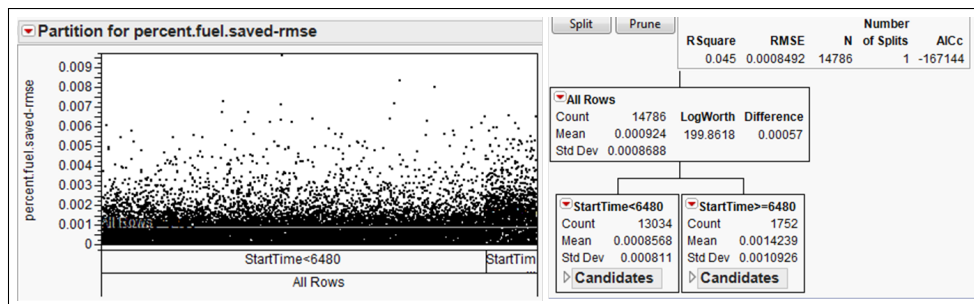


Figure 5.27: The first split in the partition tree identifying start time as the third most influential factor for inter-annual variability in HOMER fuel savings predictions when variability is due to inter-annual temperature variability

### 5.4.3 Temperature Variability: Seasonal Effects on Variability in HOMER Fuel Savings Estimates

When duration and peak load are not included as factors in the partition tree analysis, the start time of scenarios is seen to be the third most influential factor for understanding inter-annual variability in HOMER fuel savings predictions. Figure 5.27 shows this partition tree, with the first split, about the start time of September 1st, yielding an RSquare value of 0.045.

Visual exploration of this factor's influence on inter-annual variability of HOMER fuel savings predictions showed that the relationship between scenario start time and the variability in inter-annual HOMER fuel savings predictions was related to the relationship between scenario start time and mean fuel savings predictions. This relationship is similar to that seen when assessing the relationship between scenario start time and HOMER prediction variability due to solar irradiance variability. Once again, the confounding effects of the seasonal fluctuations in mean load profiles appear to explain more of the inter-annual variability in HOMER fuel savings predictions than does the inter-annual temperature variability associated with the seasons. While the relationship between scenario start time and scenario mean temperature is unimodal, the graphical representation of start-time relationship with HOMER prediction variability is bi-modal, with the latter matching the bi-modal relationship between mean fuel savings and scenario start-time. Through this analysis, the relationship between scenario season and the inter-annual variability of HOMER fuel savings predictions is considered to be minimal for the purposes of this research. An important caveat, as stated with the solar irradiance analysis, is that seasonal effects seen in climates outside the continental United States could potentially have greater influence on inter-annual variability of HOMER simulations.

#### **5.4.4 Temperature Variability: Climate Effects on Variability in HOMER Fuel Savings Estimates**

The next factor considered is the climate of the scenarios. Figure 5.28 shows that climate has little influence on the inter-annual variability of HOMER fuel savings predictions when that variability is due to inter-annual temperature variability. While the steppe climate provides for greater mean predicted fuel savings percentages than the other two climates throughout the year, there is no one climate that shows a consistently higher or lower inter-annual variability in fuel savings predictions relative to the other climates. This suggests that, when considering the effects of inter-annual temperature variability, the scenario's climate demonstrates minimal influence on the inter-annual variability of HOMER fuel savings estimates.

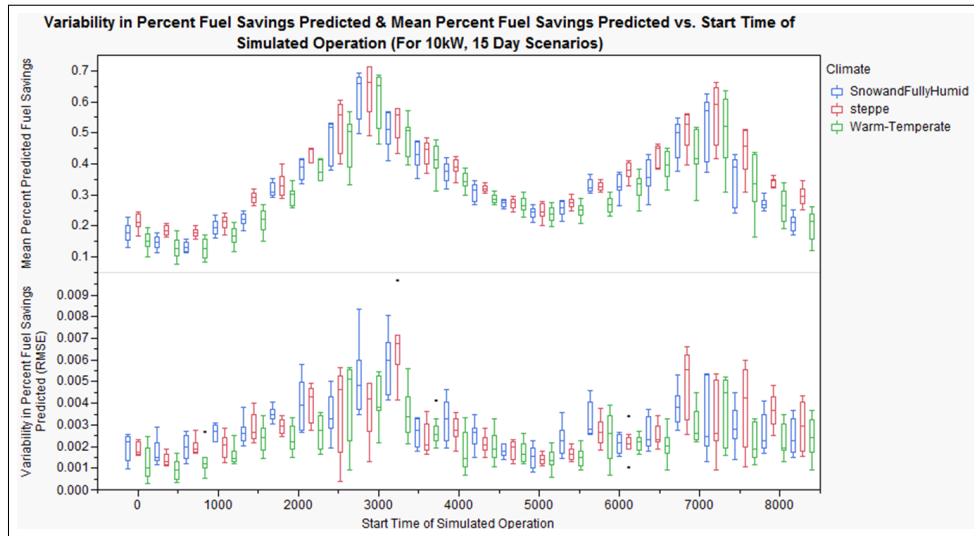


Figure 5.28: Effects of climate on inter-annual variability of HOMER fuel savings predictions due to temperature variability, shown across the seasons for 10kW and 15-day scenarios

## 5.5 Comparing the Effects of Solar Irradiance and Temperature Inter-annual Variability on the Robustness of HOMER Predictions

When the effects of inter-annual temperature variability are considered, variability of HOMER fuel savings predictions for individual peak load and duration factor levels is less than the variability for equivalent scenarios associated with only inter-annual solar irradiance variability. While the relationship between duration and inter-annual HOMER fuel savings predictions is significant for the temperature variability scenarios, the quantity of inter-annual variability is smaller than it is when due to solar irradiance variability. Figure 5.29 shows how solar irradiance inter-annual variability has a much greater influence on the inter-annual variability of HOMER fuel savings predictions than does temperature variability. For example, the HOMER fuel savings predictions for 3kW, 15-day scenarios have a median inter-annual variability of approximately 0.275% when the variability is due to inter-annual temperature variability. The 3kW, 15-day scenarios have a median inter-annual variability of approximately 2.2% when the variability is due to inter-annual solar irradiance variability.

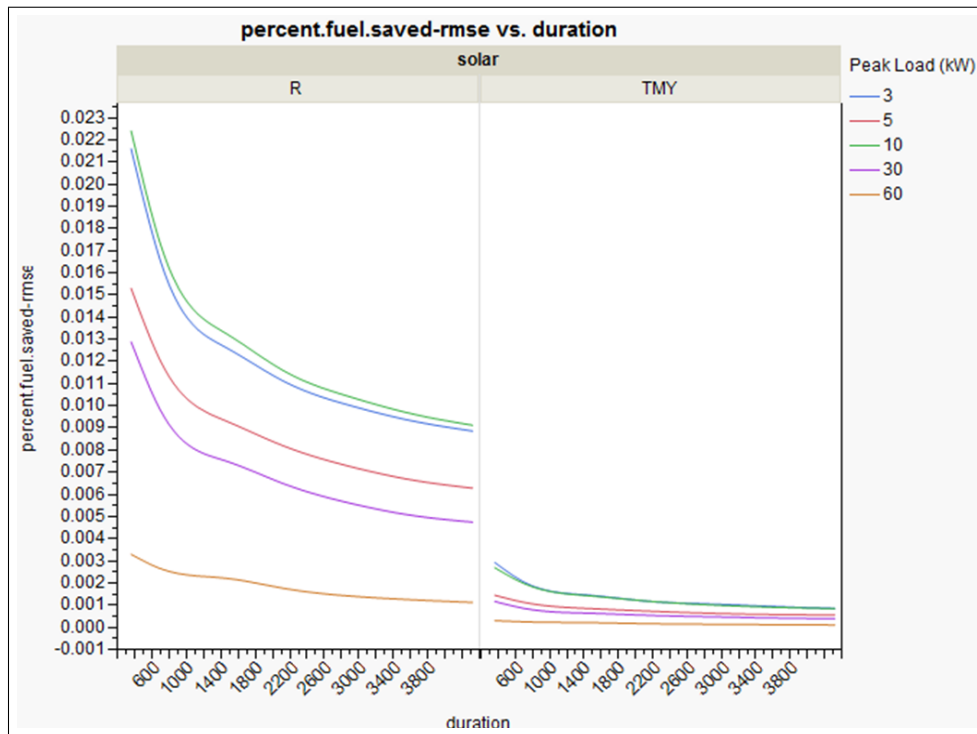


Figure 5.29: Visualization of how inter-annual variability (RMSE) of percent fuel savings differ between HOMER simulations that utilize measured temperature profiles and measured annual solar irradiance profiles ("R" graph) and HOMER simulations that utilize measured temperature profiles and TMY3 solar irradiance profiles ("TMY" graph)

Interestingly, when both solar and temperature inter-annual variability are considered in the HOMER simulations, the inter-annual variability of HOMER fuel savings predictions is actually less than the variability resulting from solar irradiance variability alone. This decrease in inter-annual HOMER prediction variability is seen in Figure 5.30. The decrease in variability can be explained by understanding the relationship between the correlated solar irradiance and temperature input files. For a given location solar irradiance and temperature values tend to fluctuate with the seasons in an inverse relationship relative to each other. In the summer, for example, temperature values tend to be at their highest while solar irradiance values tend to be at their lowest values. In the winter season, temperature values tend to be at their lowest while solar irradiance values tend to be at their highest. This inverse relationship between temperature and solar irradiance fluctuations across the seasons explains why the combination of solar irradiance and temperature data in a HOMER

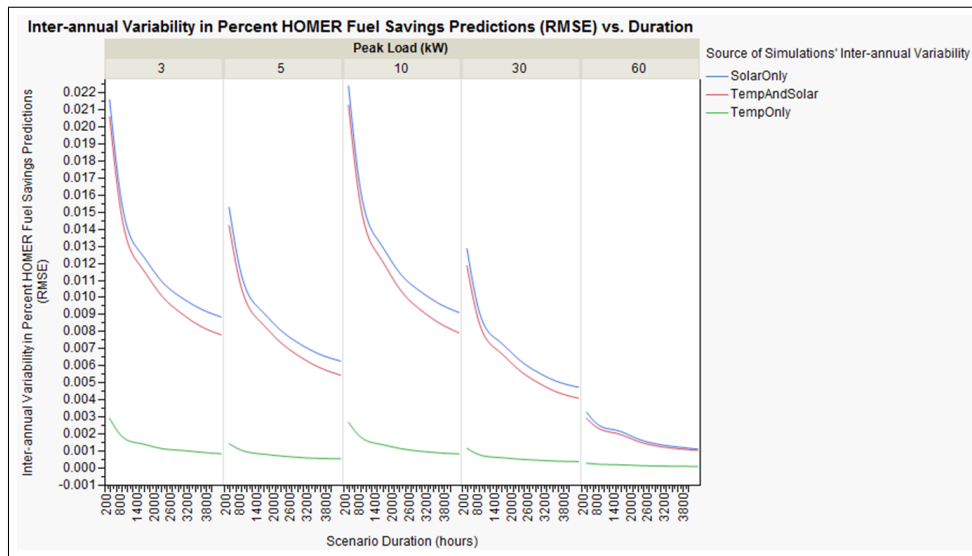


Figure 5.30: Visualization of how inter-annual variability (RMSE) of percent fuel savings differ between HOMER simulations that utilize measured temperature profiles and measured annual solar irradiance profiles ("Temp Only"), HOMER simulations that utilize measured temperature profiles and TMY3 solar irradiance profiles ("TempAndSolar"), and HOMER simulations that utilize measured annual solar irradiance files and don't consider temperature effects ("SolarOnly")

simulation would decrease inter-annual variability of the predictions. Increases in power generation that would be associated with increases in solar irradiance beyond the mean level would be partially dampened by the associated decreases in ambient temperature for the same period of time. This could explain why including both solar irradiance input profiles and correlated temperature input profiles in HOMER simulations results in a decrease in the inter-annual variability of HOMER simulations.

## 5.6 Using HOMER to Assess Grid-tie versus Standalone Converters for PV Systems

All of the experiments conducted for this research included Marine Corps AMMPS generators and a slightly modified representation of the Marine Corps GREENS renewable power system. The modification of the GREENS specifications was the representation of a single GREENS as being able to produce 1.76kW of power with its 1.76kW PV arrays, rather than limiting the power output to 1kW as is seen with the real GREENS system. The GREENS specifications were modeled in this way in the HOMER model because the

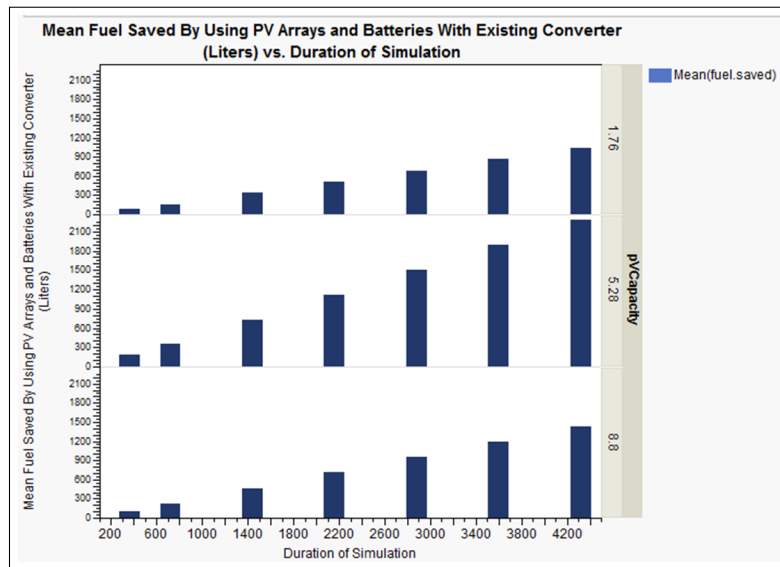


Figure 5.31: Mean fuel savings derived from employing the GREENS PV arrays and batteries with the existing standalone converter and without the controller decreasing power provided by the PV arrays

model was unable to represent the GREENS controller's limitation on power production without decreasing the modeled size of the PV arrays themselves. It is important to note that the HOMER LLC, being made aware of this difference between the existing model and the GREENS capabilities, will be able to correct the HOMER representation of GREENS in future versions. Although this representation of GREENS facilitated the analysis of HOMER robustness concerning variability of inputs, it also facilitated an assessment of how PV arrays and batteries equivalent in size to the GREENS components could support Marine Corps micropower systems if employed in a way different from the current method. This analysis has demonstrated the notable fuel savings that can be derived from employing PV arrays and battery banks in direct support of loads in conjunction with other micropower system assets. The mean fuel savings experimentally calculated across the scenarios are shown in Figure 5.31, the mean values are organized by quantity of GREENS and by the duration of the simulation. This research went a step further in the analysis of Marine Corps renewable energy power planning by assessing how the implementation of grid-tie converters would affect the fuel savings to be derived from employing renewable power sources.

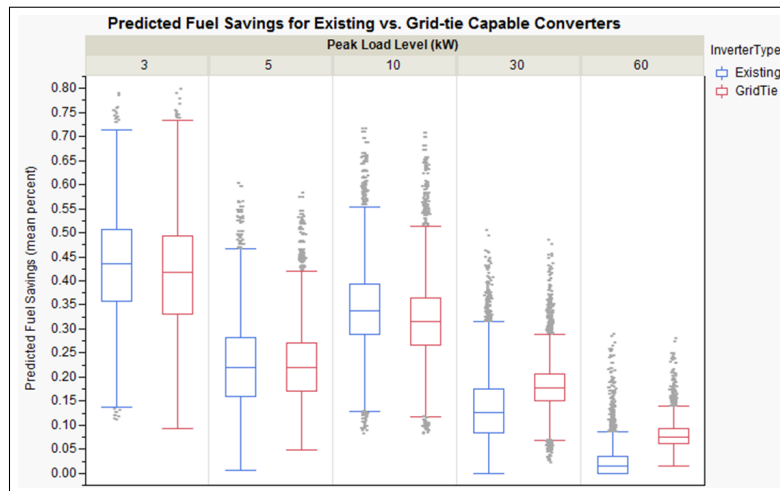


Figure 5.32: Comparison of mean fuel savings derived from employing the GREENS PV arrays and batteries with a grid-tie capable versus using a standalone converter

Following analysis of inter-annual variability in temperature and solar irradiance inputs for existing converter type, this research shifted to an assessment of HOMER predictions of grid-tie capable PV systems for the same scenarios. This analysis of converter effects on the fuel savings to be derived from GREENS systems was conducted only with measured annual solar irradiance profiles as the solar resource input and with the effects of temperature not included in the model. The only change made to the PV array systems was the specification of the inverters as being grid-tie capable. This specification change was executed to identify the potential fuel savings of the GREENS PV arrays if the converter was changed to be a grid-tie capable converter. This modification to the GREENS specifications is in addition to the previously explained modification of not limiting the PV array power production from 1.76kW to 1kW per individual GREENS system. Figure 5.32 shows the mean fuel savings predicted through the use of HOMER for the scenarios when the GREENS converter is made to be grid-tie capable compared to the mean fuel savings predicted for scenarios utilizing the existing stand-alone converter specification.

Figure 5.32 demonstrates an interesting relationship between the peak load size and the benefit of employing a grid-tie capable converter. While having a grid-tie capability showed to be of little value for the smaller micropower systems (even slightly detrimental at times) the use of grid-tie converters resulted in significant fuel savings over the use of standalone

converters when the peak load level is higher.

As the Marine Corps pushes forward in its development and fielding of renewable energy technologies, this analysis of grid-tie capable PV array performance provides valuable insight for critically assessing the Marine Corps' approach to renewable power employment. It can help answer the question of whether stand-alone systems are still the best way to go, or if fuel savings derived from grid-tie capable PV systems would be worth the investment of time and resources. These results show that the pursuit of grid-tie capabilities for PV-battery bank systems would likely only increase fuel savings for micropower systems with peak load levels of 30kW or greater.



---

## CHAPTER 6:

### Conclusions, Recommendations, and Future Research

---

This research included analysis of the robustness of the HOMER model with regard to solar irradiance and temperature variability and quantified how several factors relate to that robustness. This research also included an analysis of global dimming and its effects on solar power generation, the benefits of employing a PV array and battery bank system similar to GREENS in direct support of a micropower system, and the potential fuel saving benefits of making such a GREENS-like system grid-tie capable. In this chapter, these findings will be briefly discussed and recommendations will be provided for improving Marine Corps use of the HOMER model, PV arrays and battery banks, and power planning in general. Recommendations for future work are also provided to illustrate additional research that is needed to further support these findings and to investigate additional questions highlighted by this research.

The variability in HOMER-generated fuel savings estimates, from including PV-battery bank systems, associated with the inter-annual variability of solar irradiance and temperature profiles was found to be statistically significant, but relatively minor. The highest degree of variability seen in HOMER fuel savings estimates was seen with the 15-day, 10kW scenarios. When considering solar irradiance variability, these simulations, with mean percent fuel savings estimates of 33.8%, demonstrated a mean variability in percent fuel savings estimates of 2.2%, with a 95% confidence interval of 1.2 to 3.4%. This means that for a HOMER estimate of 33% GREENS-derived fuel savings, a consideration of inter-annual solar irradiance variability results in anticipating the fuel savings estimate to lie between 30.8 and 35.2%. A more conservative consideration of variability, using the 3.4% variability level seen as the highest value within the 95% confidence interval, would result in a fuel savings estimate between 29.6 and 36.4%. As was discussed earlier, scenarios with only slightly longer durations and larger load to PV power capacity ratios demonstrated far less variability. This shows that there is promise for Marine Corps implementation of the HOMER model in support of expeditionary power planning.

This analysis of the variability associated with the HOMER model's stochastic inputs has

quantified how changes to certain simulation factors, such as duration, influence the confidence that users can hold when using HOMER fuel consumption estimates. The following sections provide a summary of the analysis as well as some additional insights gleaned from this research. The findings and recommendations below provide information to improve Marine Corps power planning with the HOMER model and renewable energy technology.

## **6.1 Evaluation of HOMER Model Robustness with Regard to Inter-Annual Variability in Solar Irradiance and Temperature Profiles**

This research quantified the variability of HOMER fuel savings predictions that is due to inter-annual solar irradiance and temperature variability across multiple factors. It was first identified that, of the five factors assessed, the peak load level (including ratio of peak load level to PV power production capacity) and the duration of a simulated operation are the two most useful factors for explaining the variability of HOMER fuel savings predictions. Figure 6.1 and Figure 6.2 quantify the degrees of variability seen across the levels of these two factors for the 50 years of measured data. Both Figure 6.1 and Figure 6.2 illustrate how decreases in duration and increases in the peak load to PV production capacity ratio increase the variability of a scenario's HOMER fuel savings predictions. This can prove useful for power planners, as the tables quantify how changes in operation parameters influence the variability of HOMER fuel savings estimates.

Comparing Figure 6.1 and Figure 6.2 shows that inter-annual solar irradiance variability has a greater impact on the variability of HOMER-generated fuel savings predictions than does the inter-annual variability of temperature input profiles. Variability in HOMER fuel savings estimates that is due to inter-annual solar irradiance variability is roughly a power of 10 greater than variability due to inter-annual temperature variability.

The other three factors included in the DOE, simulation start time, location/climate, and composition of diesel generators, demonstrated weaker relationships with the variability of HOMER fuel savings predictions. The relationships between these factors and the variability in HOMER fuel savings estimates can be reviewed in sections 5.2.3, 5.2.4, and 5.3.5 for solar irradiance variability and 5.4.3 and 5.4.4 for temperature variability. These relation-

Variability of Fuel Savings Predicted in RMSE from the Mean Percent Fuel Savings Prediction (when variability is due to inter-annual solar irradiance variability across 50 years)									
			Duration of Simulated Operations						
			15 Days	1 Month	2 Months	3 Months	4 Months	5 Months	6 Months
Ratio of Scenario Peak Load to PV Power Production Capacity (Peak Load Level)	0.33 (3kW)	97.5% Quantile	3.10%	2.31%	1.78%	1.51%	1.35%	1.19%	1.11%
		50% Quantile	2.17%	1.61%	1.29%	1.10%	1.00%	0.92%	0.89%
		2.5% Quantile	1.17%	0.90%	0.71%	0.66%	0.66%	0.68%	0.65%
	0.30 (10kW)	97.5% Quantile	3.41%	2.61%	1.96%	1.61%	1.41%	1.27%	1.17%
		50% Quantile	2.21%	1.69%	1.31%	1.14%	1.04%	0.95%	0.90%
		2.5% Quantile	1.20%	0.95%	0.82%	0.77%	0.73%	0.73%	0.70%
	0.20 (5kW)	97.5% Quantile	2.91%	2.20%	1.57%	1.28%	1.06%	0.86%	0.78%
		50% Quantile	1.59%	1.23%	0.96%	0.79%	0.72%	0.68%	0.63%
		2.5% Quantile	0.00%	0.09%	0.21%	0.37%	0.44%	0.47%	0.46%
	0.16 (30kW)	97.5% Quantile	2.87%	2.12%	1.47%	1.13%	0.89%	0.68%	0.60%
		50% Quantile	1.34%	0.98%	0.75%	0.61%	0.54%	0.51%	0.48%
		2.5% Quantile	0.00%	0.00%	0.00%	0.19%	0.26%	0.32%	0.32%
	0.18 (60kW)	97.5% Quantile	1.62%	1.08%	0.59%	0.36%	0.25%	0.18%	0.15%
		50% Quantile	0.00%	0.00%	0.13%	0.16%	0.15%	0.13%	0.11%
		2.5% Quantile	0%	0%	0%	0%	0.01%	0.06%	0.08%

Figure 6.1: Quantifying the variability in HOMER Fuel Savings predictions associated with different duration and peak load levels, when the variability is due to inter-annual solar irradiance variability

ships provide less value than the peak load level and duration factors for quantifying the variability of HOMER fuel savings estimates.

### 6.1.1 Recommendation: Use Quantification of Variability for TMY3-Generated Vice Graham-Hollands-Generated Solar Irradiance Profiles

It is recommended that the Marine Corps use this quantification of HOMER output variability when using the NREL TMY3 solar irradiance profiles and subsequent versions of TMY profiles only. While this thesis quantifies the variability of fuel savings estimates due to inter-annual solar irradiance and temperature variability, these measures can only be marginally useful when using Graham-Hollands-generated solar irradiance profiles without additional assessment of the relationship between TMY profiles and Graham-Hollands-generated profiles. This is because the Graham-Hollands-generated profiles are not built using historical, measured solar irradiance profiles like TMY3 profiles are, making it difficult to identify the variability of Graham-Hollands-generated profiles relative to the typical profiles seen with NREL's TMY3 solar irradiance profiles. Additionally, based on the limited evaluation of HOMER output variability due to Graham-Hollands algorithms, TMY3 solar irradiance profiles are suggested to be preferable to the Graham-Hollands generated

<b>Variability of Fuel Savings Predicted in RMSE from the Mean Percent Fuel Savings Prediction</b> (when variability is due to inter-annual temperature profile variability across 50 years)									
			Duration of Simulated Operations						
			15 Days	1 Month	2 Months	3 Months	4 Months	5 Months	6 Months
Ratio of Scenario Peak Load to PV Power Production Capacity (Peak Load Level)	0.33 (3kW)	97.5% Quantile	0.57%	0.39%	0.28%	0.19%	0.16%	0.14%	0.13%
		50% Quantile	0.28%	0.19%	0.14%	0.12%	0.10%	0.09%	0.08%
		2.5% Quantile	0.11%	0.07%	0.08%	0.06%	0.06%	0.06%	0.05%
	0.30 (10kW)	97.5% Quantile	0.33%	0.24%	0.17%	0.13%	0.11%	0.09%	0.09%
		50% Quantile	0.14%	0.11%	0.09%	0.07%	0.06%	0.06%	0.06%
		2.5% Quantile	0%	0%	0.02%	0.03%	0.03%	0.03%	0.03%
	0.20 (5kW)	97.5% Quantile	0.60%	0.40%	0.26%	0.19%	0.16%	0.13%	0.12%
		50% Quantile	0.24%	0.17%	0.14%	0.12%	0.10%	0.09%	0.09%
		2.5% Quantile	0.09%	0.07%	0.06%	0.06%	0.06%	0.05%	0.05%
	0.16 (30kW)	97.5% Quantile	0.33%	0.21%	0.14%	0.11%	0.08%	0.07%	0.06%
		50% Quantile	0.11%	0.13%	0.06%	0.05%	0.05%	0.04%	0.04%
		2.5% Quantile	0%	0%	0%	0.02%	0.02%	0.02%	0.02%
	0.18 (60kW)	97.5% Quantile	0.18%	0.12%	0.07%	0.05%	0.03%	0.02%	0.02%
		50% Quantile	0%	0%	0.02%	0.02%	0.01%	0.01%	0.01%
		2.5% Quantile	0%	0%	0%	0%	0%	0%	0%

Figure 6.2: Quantifying the variability in HOMER Fuel Savings predictions associated with different duration and peak load levels, when the variability is due to inter-annual temperature profile variability

solar irradiance profiles when employing the HOMER model. This research has quantified the inter-annual variability of HOMER results due to measured inter-annual solar irradiance variability and has quantified the difference between fuel savings predictions from using TMY3 solar irradiance and the measured annual profiles across 50-year and 10-year periods. The author knows of no such analysis of variability in HOMER fuels savings predictions, and global dimming effects, associated with Graham-Hollands synthetic profiles or of any comparison of Graham-Hollands generated fuel savings predictions and mean fuel savings predictions for multiple measured annual profiles.

## 6.1.2 Recommendation: Develop and Employ Typical Meteorological Year Temperature Profiles

It is recommended that a library of synthetic temperature profiles be developed or acquired for locations for which the HOMER model is likely to be used by the Marine Corps. In section 5.5 it is shown that the variability of HOMER simulations associated with inter-annual temperature profile variability is a power of ten less than the variability associated with solar irradiance profile variability. It is assumed in this research, from the example provided by Newell's thesis and the explanation of NOCT coefficient effects in section 2.3.3, that inclusion of temperature averages or profiles in the HOMER model is important

for maintaining the fidelity of the simulations at an acceptable level. This suggests that while a synthetic temperature profile would increase simulation fidelity it would not notably increase the variability in HOMER fuel savings estimates. In fact, inclusion of correlated temperature profiles could even decrease variability in HOMER-generated estimates.

Section 5.5 showed that utilization of correlated annual solar irradiance and temperature profiles for a given scenario provides for a slight decrease in the variability of HOMER simulation output. That being said, it is unknown if this effect will be seen when TMY solar and temperature input files are utilized rather than correlated solar irradiance and temperature input files for individual years. It may also be useful for additional research to identify whether average temperature profiles would be sufficient for providing increased fidelity with minimal variability, similar to the results seen from employing measured annual temperature profiles.

## **6.2 HOMER Robustness with Regard to Global Dimming**

This research used RMSE measures of variability to discount the effects of global dimming on the robustness of HOMER with regard to inter-annual solar irradiance variability. The benefit of excluding the effects of global dimming in this analysis of inter-annual solar irradiance and HOMER fuel savings estimate variability is that this analysis shows the robustness of the HOMER model if the user considers global dimming in their employment of the model. Had this research ignored the effects of global dimming and instead measured inter-annual variability in terms of CV, the HOMER simulations would likely have shown to be much less robust than they were shown to be when global dimming effects are accounted for. This is because the more recent measured annual solar irradiance profiles demonstrate significantly less cumulative surface solar irradiance and GREENS-derived fuel savings than do HOMER simulations using measured solar irradiance profiles from several decades ago.

The analysis shown in section 5.3 quantified the effects of global dimming on HOMER fuel savings estimates. HOMER simulations conducted using TMY3 solar irradiance input profiles demonstrated a mean over-estimate of less than half a percent in fuel savings when compared to mean results of simulations utilizing annual profiles from 1961-2010. The over-estimate in fuel savings estimates increased by approximately 1 percent for the same

scenarios when TMY3 simulations were compared to mean results of simulations using annual profiles from only 2000-2010. This shows that a failure to consider the effects of global dimming when conducting HOMER simulations with TMY3 profiles can result in over-estimates of fuel savings.

### **6.2.1 Recommendation: Include Global Dimming/Brightening Effects in HOMER Modeling or Output Analysis**

It is recommended that Marine Corps use recent TMY solar irradiance profiles as resource inputs for the HOMER model along with an estimate of global dimming and brightening effects. It was shown in this research that comparisons can be made between simulations using the full range of annual measured profiles and simulations using only the most recent annual measured profiles to identify the degree to which global dimming is not reflected in TMY3 profiles. Global dimming effects could be replicated by modifying the solar irradiance profiles, or the user could simply be informed of the effects of global dimming as a consideration for their decision making.

The influence of the global dimming and brightening phenomenon is inherently unclear because it is unclear for any given location and time whether it is dimming or brightening that is occurring. The nature of global dimming/brightening influence is discussed here with regard to the locations included in this study. If global brightening continues to occur in North America over the next few years, then the difference between TMY3-generated simulations and real-world results will be diminished as the degree of HOMER fuel savings over-estimations will decrease. On the other hand, if global dimming occurs in North America over the next several years, the disparity between TMY3-generated simulations and real-world results will increase as TMY3 profiles provide increasingly larger over-estimates of available solar irradiance compared to reality.

## **6.3 Using HOMER to Weigh the Benefits of Different Generator Compositions for a Micropower System**

This research not only discussed the robustness of the HOMER model but also demonstrated ways in which the model can be used to improve power planning doctrine. Chapter 4 discussed the fuel savings and maintenance benefits of employing multiple generators of

different sizes for a micropower system rather than utilizing only a single generator that can provide the peak power required by the load. The first group of HOMER simulations discussed in section 5.2.5, those where the micropower systems did not include GREENS systems, supported the claim that increased fuel savings can be achieved by employing multiple different sized generators. The second group of HOMER simulations discussed in that section, those where micropower systems did include GREENS systems, contradicted the initial claim that scenarios with only a single, peak-load generator would consume more fuel than the other scenarios.

These surprising findings suggest that while using multiple generators results in substantial fuel savings for a non-hybrid micropower system, those benefits disappear once a PV array and battery bank system are added to the micropower system. John Glassmire from HOMER LLC, suggested that this increased relative performance of the single peak-load generator may be attributed to the way controllers operate in selecting when to charge and when to discharge batteries based on the controllers' lack of knowledge about the future.

These findings can prove useful for decreasing generator maintenance requirements in addition to decreasing fuel consumption. While these results do not specifically address the question of wet stacking due to generators operating at sub-par loads, it can be inferred by the decreased fuel consumption of the single generator scenarios that the use of GREENS does decrease the amount of time that a single-peak load generator is operating at sub-par power production levels. This decrease in generator time spent operating at sub-par power production levels would relate to decreased wet-stacking and associated maintenance issues.

### **6.3.1 Recommendation: Use Multiple Different Sized Generators When Not Employing GREENS in a Micropower System**

It is recommended that micropower system configurations including multiple different sized generators be employed when a GREENS or other such battery bank and solar array system is not included in supporting the load. It is also recommended that the benefit of having multiple generators when a GREENS system, or similar system, be reviewed with regard to the cost in transportation space, heavy lift engineering equipment, and maintenance requirements associated with the additional generator(s). While this research did not

definitively show that the inclusion of a PV-battery bank system makes a single peak-power generator preferable to multiple generators, it does provide a new insight for weighing the benefits of having multiple generators relative to the costs.

## **6.4 Fuel Savings Associated with Existing versus Grid-Tie Capable Converters for the GREENS System**

Section 5.6 showed mixed results from employing grid-tie capable converters with the GREENS system. The benefits of the grid-tie converters relative to existing converters seem to be inversely related to the ratio of peak-load level to PV power production capacity for the scenario. Little difference was seen between the fuel savings estimates of existing and grid-tie capable converters for the 3kW, 5kW, and 10kW scenarios, with load to PV power ratios of 0.59, 0.35, and 0.53, respectively. For the 30kW and 60kW scenarios, however, the fuel savings estimates derived the simulated use of a grid-tie capable converter were higher than the fuel savings estimates derived from utilizing the existing converter. These scenarios had peak load to PV power production capacity ratios of 0.29, and 0.15, respectively. For the 30kW scenarios, 50% of grid-tie derived fuel savings estimates were higher than 75% of those derived from simulating a stand-alone converter. For the 60kW scenarios, 75% of grid-tie derived fuel savings estimates were higher than 75% of fuel savings estimates derived from simulating a stand-alone converter.

One possible explanation for this relationship is that, when the stand-alone converter is utilized, the solar array and battery bank must be able to provide all of the power required by the load at a given time in order to provide any power to the load at that time. When the load size is increased and the size of the GREENS is not increased at an equivalent rate (i.e., where there is a decrease in the ratio of peak load to PV power production capacity) the amount of time that the GREENS can provide power to the load is decreased. When a grid-tie converter is used, on the other hand, the GREENS can provide power to the system regardless of whether it can cover the entire load by itself. This means that at certain times the GREENS can provide power simultaneously with a small generator to cover a load that would otherwise require the use of a larger generator. This results in an increased utilization of GREENS in grid-tie converter scenarios and a related increase in GREENS-derived fuel savings.



#### **6.4.1 Recommendation: Develop or Acquire Grid-Tie Converters Only for Hybrid Micropower Systems with Peak Power Levels Greater than 30kW**

The question of whether or not to acquire rugged, grid-tie capable converters does not have a simple answer. While giving users the option of operating individual GREENS in either a grid-tie or stand-alone method would provide for increased fuel savings, it is not clear whether that would be worth the cost of developing or acquiring a grid-tie capable converter for all hybrid micropower systems. While grid-tie converters exist commercially, it would be more difficult to find or develop grid-tie converters that could meet the ruggedness requirements for use in an expeditionary environment. If the Marine Corps intends to use GREENS-like systems to maximize the fuel savings of larger micropower systems, those with peak power levels of 30kW or higher, then it is more likely that a grid-tie converter would be worth the costs. If the Marine Corps intends to only use GREENS-like systems to support smaller micropower systems, as seen in the 3kW, 5kW and 10kW scenarios, then it is more likely that investing in grid-tie converters would not be worth the costs.

### **6.5 Future Work**

#### **6.5.1 Future Work: Analysis of the Inter-Annual Variability of Graham-Hollands Generated Solar Irradiance Profiles**

The Graham-Hollands algorithm was utilized by Newell in his 2010 thesis, and the resulting HOMER fuel savings estimate demonstrated an unacceptable degree of error when compared to a HOMER simulation using a measured solar irradiance profile. While it would be nice to always be able to use TMY3 solar irradiance profiles, the TMY profile requirement of historical data collection precludes the constant availability of TMY profiles for solar resource inputs. For this reason, it is necessary to quantify the variability of Graham-Hollands solar irradiance profiles.

As was discussed earlier, this thesis identified the variability of HOMER fuel savings estimates associated with the inter-annual variability of measured solar irradiance profiles. While this provides a quantification of variability in HOMER fuel savings estimates generated using TMY3 profiles, these measures of variability cannot be used when Graham-

Hollands-generated solar irradiance profiles are used as the HOMER solar resource. Analysis of the variability between Graham-Hollands-generated solar irradiance profiles and TMY3 solar irradiance profiles would allow this thesis' quantification of inter-annual variability due to solar irradiance profile variability to be appropriately applied for simulations using Graham-Hollands-generated solar irradiance profiles. This could be accomplished with an experiment that quantifies the variability of fuel savings estimates associated with employing Graham-Hollands-generated solar irradiance profiles and compares Graham-Hollands generated fuel savings predictions and fuel savings predictions for measured annual solar irradiance profiles.

### **6.5.2 Future Work: Additional Research Into the Effects of Global Dimming and Brightening**

It is recommended that additional research into global dimming and brightening be conducted to increase the Marine Corps' understanding of the phenomenon's implications for solar power assets. An improved understanding of the causes of global dimming and brightening could potentially assist in improved forecasting of solar irradiance profiles for future years and provide associated improvements in the fidelity of HOMER simulations.

### **6.5.3 Future Work: Quantifying the Maintenance Benefit of Different Generator Composition Scenarios and Investigating Controller Improvements**

Future research would be required to quantify how much the generator compositions of different scenarios relate to frequency of generators operating at low loads relative to their peak capacity. This would allow both those using HOMER operationally and those using HOMER to improve power planning doctrine to identify which composition of generators could be expected to result in the least amount of wet stacking and maintenance hours required for each generator.

It is also recommended that future research be conducted into the way in which controllers dictate the charging and discharging of batteries for a hybrid power system. If advances have been made in controllers, improving the controller decision making process for charging and discharging of batteries, such controller improvements could potentially provide for

increased efficiency in Marine Corps expeditionary power systems.

#### **6.5.4 Future Work: Continued Validation of the HOMER Model**

This research was conducted under the assumption that Newell's assessment of the HOMER model as providing sufficient fidelity was correct. While nothing has been seen to counter this assumption, additional experimentation is required to more definitively assess the model's fidelity. More specifically, Newell's assessment of the HOMER model as being sufficiently accurate is dependent on ascribing the last 17 percent of variability seen in the initial experiment to an incorrect derating factor. A follow-on experiment was not executed to validate this assumption and support the assessment of the HOMER model's fidelity. It is recommended that future research be conducted to validate the assumption that the HOMER model's over-estimate in fuel savings was due to an incorrect solar panel derating factor for the NPS solar panels utilized in Newell's experiment.

#### **6.5.5 Future Work: Marine Corps Approach to Solar Power Asset Evaluation**

The Marine Corps currently evaluates the capabilities of solar power assets by assessing their projected performance in extreme environments rather than assessing their projected performance across the range of most likely environments. Marine Corps analysis of power generation assets includes an assessment of performance in extreme heat and extreme cold. While evaluating equipment for these extreme conditions will ensure the Marine Corps has equipment that is capable of operating in any climate and place, it does not help in the pursuit of optimal system performance and power management across the range of likely environments.

An analysis of equipment should include a balance between assessing equipment reliability and performance. In both of these areas one train of thought argues that quality spread is a better mode of assessment than assessing performance in extreme conditions. To do this, one could identify the locations where Marine Corps deployments are most likely to occur and weight the performance of equipment in each environment according to the perceived likelihood of deployment to that region or environment. In this regard, the weighted performance refers to both measured reliability, in terms of operating time and maintenance requirements, and energy production performance of the equipment. Methods for

weighting the likelihood of Marine Corps deployment can include values such as national instability rankings, perceived economic and political challengers to U.S. hegemony in regions across the world, and/or the inclusion of regions falling within the arc of instability. The arc of instability is a term describing a region of the world "stretching from the Andean region of Latin America across Sub-Saharan Africa, the Middle East and the Caucasus, and through the northern parts of South Asia," which is deemed to contain countries particularly prone to political instability [44]. The prevalence of "migration, demographic decline, and economic stress" throughout the countries within the arc of instability increases the likelihood of conflict in the region [45]. This thesis has shown how historical solar irradiance and temperature data can be used to assess equipment performance across many different environments and seasons. By basing equipment analysis on factors such as these, rather than only the most extreme scenarios, the Marine Corps could better work toward maximizing its expeditionary energy efficiency and effectiveness across the range of operating environments.

#### **6.5.6 Future Work: HOMER Robustness Concerning Load Profile Variability**

The need for an analysis of how variability in load profiles affects HOMER fuel savings estimates was presented in Chapter 3. While the effects of variability in load profiles was originally intended to be assessed in this research, a lack of sufficient measurements of load profiles over time prevented the execution of that analysis. While it would be preferable for future analysis of this factor to be based on real world measures of load profile variability, a DOE that produces synthetic load profiles with specified degrees of variability could also provide valuable insight into variability in the load profile model resource.

#### **6.5.7 Future Work: Spatial Solar Irradiance and Temperature Variability**

A HOMER user's decision to employ either a TMY3 solar irradiance profile or a profile derived with the Graham-Hollands algorithm is a cost-benefit decision. For the TMY3 option, greater fidelity of the profile is acquired at the expense of limitations on locations for which the method can be employed. TMY3 solar irradiance profiles can only be utilized near the sites that have been established to collect measurements and NREL has synthesized the

data to compile a TMY3 profile. For the Graham-Hollands option, the increased flexibility in location applicability comes with a cost in the fidelity of the solar irradiance profile. A clarification of this cost-benefit relationship is necessary to identify the best solar resource option for the Marine Corps in different situations. Such a clarification could be achieved through a quantification of spatial variability effects on solar irradiance and temperature profiles.

While an introduction to spatial solar irradiance variability was provided in section 3.2, greater analysis is required to make this understanding of spatial variability useful. Quantification of how distance from the TMY3 measurement location affects the variability of TMY3 profiles and HOMER fuel savings estimates is needed to help determine the number and spread of TMY3 measurement sites necessary to make the Marine Corps' use of TMY solar irradiance profiles for the HOMER model more feasible for expeditionary scenarios. Similar research for improving the Marine Corps' understanding of temperature spatial variability would be beneficial for the same reasons.

THIS PAGE INTENTIONALLY LEFT BLANK

---

## APPENDIX: ReadMe for the Interface Built to Access HOMER 3.0 API

---

README for managing and submitting HOMER experiments on reaper, SEED Center's cluster

Stephen C. Upton

SEED Center for Data Farming

12/3/2013

modified: 5/13/2014

Overview Running HOMER on our cluster required development of several software artifacts, as well as using the HOMER 3 software components. The HOMER 3 components included a HOMER executable and several java libraries. The other software artifacts described below were written to configure a set of HOMER "experiments" and generate supporting files in order to run HOMER on our cluster. Our cluster uses the open source software application called "HTCondor" (<http://research.cs.wisc.edu/htcondor/>) for distributing the runs across the machines in the cluster.

The other two pieces of software that were written are called HOMERRunner and HOMERFarmer. HOMERRunner, written in java, uses the HOMER 3 APIs, and takes a single set of input in the form of: (1) a HOMER 3 scenario; (2) a city name; (3) a specific year, e.g., 1961; (4) a start time; (5) an end time, where the times specify a duration during the year; and (6) a solar irradiance data file and a temperature file, both associated with an individual city and a specified year. HOMERRunner then takes those as input, modifies the scenario input file, using the HOMER 3 API, sets the latitude and longitude of the city, the azimuth of the PV component based on city data, as well as adjusting the solar and temperature input to conform to the time period specified, and calls the HOMER executable. Once the HOMER executable has completed, output is directed to a CSV (comma-separated value) output file, with the file name constructed from the input settings.

HOMERFarmer, also written in java, is a wrapper around HOMERRunner and basically runs HOMERRunner over multiple inputs, collected together in what we call an "experi-

ment". A collection of experiments is considered a "run". An experiment is just a set of input settings specified in a CSV input file. An experiment file, or a subset of an entire run, is considered a single job. A single job is then run on a single processor on a machine as scheduled by the HTCondor software. All the output is then gathered in a centralized location and post-processed.

HOMER Input: 1. DOE file an experiment file that lists scenario file, solar file, temperature file, start time, and end time, in that order, in a .csv file (the city and year are extracted either from the solar file or the temperature file, depending on the type of experiment) 2. scenario file a .hm3 HOMER formatted input file 3. solar file a plain text file with 8760 lines, one per hour, representing solar irradiance at that time 4. temp file a plain text file with 8760 lines, one per hour, representing temperature at that time

Other software artifacts (in /Users/condor/models/HOMER on the reaper cluster):

1. clean\_DOE\_file.scala usage: scala <pathtoscript>/clean\_DOE\_file.scala <full path to DOE file name> purpose: removes paths from DOE file for scenario file, solar file, and temperature file entries
2. split\_experiments.scala usage: scala <pathtoscript>/split\_experiments.scala <full path to experiment file> <name of your experiments dir> <source to get year from; either "solar" or "temp"> [optional splitBy -default "scenario:city:year"] purpose: splits the DOE file into a set of more manageable job groups; default is to split by scenario, city, and year
3. generate\_submit\_files.scala usage: scala <pathtoscript>/generate\_submit\_files.scala <full path to study directory> <name of your experiments dir, relative to study directory> <full path to your scenario dir> <full path to your data dir> <name of your submit dir, relative to study directory> [optional: full path to your template file; default is studyDir/submit-template.dat] purpose: generates the condor submit files for a HOMER experiment using the submit-template.dat file
4. submit-template.dat file used as template to generate condor submit files for running a HOMER experiment
5. generate\_ppsubmit\_files.scala usage: scala <pathtoscript>/generate\_ppsubmit\_files.scala



<full path to study directory> [optional: full path to your post-processor submit template file; default is <homerdir>/ppsubmit-template.dat]

6. ppsubmit-template.dat file used as template to generate condor submit files for post-process a HOMER experiment

7. concat.output.by.city.R R script to concatenate the output from a set of experiments, by city

8. combine.fuel.saved.R ((ran from the parent directory of the PV/NoPV directories, e.g., Input) usage: Rscript <pathtoscript/combine.fuel.saved.R <use.for.year (solar | temp)> <solar category (R | T)> <temp category (R | G)> <inverter type (Existing | GridTie)> purpose: concatenates the output from an experiment group that has PV and NoPV directories, with output associated with running a scenario that has PV components and one that has NoPV components, but is the same scenario otherwise. Computes the fuel saved, i.e., the difference in fuel usage with PV components and one without PV components. This is calculated using the same scenario, city, year, start time, and duration settings.

9. check.missing.output.R (ran from study directory) usage: Rscript <pathtoscript/check.missing.output.R <full path to study directory> <name of your experiments dir, relative to study directory> <name of your Output dir, relative to study directory> <source to get year from; either "solar" or "temp"> purpose: checks to see which scenario/city/year/start time/duration experiment output is missing so that the user can re-run if there was an issue.

Procedure: 1. first run clean\_DOE\_file.scala for each DOE file to remove paths, if needed. Current configuration assumes that the scenario files, solar files, and temperature files will be located in the execute directory of the condor job. If desired, changes can be made to the submit-template.dat default and the runHomerOnNode.bat file to use zipped up files; just ensure the paths in the DOE files reflect what those paths will be

2. run split\_experiments.scala to divide up the DOE file into more manageable "chunks"; default is to group by scenario, city, year, i.e., in the generated experiment file will only be the jobs for a specific scenario in a specific city for a specific year, e.g., Experiment1.hm3, Boulder, 1961

3. run generate\_submit\_files to generate the condor submit file for each of the experiment files generated in step 2.

4. go into the submit directory and submit all the condor jobs, i.e., for f in 'ls' ; do condor\_submit \$f ; done

Procedure to run post-processor: 1. run generate\_ppsubmit\_files.scala in the study directory 2. go into the ppsubmit directory and submit all the condor jobs, i.e., for f in 'ls' ; do condor\_submit \$f ; done

Procedure to compute fuel saved 1. run combine.fuel.saved.R (ran from the parent directory of the PV/NoPV directories, e.g., Input)

Procedure for running the regressions:

1. open up R in the combined directory (where your combined file for the experiment is located).
2. source(" /models/HOMER/fit.regressions.R")
3. library(plyr)
4. rr <- read.csv("nameoffile with all data"), e.g., read.csv("Existing.withPercent.withPV.csv")
5. rg <- ddply(rr,.(InverterType,scenario,city,StartTime,duration,solar,temp), function(x) fit.model(x,"percent.fuel.saved","percent.fuel.saved"))
6. rg.pv <- ddply(rg,.(InverterType,scenario,city,StartTime,duration,solar,temp), function(x) fit.model(x,"PV.production","PV.production"))
7. hh <- join(rg,rg.pv,by=c("InverterType","scenario","city", "StartTime","duration","solar", "temp"))
8. write.csv(hh,"Existing.withPercent.withPV.regressions.csv", quote=FALSE,row.names=FALSE)

---

## References

---

- [1] T. Lambert, P. Gilman, and P. Lilienthal, *Micropower System Modeling with Homer*. John Wiley and Sons, Inc., 2006, pp. 379–418. [Online]. Available: <http://dx.doi.org/10.1002/0471755621.ch15>
- [2] R. Charette. (2011). Expeditionary energy strategy and implementation plan presentation. Expeditionary Energy Office. [Online]. Available: [http://www.jhuapl.edu/ClimateAndEnergy/Presentations/2011/RT\\_6\\_Charette.pdf](http://www.jhuapl.edu/ClimateAndEnergy/Presentations/2011/RT_6_Charette.pdf)
- [3] J. F. Amos. (2011). USMC expeditionary energy strategy. United States Marine Corps. [Online]. Available: <http://www.hqmc.marines.mil/Portals/160/Docs/USMC%20Expeditionary%20Energy%20Strategy%20%20Implementation%20Planning%20Guidance.pdf>
- [4] D. Parsons, “Marines hope to preserve advances in renewable energy,” Jun 2013. [Online]. Available: <http://www.nationaldefensemagazine.org/archive/2013/June/Pages/MarinesHopetoPreserveAdvancesinRenewableEnergy.aspx>
- [5] R. E. Mabus. (2012, Mar). Statement before the U.S. Senate Subcommittee on Water and Power of the United States Senate Committee on Energy and Natural Resources. [Online]. Available: <http://www.gpo.gov/fdsys/pkg/CHRG-112shrg74184/html/CHRG-112shrg74184.htm>
- [6] United States Marine Corps. Human resources and organizational management website: USMC Expeditionary Energy Office (EEO). United States Marine Corps. [Online]. Available: <http://www.hqmc.marines.mil/hrom/NewEmployees/AbouttheMarineCorps/Organization/ACMC/ExpeditionaryEnergyOffice.aspx>
- [7] United States Marine Corps. (2011, Apr). ALMAR011/11: Marine Corps expeditionary energy strategy. United States Marine Corps. [Online]. Available: <http://www.marines.mil/News/Messages/MessagesDisplay/tabid/13286/Article/109473/marine-corps-expeditionary-energy-strategy.aspx>
- [8] D. Hesterman, “Alternative energy on the frontlines,” March 2011. [Online]. Available: <http://scicom.ucsc.edu/publications/essays-profiles-pages/essay-hesterman.html>
- [9] M. Schwartz, K. Blakeley, and R. O’Rourke, “Department of Defense energy initiatives: background and issues for Congress,” Congressional Research Service, *CRS Report for Congress* R42558, Dec. 2012.

- [10] United States Marine Corps. Marine Corps Expeditionary Energy Office website: EXFOB. United States Marine Corps. [Online]. Available:  
<http://www.hqmc.marines.mil/e2o/ExFOB.aspx>
- [11] United States Marine Corps, *Guide to Employing Renewable Energy and Energy Efficiency Technologies*. Washington, DC: United States Marine Corps, September 2012. [Online]. Available: <http://www.hqmc.marines.mil/Portals/160/Docs/X-File%20Guide%20to%20Renewable%20Energy%20and%20Energy%20Efficient%20Technologies%20Sep%2012.pdf>
- [12] C. Hedelt, "MCSC helps Marines go green," December 2012. [Online]. Available:  
<http://www.marcorsyscom.marines.mil/News/PressReleaseArticleDisplay/tabid/8007/Article/136008/mcsc-helps-marines-go-green.aspx>
- [13] United States Marine Corps. (2011). SPACES extract from TM 12359A-OD. Marine Corps Systems Command. [Online]. Available:  
<http://www.marcorsyscom.usmc.mil/sites/pdmeps/DOCUMENTS/H0011.pdf>
- [14] Marine Corps Systems Command, *Principal Technical Characteristics of Expeditionary Power Systems Equipment*. Washington, DC: United States Marine Corps, Nov 2011.
- [15] J. Gerdes, "Marines push to front lines in renewable energy innovation," Jun 2013. [Online]. Available: [http://e360.yale.edu/feature/marines\\_push\\_to\\_front\\_lines\\_in\\_renewable\\_energy\\_innovation/2667/](http://e360.yale.edu/feature/marines_push_to_front_lines_in_renewable_energy_innovation/2667/)
- [16] United States Marine Corps. (2013, January). Brief to industry: mobile electric hybrid power sources (MEHPS) analysis of alternatives (AOA). Brief to Industry. United States Marine Corps, Expeditionary Energy Office. [Online]. Available:  
[http://www.hqmc.marines.mil/Portals/160/FINAL%20MEHPS%20Brief%20to%20Industry\\_0201.pdf](http://www.hqmc.marines.mil/Portals/160/FINAL%20MEHPS%20Brief%20to%20Industry_0201.pdf)
- [17] K. Hantson, "Armor and mobility: Marine Corps Expeditionary Energy Office update," September 2013. [Online]. Available:  
[http://nsrdec.natick.army.mil/about/shelter/2013\\_HighResolutionArmorandMobilitycutfullpageadds\\_Sep\\_JOCOTAS.pdf](http://nsrdec.natick.army.mil/about/shelter/2013_HighResolutionArmorandMobilitycutfullpageadds_Sep_JOCOTAS.pdf)
- [18] *Making the Soldier Decisive on Future Battlefields*. The National Academies Press, 2013. [Online]. Available: [http://www.nap.edu/openbook.php?record\\_id=18321](http://www.nap.edu/openbook.php?record_id=18321)
- [19] A. A. Alrowaie, "The effect of time-advance mechanism in modeling and simulation," *DTIC Document*, Tech. Rep., 2011.

- [20] A. Buss and P. Sanchez, "Simple movement and detection in discrete event simulation," in *2005 Winter Simulation Conference*, 2005, pp. 992–1000.
- [21] F. C. Sloane and S. Gorard, "Exploring modeling aspects of design experiments," *Educational Researcher*, vol. 32, no. 1, pp. 29–31, 2003.
- [22] (2013). When do winter, spring, summer, and fall begin. [Online]. Available: <http://www.almanac.com/content/first-day-seasons>
- [23] M. K. Williams and S. L. Kerrigan, "How typical is solar energy? a 6 year evaluation of typical meteorological data (TMY3)," in *Proceedings of World Renewable Energy Forum 2012*, 2012. [Online]. Available: <http://locusenergy.com/wp-content/uploads/2013/10/How-Typical-is-Solar-Energy-A-6-Year-Evaluation-of-TMY3-Locus-Energy-White-Paper.pdf>
- [24] S. Wilcox and W. Marion, *Users Manual for TMY3 Data Sets*. Golden, CO: National Renewable Energy Laboratory, 2008.
- [25] V. Graham and K. Hollands, "A method to generate synthetic hourly solar radiation globally," *Solar Energy*, vol. 44, no. 6, pp. 333–341, 1990.
- [26] B. Sullivan, "The effect of temperature on the optimization of photovoltaic cells using SILVACO atlas modeling," M.S. thesis, Department of Electrical and Computer Engineering, Naval Postgraduate School, Monterey, CA, 2010.
- [27] S. Dubey, J. N. Sarvaiya, and B. Seshadri, "Temperature dependent photovoltaic (PV) efficiency and its effect on PV production in the world—a review," *Energy Procedia*, vol. 33, pp. 311–321, 2013.
- [28] R. Faranda and S. Leva, "Energy comparison of MPPT techniques for PV systems."
- [29] E. Skoplaki, A. Boudouvis, and J. Palyvos, "A simple correlation for the operating temperature of photovoltaic modules of arbitrary mounting," *Solar Energy Materials and Solar Cells*, vol. 92, no. 11, pp. 1393–1402, 2008.
- [30] HOMER Energy, LLC. *HOMER graphical user interface: the micropower optimization model*.
- [31] NREL: glossary of solar radiation resource terms. [Online]. Available: [http://rredc.nrel.gov/solar/glossary/gloss\\_d.html#directnormalirradiance](http://rredc.nrel.gov/solar/glossary/gloss_d.html#directnormalirradiance)
- [32] B. Newell, "The evaluation of HOMER as a Marine Corps expeditionary energy pre-deployment tool," M. S. thesis, Department of Electrical and Computer Engineering, Naval Postgraduate School, Monterey, CA, 2010.

- [33] S. Wilcox and C. Gueymard, “Spatial and temporal variability of the solar resource in the united states,” *Washington, DC: NREL/DoE [National Renewable Energy Laboratory/Department of Energy]*, 2010.
- [34] Z. Simic and V. Mikulicic, “Small wind off-grid system optimization regarding wind turbine power curve,” in *AFRICON 2007*. IEEE, 2007, pp. 1–6.
- [35] Powering health: Reciprocating engines (generators). United States Agency for International Development. [Online]. Available: <http://www.poweringhealth.org/index.php/topics/technology/generators>
- [36] M. Kottek, J. Grieser, C. Beck, B. Rudolf, and F. Rubel, “World map of the koppen-geiger climate classification updated,” *Meteorologische Zeitschrift*, vol. 15, no. 3, pp. 259–263, 2006.
- [37] B. Newell, private communication, Mar 2013.
- [38] B. Müller, M. Wild, A. Driesse, and K. Behrens, “Rethinking solar resource assessments in the context of global dimming and brightening,” *Solar Energy*, vol. 99, pp. 272–282, 2014.
- [39] M. Wild, “Global dimming and brightening: A review,” *Journal of Geophysical Research: Atmospheres (1984–2012)*, vol. 114, no. D10, 2009.
- [40] G. Stanhill and S. Cohen, “Global dimming: A review of the evidence for a widespread and significant reduction in global radiation with discussion of its probable causes and possible agricultural consequences,” *Agricultural and Forest Meteorology*, vol. 107, no. 4, pp. 255–278, 2001.
- [41] HOMER, LLC. HOMER history. [Online]. Available: <http://homerenergy.com/history.html>
- [42] M. Walker, private communication, Feb 2013.
- [43] J. Glassmire, private communication, Mar 2014.
- [44] C. T. Fingar, *Global Trends 2025: A Transformed World*. DIANE Publishing, 2009.
- [45] J. Mattis, “The JOE 2010 joint operating environment,” DTIC Document, Tech. Rep., 2010.

---

## Initial Distribution List

---

1. Defense Technical Information Center  
Ft. Belvoir, Virginia
2. Dudley Knox Library  
Naval Postgraduate School  
Monterey, California